

Aus der Klinik für Augenheilkunde  
der Medizinischen Fakultät Charité – Universitätsmedizin Berlin

DISSERTATION

Die Rolle von FoxP3 bei der altersbedingten Makuladegeneration.

The role of FoxP3 in Age-related macular degeneration.

zur Erlangung des akademischen Grades

Medical Doctor - Doctor of Philosophy (MD/PhD)

vorgelegt der Medizinischen Fakultät

Charité – Universitätsmedizin Berlin

von

Ahmed Samir Ahmed Alfaar

Datum der Promotion: 29. November 2024



## Table of contents

List of tables	II
List of figures	III
List of abbreviations	IV
Abstract	1
Zusammenfassung	2
1 Introduction	3
2 Methods	7
3. Results	12
Mouse models:	12
Dry AMD	12
Wet AMD	12
Human Eyes	13
Cultured Cells	13
4. Discussion	16
5. Conclusions	19
Reference list	20
Statutory Declaration	27
Declaration of your own contribution to the publications	28
Excerpt from Journal Summary List	30
Printing copy(s) of the publication(s)	31
Curriculum Vitae	55
Acknowledgments	72

## List of tables

Table 1 Patients Characteristics of the examined eyes.....	8
--	---

## List of figures

Figure 1 Functions of the RPE (Adapted from 2).....	3
Figure 2 Fundus photo in AMD patient. (4).....	4
Figure 3 Prevalence of age-related macular degeneration.....	5
Figure 4. Summary of methods.....	11

## List of abbreviations

AMD	Age-related macular degeneration
BSA	Bovine serum albumin
DAPI	4',6-Diamidine-2-phenylindole
GFP	Green fluorescent protein
C	Celsius
C3, C3a, C5a	Complement factor 3, -3a, -5
Ca <sup>2+</sup>	Calcium
CFH	Complement factor H
CNV	Choroidal neovascularization
CRISPR/Cas9	Clustered Regularly Interspaced Short Palindromic Repeats/CRISPR-associated 9
CXCR4	CX-chemokine receptor 4
CX3CR1	CX3-chemokine receptor 1
FoxP3	Forkhead-box-protein P3
H	hours
IFN- $\gamma$	Interferon- $\gamma$
IL-1 $\beta$	Interleukin-1 $\beta$
MCP-1	Monocyte chemoattractant protein-1
PBS	Phosphate-buffered saline
RPE	Retinal pigment epithelium
RT	Room temperature
TBS	TRIS-buffered saline
TGF- $\beta$	Transforming growth factor- $\beta$
Treg	Regulatory T cell
TNF $\alpha$	Tumor Necrosis Factor-alpha
VEGF-A	Vascular endothelial growth factor-A
WT	Wild type

## Abstract

Age-related macular degeneration (AMD) is a leading cause of blindness among the elderly in the developed world. It is characterized by loss of the retinal pigment epithelial (RPE) cells followed by a subsequent decline in the number of photoreceptors and the choriocapillaris with the possible development of new vessels. In the normal eye, retinal pigment epithelium is an essential component of the outer blood-retina barrier that protects the eye against inflammation. Inflammatory mechanisms during the development of disease in the eye are yet to be fully understood. Forkhead-Box-Protein P3 (FoxP3) was until recently believed to be solely expressed by regulatory T cells but has recently been identified in RPE cells. As the functional role of FoxP3 in the RPE is so far unknown, we investigated its function under the hypothesis that FoxP3 is a general regulator of RPE reactions to different stress conditions.

To test our hypothesis, we examined FoxP3 expression, localization, and phosphorylation in murine eyes and ARPE-19 cell-line cultures under different stress conditions. Such stress conditions included sub-confluency, aging, stimulation by IL-1 $\beta$  (as a component of inflammation), autoimmune uveitis, exposure to cigarette smoke and laser, and mechanical injury. In addition, we confirmed FoxP3 expression in the RPE in human eyes with AMD. FoxP3 expression and localization were examined using immunofluorescence, immunohistochemical, and PCR or dot-blot studies. Bio-Plex bead analysis was used to measure the levels of cytokine secretion. Knockout FoxP3 was conducted using CRISPR/Cas9 technology to test the effect of its importance in the development of RPE cells' stress response.

The knockout of the FoxP3 gene resulted in the halting of ARPE-19 cellular growth and/or cell death under the Crisp/Cas9 treatment-induced stress. Under stress conditions, including non-confluency, RPE cells increased the expression of FoxP3 and its translocation into the nucleus. Confluent cells with a more mature and stable phenotype showed FoxP3 localization in the cytosol and upon mechanical injury or exposure to IL-1 $\beta$  translocation into the nucleus. Moreover, inflammation promoted the phosphorylation of FoxP3.

Those results imply a regulatory role for FoxP3 in the RPE during chronic inflammation and degeneration and its importance for withstanding stress conditions.

# Zusammenfassung

Die altersbedingte Makuladegeneration (AMD) ist eine der häufigsten Ursachen für Erblindung bei älteren Menschen in entwickelten Ländern. Sie ist durch den Verlust von Pigmentepithelzellen der Netzhaut (RPE) gekennzeichnet, gefolgt von einer damit verbundenen Degeneration der Photorezeptoren und Choriocapillaris. Das RPE ist ein wesentlicher Bestandteil der äußeren Blut-Netzhaut-Barriere, etabliert das Immunprivileg der Retina und schützt das Auge von entzündlichen Vorgängen. Da bei der AMD wesentliche Hinweise auf ein Versagen der Kontrolle entzündlicher Vorgänge durch das RPE deuten, könnten Entzündungsmediatoren Targets für therapeutische Ansätze sein. Allerdings ist der Entstehungsmechanismus der Erkrankung nicht im Detail verstanden. Das Forkhead-Box-Protein P3 (FoxP3) ist ein charakteristischer Marker regulatorischer T-Zellen, wurde aber in jüngster Zeit auch in RPE-Zellen identifiziert. Unter der Hypothese, dass FoxP3 in RPE-Zellen eine regulatorische Rolle in AMD relevanten Stressbedingungen spielt, haben wir die Funktion des FoxP3 im RPE untersucht.

Somit haben wir die Expression, Lokalisation und Phosphorylierung von FoxP3 in murinen Augen und ARPE-19 Zellkulturen unter verschiedenen Stressbedingungen untersucht. Diese Stressbedingungen umfassten den Verlust der epithelialen Integrität, das Alter, die Exposition von IL-1 $\beta$  (als Bestandteil einer Entzündung), autoimmune Uveitis, die Exposition gegenüber Zigarettenrauch und Laser sowie mechanische Verletzungen. Außerdem haben wir die Expression von FoxP3 im RPE menschlicher Augen mit AMD untersucht. Die Expression und Lokalisation von FoxP3 wurden mittels Immunfluoreszenz, Immunhistochemie und PCR sowie durch Dot-Blot-Studien untersucht. Die Zytokin-Sekretion wurde mit Hilfe von Bio-Plex-Beadsanalysen gemessen. Mit Hilfe der CRISPR/Cas9-Technologie wurde FoxP3 genomisch ausgeknockt, um die FoxP3 Funktion für das RPE unter zellulären Stress zu demonstrieren.

Das Ausschalten des FoxP3-Gens führte zum Stillstand des Wachstums der ARPE-19 Zellen, sowie Zelltod in Antwort auf den Zellstress durch die Crsip/Cas9 Behandlung. Die verschiedenen Stressbedingungen, einschließlich dem Verlust der epithelialen Integrität, führten zur erhöhten Expression von FoxP3 als auch zur Translokation in den Zellkern. Konfluente Zellen stellen einen besser differenzierten, stabilen Phänotyp dar, bei dem FoxP3 aus dem Zytosol bei mechanischer Verletzung oder Exposition gegenüber IL-1 $\beta$  im Nukleus akkumulierte. Darüber hinaus förderte der Entzündungsmediator die Phosphorylierung von FoxP3.

Diese Ergebnisse deuten im RPE auf eine regulatorische Rolle des FoxP3 im Entzündungsprozess und bei retinaler Degeneration sowie auf eine Bedeutung Stressbedingungen zu widerstehen.



# 1. Introduction

## 1.1 Anatomy and physiology

### 1.1.1 Blood Eye barrier

The blood-ocular barrier is composed of two barriers: anteriorly, the blood-aqueous barrier built by the tight junctions of the non-pigmented ciliary body, and the iris epithelium separating blood vessels from the aqueous humor. Posteriorly, the blood-retinal barrier is formed by the tight junctions of the endothelial cells in the inner retina and by the tight junctions of the retinal pigment epithelium (RPE). These barriers establish an immune privilege of the eye and provide selective transport of water and exchange of molecules between the bloodstream and the inner eye [1].

Both anterior and posterior barriers can acutely fail under conditions such as uveitis or in the event of trauma. Moreover, chronic degenerative diseases develop slowly in a vicious circle of inflammation, change in the immunogenic phenotype of barrier cells, and loss of barrier cells due to reduced metabolic activity and attack by an innate immune reaction.

### 1.1.2 RPE Function

The RPE maintains the photoreceptor outer segment function [2]. Bruch's membrane, and the tight junctions of the RPE, form a physical barrier against immune cells that is further enhanced by the secretory activity of the RPE. The profile of factors secreted by the RPE includes a variety of immune inhibitory factors and is regulated by receptors for pro-inflammatory cytokines. In this way, the RPE represents an active immune inhibitory barrier that helps to establish the immune privilege of the retina [3]. Besides such an immune regulatory function, RPE possesses multiple roles whereby it helps in the regulation of the microenvironment of the outer retina and supports the proper functioning of photoreceptors.

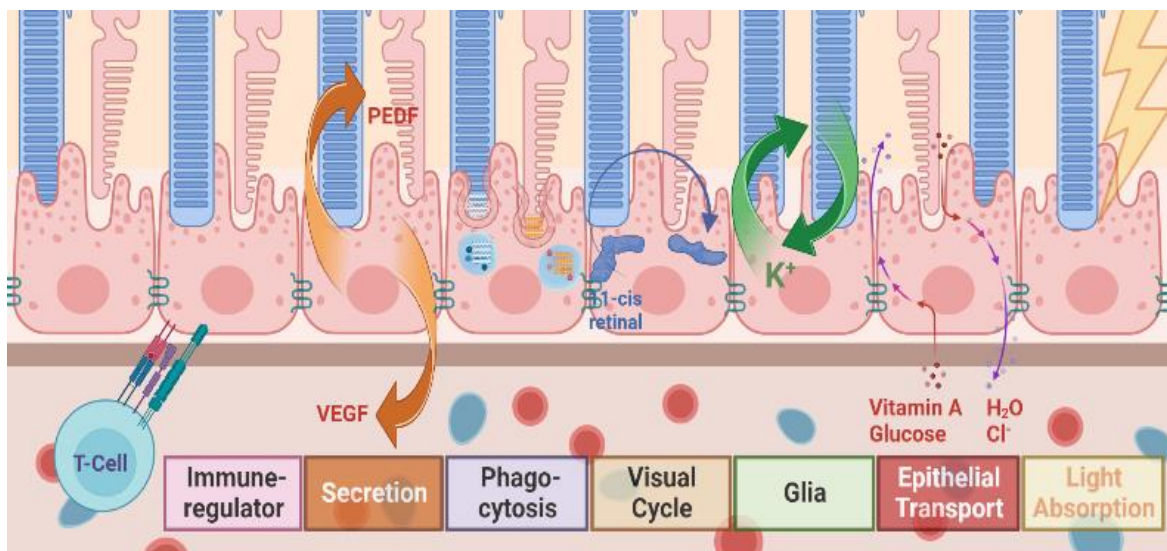


Figure 1 Functions of the RPE.

Adapted from Ref. No. [2]: Strauss O (2005) The retinal pigment epithelium in visual function. *Physiol Rev* 85:845–881.



Figure 2 Fundus photo in AMD patient.

From Ref. [4]: Leung R (2006) Back of the eye glossary: Age-related macular degeneration (AMD). *Community Eye Heal J* 19:10

## 1.2 Age-Related Macular Degeneration

### 1.2.1 Epidemiology

Age-related macular degeneration AMD is the most common cause of blindness in aging populations, including high-income countries. Its prevalence has been traditionally highest among European countries and is now rising among the upper middle-income countries as with ever higher life expectancies due to the improved general health of their populations (Figure 3). In total, AMD represents 8.7% of all causes of blindness worldwide. In addition, the burden of years lived with a disability is increasing in both developed and developing countries due to the untreatable nature of the disease. As aforementioned, improved general health has resulted in more patients living with the burden of the disease. This burden is even high in many European countries, also attributed to health policies that may not cover new medications. It is estimated that there were 196 million patients in 2020, with a predicted 288 million patients in 2040 [5].

### 1.2.2 Pathology

Early stages of AMD are associated with increased formation of *drusen* (under RPE) and subretinal drusenoid deposits (Between RPE and photoreceptors) without RPE changes. Drusen are accumulations of extracellular lipid-rich material that represent a risk factor for AMD. The late stages of the disease show a disintegration of the RPE and scarring of the macula, which is the center of vision in the human retina.

### 1.2.3 Pathogenesis; a disturbed inflammatory reaction

Risk factors for the development of AMD include age, cardiovascular disease, atherosclerosis, smoking, obesity, and race [6–9]. Reactive oxygen species, lipofuscin, thickening of Bruch's membrane, loss of hydraulic conductivity of Bruch's membrane, photo-oxidation by blue light, and increased autofluorescence during one's lifetime are other observed risk factors of the disease. On the other hand, Lutein and Zeaxanthin Vitamins C, D, and E and Zinc Oxide and other antioxidants are believed to minimize the risk of AMD [10–14]. Gene-wide association studies have identified multiple risk-associated genes, including, at the time of writing these lines, 262 variants and risk alleles reported for 159 genes on EBI GWAS Database [15]. Multiple studies have shown CFH, ARMS2, HTRA, and other complement pathway genes to be involved in the development of

the disease [16, 17]. ARMS2 acts as a surface complement regulator that activates the clearance of cellular debris, and its polymorphisms may be responsible for the accumulation of drusen [18].

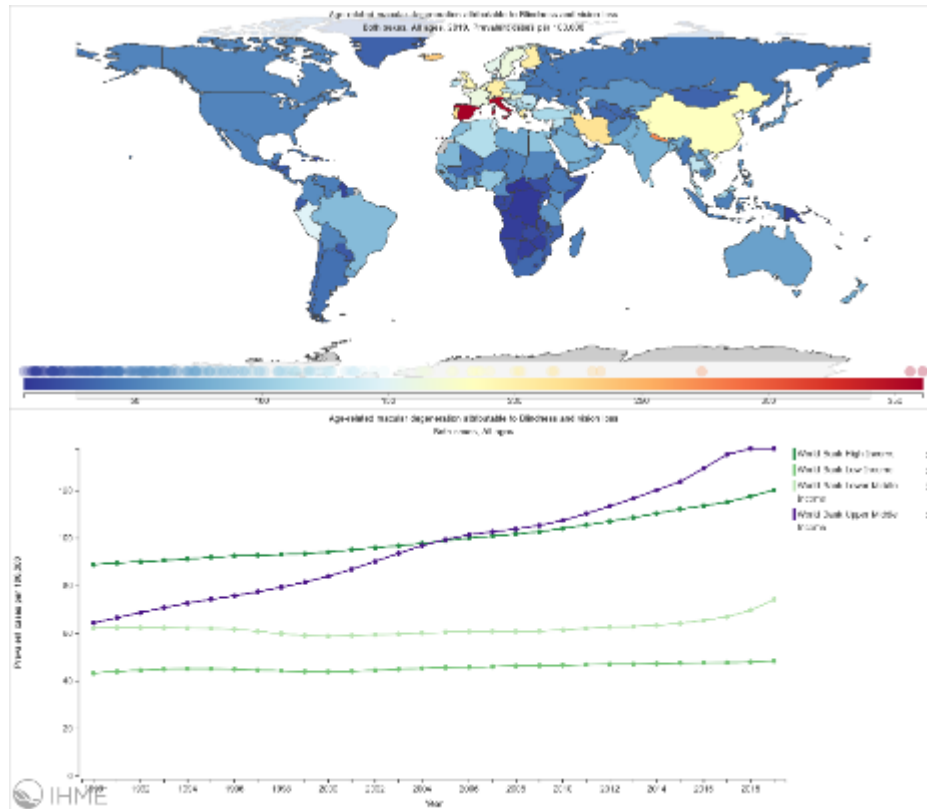


Figure 3 Prevalence of age-related macular degeneration.

Source: [19] Global Burden of Disease (GBD), Institute for Health Metrics and Evaluation (IHME), <https://www.healthdata.org/gbd>

There is recurring evidence that senescence, the buildup of gene defects, and oxidative stress lead to the inability of cells to clear up cellular debris with an accumulation of lipofuscin. All these factors, in addition to the accumulation of terminal complement complexes in the RPE/Choroid, participate in the production of a chronic proinflammatory change in the immunogenic phenotype of the RPE, switching it from immune inhibition to immune stimulation. RPE would then stimulate  $\text{TNF}\alpha$  secretion by invading monocytes and drive the development of an inflammasome, as well as drive other immune-stimulatory steps. RPE cells react to cytokines and chemokines secreted by T cells and macrophages with the release of VEGF-A, suggesting a role that may result in further inflammation and, possibly, the development of the wet form of AMD [20–22]. A similar pro-inflammatory response from RPE has been observed in the mediators of the invading mononuclear phagocytes with the further secretion of MCP-1/CCL2 and complement by the RPE and the consequent attraction of monocytes [20–22]. When the loss of the RPE cells is too fast, a complete loss of immune control happens, followed by chronic loss of the RPE and, thus, photoreceptors.

RPE can activate the pro-inflammatory phenotype M1 of Monocytes. However, some monocytes may escape such control and initiate an immune activity in a stressed RPE [20], accumulating inflammasomes as a reaction to an overactive complement system (mediated by C5a) [23–25] that would have already been showing genetic polymorphism in patients of age-related macular degeneration (AMD) [25–28]. The entire

cascade of a shift from immune-inhibitory activity to inflammation has not been fully mapped out, but is hopefully targetable.

In a recent study, we showed that RPE cells, under stress conditions, express the transcription factor FoxP3 (forkhead box P3), a factor that is known to be expressed in regulatory T cells (Treg) [26, 29, 30]. As mentioned, RPE was found to express FoxP3 under oxidative stress, a risk factor for AMD, or as a reaction to anaphylatoxins, resulting in the expression of complement factors/receptors and cytokines associated with increased FoxP3 phosphorylation [25, 26]. In Treg cells, FoxP3 activity transiently increases in T cells after activation. It determines the differentiation into regulatory cells (Tregs) associated with protein translocation to the nucleus and an increased ability to suppress inflammation and help tissue regeneration [31, 32]. This activity, however, dissipates if cells keep the effector phenotype and the FoxP3 protein remains in the cytosol [33–35]. Thus, we assumed a potentially comparable function of FoxP3 in the RPE, including the determination of the immunogenic phenotype and the switching of this phenotype towards a pro-inflammatory type.

The level of FoxP3 regulatory function is associated with splicing variants and several post-translational modifications that help govern the phenotype [31]. Besides, the epithelium of other immune-privileged organs expressed FoxP3 [36, 37] and particular cancer cells [38, 39]. Therefore, we assumed that FoxP3 could be a regulatory factor for the role of RPE as an immune barrier in diseases like AMD.

### **3.3 Goal and hypotheses**

We hypothesized that FoxP3 plays a similar role in RPE to its function in T Regs in the regulation of the immunogenic phenotype. We further assumed that the FoxP3 effects on the RPE function are similar to those on T cells. Therefore, we planned to study the expression and intracellular distribution of FoxP3 in RPE cells in AMD models as well as human specimens and examine which functional status of FoxP3 correlates with disease progression.

To test this hypothesis, we investigated FoxP3 functional status in models with AMD relevance with a focus on the effects of IL-1 $\beta$ , a factor secreted by monocytes that accumulate close to the RPE in the outer retina and that might trigger the initial steps towards a change the RPE function. In the following sections, we will delve into the methodologies utilized, the results obtained, and the subsequent discussions that further establish our hypothesis, all of which are detailed in our published work [40].

## 2. Methods

### 1.3 Ethical aspects

We followed the Association for Research in Vision and Ophthalmology ARVO *Statement for the Use of Animals in Ophthalmic and Vision Research*. Mouse experiments were approved by the LaGeSo (Nr. G0039/19), while the IACUC approved the smoke exposure experiment at MUSC (Nr. 00399). The experimental autoimmune uveitis experiment in Lewis rats was approved by the government of Upper Bavaria (Nr. ROB-55.2–1-2532.Vet\_02-15–225). The local Ethics Committee at Charité authorized the use of iPSC-RPE cells under the registration number EA1/024/17 [40].

### 1.4 Animal Experiments

- 1.4.1 **Animal models:** *Cx3cr1<sup>GFP/GFP</sup>* mice are hyperinflammatory and develop features of dry AMD in the retina, including monocyte accumulation, cytokine signaling, and loss of RPE cells manifesting with age [41]. We used C57BL/6J mice for laser-induced choroidal neovascularization (CNV) and as controls for the *Cx3cr1<sup>GFP/GFP</sup>* mice on the C57BL/6 J genetic background. Albino/Lewis rats were employed to test the effects of Autoimmune uveitis.
- 1.4.2 **Environment:** The animals were maintained in regular environmental conditions with unrestricted access to food and water, and exposed to a 12-hour cycle of light and darkness.
- 1.4.3 **The laser-induction of CNV** as mentioned before [42]: The mice were given anesthesia using a combination of 1% ketamine hydrochloride and 0.1% xylazine, after which their pupils were dilated with a mixture of 2.5% phenylephrine-hydrochloride and 0.5% tropicamide. Argon laser was used to apply four burns around the optic nerve (Power:120 mW, Time:100 ms, Size: 50  $\mu$ m). We excluded eyes that experienced retinal bleeding after the laser. The outer retina was fixed and prepared after 14 days as flat-mount and stained with phalloidin for cell borders, anti-CD102 for blood vessels, and anti-FoxP3.
- 1.4.4 **Experimental autoimmune uveitis** was performed as aforementioned [43]: Lewis rats were given subcutaneous immunization of retinal S-antigen peptide PDSA<sub>g</sub> in CFA. Cryosection was conducted on the eyes after the experiment was terminated after 30 days.

### 1.5 Immunohistochemistry of RPE/choroid flatmounts

We prepared RPE/choroid flatmounts from mouse eyes, guided by a recently published work [42]. After removal of the eyes, they were fixed in 4% paraformaldehyde for 12 minutes at room temperature and sectioned at the limbus. The retinae were separated from the RPE/choroid/sclera and sectioned into 6-8 radial sections. The RPE/choroid/sclera tissue was incubated in 5% Triton X-100 in TBS overnight at 4 °C, followed by incubation in blocking buffer (5% BSA in TBS) for 1 hour. Subsequently, the tissue was exposed to rabbit polyclonal anti-FoxP3 antibody and ActiStain555-conjugated phalloidin for 48 hours. Laser scars were highlighted using

Rat anti-mouse CD102 (1:200). The samples were washed multiple times, then incubated for 1 h at room temperature with Alexa Fluor®-conjugated secondary antibodies and then fixed in DAKO fluorescence mounting medium (Agilent). Imaging was performed using an LSM 510 confocal laser-scanning microscope (Zeiss) and ZEN 3.1 Blue Edition software.

## 1.6 Immunohistochemistry of sagittal sections

### 1.6.1 Human AMD samples

**Minnesota Lions Eye Bank** provided the eyes of donors affected by AMD and age-matched controls.

**TABLE 1 PATIENTS CHARACTERISTICS OF THE EXAMINED EYES**

Patient Characteristic	Non-Geographic Atrophy (Non-GA)	Geographic Atrophy (GA)
Number (Eyes)	4	3
Sex	three males and one female	two females and one male
Mean age in years (mean $\pm$ SD)	85.75 $\pm$ 1	85 $\pm$ 2.6
Time of death-to enucleation	193.75 $\pm$ 9 min (3:14 h)	278.5 $\pm$ 60 min (4:38 h)
Cause of Death	intracerebral hemorrhage, cardiac arrest, lung cancer, and dementia	breast cancer, congestive heart failure, and an acute cardiac disease
	Range of death-to-cooling 1 - 2:25 h	

At the central pathology department, the posterior segment was fixed for 4 h in 4% PFA, then dissected, embedded in paraffin, and sectioned.

To conduct immunohistochemistry, horse serum was added to prevent non-specific binding. Next, the sample was exposed to a primary antibody, rabbit polyclonal FoxP3 (Novus Biologicals; the same antibody as used for ARPE-19 staining below), at 4 °C overnight. After that, the sample was incubated with a secondary AP-coupled anti-rabbit antibody for 1 hour at room temperature. The positive staining was then visualized using a Fast Red substrate kit (Sigmafast Fast Red TR/Naphthol AS-MX, Sigma/Merck) and captured using a DM5500 microscope (Leica). A human lymph node sample was used to verify the staining.

### 1.6.2 Animal Eyes

To fix the rat eyes, Tissue Tec OCT (Paesel and Lorey) was used, and they were then rapidly frozen in methyl butane (Merck) at -70°C. After that, air-dried cryosections with a thickness of 8  $\mu$ m were prepared using a CryoStat Microm HM560 Microtome from Thermo Scientific. These sections were first placed in ice-cold acetone and left to dry, after which they were incubated overnight at 4°C in a humid chamber with rabbit anti-rat FoxP3 antibody (Novus Biologicals) diluted to 1:100 in PBS/3% donkey serum. The cryosections were then washed and treated with Cy3-conjugated affinipure donkey anti-rabbit IgG(H + L) as a secondary antibody (Jackson Laboratories). They were consequently incubated for 1 h at RT in the dark and then washed again. The sections were mounted with Vectashield HardSet with DAPI H-1500 (Biozol). Photos were captured using an Axio Observer 7 with ApoTome (Zeiss).

## 1.7 Cell culture

Inducible stem cells (iPS-RPE) obtained from an iPS cell line (CRTDi004-A) were used to differentiate human RPE cells. These cells were grown on filter inserts until they reached a transepithelial resistance of 600  $\Omega$ cm<sup>2</sup>

and were then kept in mTeSR™ plus medium (Stemcell Technologies) at 37°C and 5% CO<sub>2</sub>. ARPE-19 cells were grown separately in DMEM/F12 (Thermo Fisher) supplemented with Glutamax, 10% FCS, and 50 U penicillin/50 mg streptomycin at 37°C and 5% CO<sub>2</sub>. Cells were grown to reach two densities: confluent (single layer) and non-confluent (50–70% confluency). The medium was replaced with serum-free medium for 24 h before the experiments. Moreover, we conducted parallel experiments with no medium exchange. IL-1β 100 ng/ml (Sigma Aldrich/Merck) was applied to cells at 6 min, 1 h, or 2 h, respectively, at 37 °C and 5% CO<sub>2</sub>, supernatants were collected, and cells were harvested. Confluent and non-confluent cultures reached a density of 30.000 and 20.000 cells/cm<sup>2</sup>, respectively.

### 1.8 Generation and characterization of APRE-19 KO cells

The CRISPR-Cas9 experiments were conducted as per published protocols [44–46]; CXCR4 and FoxP3 sequences are described in the publication. Thereafter, cells were cultured and monitored at 1,3,6 day in order to edit efficiencies, and the numbers of viable cells/proliferation rates were compared to electroporated with Cas9 RNPs without targeting control. Cas9 RNPs can remain in the cells for 3 days; therefore, we continued monitoring them [47]. Analysis was conducted using the TIDE web tool [48].

### 1.9 Calcium imaging

To perform calcium imaging on ARPE-19 cells, 15mm glass coverslips were used with a cell density of  $8.5 \times 10^3$  cells/cm<sup>2</sup>, following an overnight serum-free incubation as previously described [26]. The coverslips were loaded with fura-2/AM (2 μM, Invitrogen) for 40 minutes, and then placed in a custom-made recording chamber with the addition of IL-1β (100 ng/mL) and various agonists/blockers such as (R)-(+)-BayK 8644 (10 μM, Tocris), Thapsigargin (1 μM, Acros), Ruthenium Red (1 μM, Alomone), Dantrolene (1 μM), and LY294002 (50 μM; Cayman Chemical Tallinn) mentioned in the publication. The fluorescence ratio imaging system was utilized to capture and analyze the images using the MetaFluor software, with excitation wavelengths of 340/380 nm and an emission wavelength of 505 nm. Changes in intracellular free Ca<sup>2+</sup> were measured as changes in the ratios of the fluorescence of the two excitation wavelengths (dF/F) to the baseline (ddF/F). The Zeiss Axiovert 40 CFL inverted microscope, Visichrome High-Speed Polychromator System, and CoolSNAP EZ CCD camera were used for imaging.

### 1.10 Immunofluorescence staining of ARPE-19 cells after stimulation with IL-1β

Cells were cultured on 15-mm coverslips to either reach confluence or remain non-confluent, and then fixed in 4% PFA for 10 minutes or treated with ice-cold methanol for 15 minutes. To permeabilize the cells, they were exposed to 5% Triton X-100 in TBS for 10 minutes. Alternatively, cells were blocked in 5% BSA in TBS for 30 minutes before being incubated overnight at 4°C with the primary antibody (rabbit polyclonal FoxP3, Novus Biologicals). After incubation with an appropriate secondary antibody conjugated with AF647 or Cy3 for 1 hour at room temperature, nuclei were counterstained with DAPI (Sigma). The coverslips were then mounted using fluorescent mounting Medium (DAKO) or Entellan (Merck) and visualized using various microscopy techniques, such as an LSM 510 confocal laser-scanning microscope (Zeiss) and ZEN software 3.1 Blue Edition (Zeiss), a Zeiss Axioskop 2plus and Axio Observer 7 with ApoTome (Zeiss), or a Zeiss Axioskop 2plus (Carl Zeiss). Images were captured using a Sony CyberShot DSC-S70 3.3 mp digital camera (Carl Zeiss). The integrated density of pixels within the nucleus was measured using ImageJ software [49].

### 1.11 Dot blotting

ARPE-19 cells were cultured on Transwell plates for four weeks at either confluent or subconfluent density, with a medium change to serum-free one night before the experiment. After incubation with IL-1 $\beta$  (100 ng/ml, Sigma Aldrich) or PBS for one hour, the cells were washed with ice-cold PBS and then collected in a sucrose isolation buffer. Following homogenization, the cytosol and nuclear fraction were separated by centrifugation at 700g for 5 min and collected into a predefined solution as per the protocol to perform dot blotting. [26]. In brief, 1.5  $\mu$ g of protein was loaded into each well of 96-well plates (Bio-Dot<sup>®</sup> Microfiltration Apparatus; Bio-Rad Laboratories Inc.) and then vacuum transferred onto nitrocellulose membranes. The membranes were then incubated with primary antibodies against Phospho-FoxP3 (Ser 418, Abgent Biotech) or FoxP3 (Cell Signaling Technologies) overnight. Normalization was achieved using antibodies against GAPDH for the cytoplasm (Cell Signaling Technologies) and histone H3 for the nuclear fraction (Cell Signaling Technologies). Horseradish peroxidase-conjugated secondary antibodies (Santa Cruz Biotechnology) were then applied, followed by detection using Clarity<sup>™</sup> Western ECL Blotting Substrate (Bio-Rad Laboratories, Inc.) and chemiluminescent imaging. The protein dots were quantified using ImageJ software. [49].

### 1.12 RNA isolation, cDNA synthesis, and RT-PCR

RNA isolation, cDNA synthesis, and RT-PCR were conducted on ARPE-19 cells and murine samples. Murine Retinae and RPE were collected and stored in liquid N<sub>2</sub>. The resulting choroid and RPE cells were mixed with Qiazol Lysis Reagent (Qiagen) and Precellys ceramic beads (PepLab Biotechnology). RNeasy Mini Kit (Qiagen) was used to separate the RNA. A high-Capacity cDNA Reverse Transcription Kit (Applied Biosystems) was applied to prepare for RT-qPCR using TaqMan Fast Universal PCR Master Mix (Thermo Fisher Scientific) on the QuantStudio 3 Real-Time PCR System (Applied Biosystems). Primer and probes were purchased (Thermo Fisher) or designed using Primer Express 3.0 and synthesized (BioTez). The target mRNA expression was quantitatively analyzed with the standard curve method. All expression values were normalized to the housekeeping gene 18S rRNA.

### 1.13 Cytokine/chemokine secretion

We collected supernatants from confluent and subconfluent ARPE-19 cell cultures without exchange of medium (DMEM with 5% FCS and stable glutamine) for two weeks. We applied a scratch using a pipet 24 h before the experiment to induce mechanical stress. We measured secretion in supernatants after treatment with 100 ng recombinant human IL-1 $\beta$ /ml medium (OriGene) after 6 min, 1 h, and 2 h of incubation with IL-1 $\beta$ . Cells were collected and directly frozen at -80 °C. The supernatants were thawed and examined by human Bio-Plex beads (Bio-Rad Laboratories Inc.) for the presence of IL-1 $\alpha$  IL-1 $\beta$ , IL-1ra, IL-6, IL-8/CXCL8, IL-10, IL-12 (p70 and p40), IL-13, IL-17, IFN- $\gamma$ , MCP-1/CCL2, MCP-3/CCL7, PDGF, and VEGF. We have presented ARPE-19-specific analytes. The median values of fluorescence of bioplex analysis for a minimum of 50 samples were calculated per analyte and sample.

### 1.14 Data analysis

The mean values  $\pm$  SEM are presented for all data. The Mann–Whitney U test was used to determine statistical significance for Ca<sup>2+</sup>-Imaging and protein secretion analyses, while the Student's t-test was used for immunocytochemistry, western blot, and gene expression analyses. The p values were denoted as \*p < 0.05,



\*\*p < 0.01, and \*\*\*p < 0.001. GraphPad Prism (Version 9.3.1), Sigma Plot 14.0 (Systat), R version 4.0, and Excel 2016 were used for calculations.

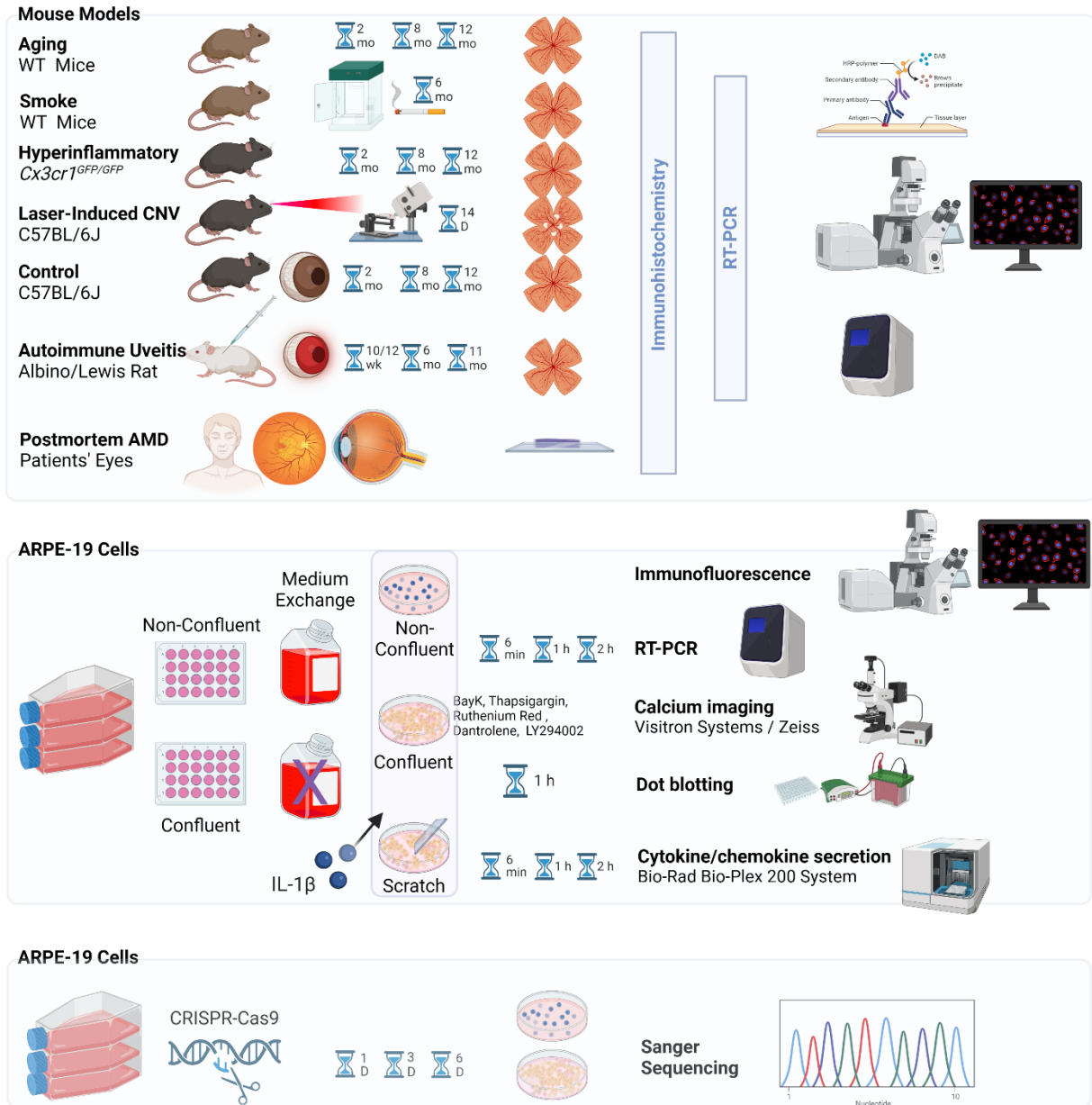


Figure 4 Summary of Experiments

### 3. Results

#### Mouse models:

##### Dry AMD:

**Cx3cr1<sup>GFP/GFP</sup> mouse** (hyperinflammatory model) lacks the fractalkine receptor Cx3cr1 resulting in hyperinflammation phenotype with retinal changes like in AMD in aged mice [50]. Thus, we examined the expression of FoxP3 in both *Cx3cr1<sup>GFP/GFP</sup>* mice and their wild-type littermates. The 2-month-old WT mice showed a regular pattern of RPE cells and an absence of FoxP3 expression. At the age of 8 months, we found a patchy FoxP3 expression with a FoxP3 localization exclusively in the cytosol. In the 8-month-old *Cx3cr1<sup>GFP/GFP</sup>* mice, RPE cells showed a regular cell border pattern, with more homogenous FoxP3 expression appearing mainly in the nucleus. In the 12-month *Cx3cr1<sup>GFP/GFP</sup>* mice, RPE cells were enlarged and irregular with up to three nuclei, with an intense, homogeneous, and exclusively nuclear FoxP3 localization. The 12-month WT had signs of RPE degeneration, mainly the multi-nuclei. FoxP3 expression in WT was stable after 8 months but showed a shift in the localization into the nucleus at the age of 12<sup>th</sup> months. The localization of FoxP3 to the nucleus was confirmed in 12-month-old *Cx3cr1<sup>GFP/GFP</sup>/WT* retinas using a combined DAPI/FoxP3 staining [40].

**FoxP3 in albino (Lewis, Autoimmune Uveitis model) rats and aging mice** showed an already established FoxP3 expression in the cytosol at the 10<sup>th</sup> week, probably due to early stress caused by lack of pigment and light exposure. In comparison, **aging mice** retinae showed increasing FoxP3 to the 11<sup>th</sup> month, where its level was similar to that of the autoimmune uveitis model. Moreover, cells with increased FoxP3 were found in the choroidal vessels (representing Treg cells), with similar cells with more nuclear FoxP3 invading the outer segment of the photoreceptor layer with high expression of FoxP3 in the RPE [51, 52]. The FoxP3 expression in RPE cells was found unchanged between 10 weeks and 6 months and significantly increased from 6 months to 11 months ( $p < 0.0001$ ).

##### Wet AMD:

The **laser-induced CNV mouse** model had features of the wet type of AMD: growth of choroidal blood vessels into the retina after a break (laser spot) in the RPE. In addition, the laser impact provoked a more robust regional inflammatory response than the *Cx3cr1<sup>GFP/GFP</sup>* model. Retinal flatmounts of the laser-induced CNV showed outlining FoxP3-positive RPE cells and peripherally to the laser spot. Surrounding the laser spot, RPE was homogeneously FoxP3-positive and localized to the nuclei, similar to the *Cx3cr1<sup>GFP/GFP</sup>* mouse, along with disturbed structure as described before [53].

The constant exposure of WT mice to **cigarette smoke** was correlated with FoxP3 expression in RPE. Previous experiments indicated changes in signature gene expression and mitochondrial alterations representing oxidative injury [54]. In our experiment, the dot-blots analysis of FoxP3 in the RPE of the passive smoker mouse showed eight folds the expression of that compared to room air-preserved animals.

The increased expression and localization to the nucleus of the transcription factor FoxP3 that correlated with increasing grades of inflammation suggested upregulation of pro-inflammatory cytokine genes. We conducted **mRNA expression of FoxP3, IL-1 $\beta$ , MCP-1, and Cxcl1** (corresponding to human IL-8 in mice [55]) at the same 8- and 12-month milestones in RPE/choroid of WT and *Cx3cr1<sup>GFP/GFP</sup>* mice. In 12-month-old *Cx3cr1<sup>GFP/GFP</sup>* mice, mRNA expression levels of FoxP3, IL-1 $\beta$ , MCP-1, and CXCL1 were significantly higher

compared to WT mice. A comparison of the 8<sup>th</sup> to 12<sup>th</sup> month showed that IL-1 $\beta$ , MCP-1, and CXCL1 were stable in WT mice but had significantly increased in *Cx3cr1<sup>GFP/GFP</sup>* mice.

### Human Eyes

Exploiting the findings of increased Foxp3 expression and its nuclear localization combined with increased expression of pro-inflammatory cytokines in the mouse model of subretinal inflammation as a mode of dry AMD, we examined the expression of FoxP3 in the donor health human retinae and those from dry AMD patients. The sections showed no expression of FoxP3 utilizing **immunohistochemistry** in age-matched control retinae but an expression of it in the AMD patients' retinae, especially in areas of RPE atrophy and also in intact regions distant from the damage.

### Cultured Cells

Human RPE cells differentiated from induced pluripotent stem cells (iPS-RPE) from healthy donors and cells from the ARPE-19 cell line were utilized in our study. The ARPE-19 cell line has previously been employed as a model to investigate AMD-like conditions. Previous studies have demonstrated that anaphylatoxins C3a and C5a affect FoxP3 phosphorylation [26]. In the group of experiments described below, we investigated the sub-confluent RPE status as a stress condition [56, 57], representing unstable cells in contrast to confluent cells.

We deleted the FOXP3 gene from ARPE-19 cells using CRISPR/Cas9 editing and compared these cells to those with deleted CXCR4 receptor gene as per protocol [45]. It showed no difference between non-targeting the cell cultures of FOXP3 KO and CXCR4 KO edited cells and no affection of the proliferation rates compared to non-treated cells. The percentage of FOXP3 KO cells or CXCR4 KO cells inside both treated groups was comparable. However, in the following days, the percentage of CXCR4 KO cells increased and remained stable until the sixth day. In the cultures of FOXP3 KO editing, however, the percentage of edited cells did not significantly change. Given the comparable proliferation rates in the two edited cell cultures, we concluded that the FOXP3 KO cells would show a reduced survival rate under the stress condition of genome editing.

Chronic inhabitation of the monocytes might cause the shift of the RPE immunogenic phenotype through secreting monokines, e.g., IL-1 $\beta$ , supported by AMD models [20, 58, 59]. Therefore, we designed experiments to test the effect of IL-1 $\beta$  on ARPE-19 on FoxP3 expression and localization together with the secretory function of the cells in confluent and non-confluent growth status, representing stable and non-stable and non-stable statuses.

I combined the evaluation of response to IL-1 $\beta$  (100 ng/ml) using immunofluorescence of confluent and non-confluent ARPE-19 cells in order to examine the mobilization of FoxP3 detected using FoxP3 immunolabeling. Before the application in both non-confluent and confluent cells, we detected an expression of FoxP3. However, in the sub-confluent cell culture, FoxP3 appeared mainly in the nuclei, whereas in the confluent cell culture, FoxP3 appeared mainly in the cytosol. In response to exposure to IL-1 $\beta$ , nuclear FoxP3 localization did not change in non-confluent cells, but in confluent cells, nuclear FoxP3 localization increased rapidly, with a peak after 1 hour and a full recovery of the control situation after two hours. In parallel, Ca<sup>2+</sup> imaging showed that non-confluent cells could respond to IL-1 $\beta$  stimulation with an increase of intracellular free Ca<sup>2+</sup>, indicating that the sub-confluent cells were generally able to react to IL-1 $\beta$  and therefore show IL-1 $\beta$  receptor expression. Thus, the FoxP3 localization determining pathways were fully active in the sub-confluent cells

because of IL-1 $\beta$  receptor stimulation, while few confluent cells showed a measured response. Confluent cells did not or very rarely respond with a Ca<sup>2+</sup> increase to IL-1 $\beta$  stimulation. The FoxP3 expression in both cell culture conditions, confluent and subconfluent, indicated that these cells represented an already stressed situation. The IL-1 $\beta$  reactions showed that the sub-confluent cells represented an even higher stressed condition. We investigated the role of cell culture stress on FoxP3 localization by maintaining the cells for 14 days without changing the medium. With this maneuver, we were even able to increase the amount of FoxP3 protein in the nucleus of sub-confluent cells.

To substantiate the IL-1 $\beta$  response in sub-confluent cells, being a specific endogenous pathway in these cells, and to generate a deeper description of the signaling pathway, I analyzed the Ca<sup>2+</sup> transporting mechanisms contributing to IL-1 $\beta$  induced Ca<sup>2+</sup> signal. For that task, I examined the effect of different ion channels and Ca<sup>2+</sup> store blockers on the response to IL-1 $\beta$ . IL-1 $\beta$  had evoked an intracellular increase of Ca<sup>2+</sup> that was affected by BayK8644 (L-type Ca<sup>2+</sup> channel blocker), thapsigargin (the sarcoplasmic Ca<sup>2+</sup>-ATPase (SERCA) blocker), and/or dantrolene (ryanodine receptor blocker). These blockers reduced the peak and the kinetic (time-to-peak) of the IL-1 $\beta$  evoked Ca<sup>2+</sup> signal. Furthermore, the blockers did not change the sustained phases of the signal. Thus, the rise of the IL-1 $\beta$  evoked Ca<sup>2+</sup> signal depended on the release of Ca<sup>2+</sup> from intracellular Ca<sup>2+</sup> stores and the subsequent activation of ryanodine receptors that, in turn, activated L-type Ca<sup>2+</sup> channels. The often in IL-1 $\beta$  signaling cascades participating PI3-Kinase was not involved as indicated by the effect of LY294002 (PI3-kinase blocker).

Besides localization, the phosphorylation of cytosolic and nuclear FoxP3 represents a marker of its activity [26]. Accordingly, we measured the phosphorylation of FoxP3 (P-FoxP3) in both confluent and non-confluent cells in response to IL-1 $\beta$  exposure using dot blot densitometry analysis. IL-1 $\beta$  led in confluent RPE to an increase in the P-FoxP3 by 200%, slightly higher than that of FoxP3. The sub-confluent cells showed no changes in the nuclear P-FoxP3 but showed a slight increase of FoxP3 by 30%. Cytosolic P-FoxP3 and FoxP3 remained unchanged by IL-1 $\beta$  stimulation. Thus, under the stress conditions, sub-confluent and confluent, the P-FoxP3 appeared to be differentially regulated in contrast to the total FoxP3 content in the nucleus.

In order to correlate the activation of the transcription factor FoxP3 with RPE cell function, we analyzed the secretory activity under stimulation by IL-1 $\beta$ , an activator of FoxP3. We conducted a secretome analysis with targets that were used in our animal models: IL-6, IL-8, and MCP1. Both confluent and non-confluent ARPE-19 cells reacted with an increase in IL-8 and IL-6 secretion in response to IL-1 $\beta$  stimulation. However, the reaction was much faster in the confluent cells, then reached equal states at 2h. Non-confluent cells only showed increased secretion of MCP-1. The profiles of secreted factors were different between confluent and non-confluent cells. Where non-confluent cells promptly reacted with a substantial increase in MCP1 secretion, the confluent cells showed mainly a substantial increase in IL-8 and IL-6, for which these cells required more time. The reaction was more pro-inflammatory in non-confluent cells, with strong increases in MCP1 and IL-6 secretion and a mild increase in IL-8 secretion. In contrast, confluent cells showed a weak change in the MCP1 secretion by only 30% but robust increases in IL-8 and IL-6 secretion. Here, IL-8 secretion indicates a reaction for cell protection.

We not only observed changes in FoxP3 localization and secretion profiles induced by IL-1 $\beta$ , but also found that tissue damage served as a stimulus for FoxP3 translocation from cytoplasm to nucleus. When we created a scratch through the confluent monolayer of ARPE-19 cells, we noticed that FoxP3 translocated into the nucleus of the injured culture 24 hours later, accompanied by an altered secretion profile induced by IL-1 $\beta$ .

Interestingly, we found an increase in IL-8 and VEGF-A levels, while MCP1 and IL-6 remained unchanged. This secretion profile appeared to promote the reduction of cell stress and proliferation.

## 4. Discussion

Our current results showed that FoxP3 was upregulated in the aging retina and in situations of RPE degeneration and inflammation in both human and murine models [40]. This indicated a vital role in age-dependent retinal diseases that are characterized by chronic low-grade inflammation.

The current model of FoxP3's impact on the pathology, as evident in animal models and in *in vitro* studies, is believed to be a multistep process. In the first step, stressed cells start to express FoxP3, which is mostly localized in the cytosol. In the following steps, activation of FoxP3 occurs via translocation into the nucleus, including phosphorylation. In inflammations, the translocation into the nucleus is only transient, whereas, in degenerative situations, cells show a permanent nuclear FoxP3 localization. In the nucleus, FoxP3 changes the gene expression and, subsequently, the secretory activity of the RPE in a way that fosters local inflammation. Thus, FoxP3 is believed to be a master regulator of the immunogenic phenotype of RPE cells in chronic low-grade inflammation with degenerative tissue damage. The following data from this study support this model.

Upon exposure to different stress conditions, including oxidative stress, cytokine IL-1 $\beta$ , and the loss of structural integrity (e.g., by reduced density or scratch injury), FoxP3 shows different activation statuses in the RPE. This indicates an active gene expression transcription regulation role in such situations. The expression of FoxP3 itself seemed to be mandatory for the ARPE19 cells to survive the culture conditions, as these cells showed permanent FoxP3 expression. We believe that such cultured cells did not reach enough maturity (which normally takes months in cultures [56]), but it is under a stress state similar to mouse retinae, setting FoxP3 to low-grade activation for their active search of integrity (or for there not reached integrity). Therefore, the FoxP3 was crucial for those cells undergoing growth and could not grow after the editing with CRISPR/Cas9. The FoxP3 gene is X-linked, and knocking it from a male-originating ARPE19 resulted in the efficient deletion of the gene, indicating that the resulting phenotype of stunted growth was due to the role of FoxP3 in the cells. In human AMD-free retinae or young mice up to the age of 6 months, the RP showed no FoxP3 expression. In aging mice or in a mouse model with features of RPE loss under chronic low-grade inflammation with age, RPE cells showed *de novo* expression of FoxP3 in early stages of tissue alteration; here, however, with a prominent localization in the cytosol. In a similar pattern, we assume that its activation in RPE age-related alterations, inflammation, or damage is a cellular tactic to initiate repair. There were similar results when localization and variation of the FoxP3 expression were reviewed in relation to cell confluency. Most stressed cells (non-confluent) in culture and diseased ones showed primarily nuclear expression, while less stressed cells (confluent) and those not affected by direct injury (laser, scratch, degeneration) showed mainly cytoplasmic expression. The cytosolic localized FoxP3 represented a pool of activatable transcription factors. Stimulation of confluent ARPE-19 cells with cytosolic localized FoxP3 by IL-1 $\beta$  led to a short and transient shift of FoxP3 into the nucleus for an hour before returning to its prior status. Along with the difference in response to IL-1 $\beta$ , we assume it is the leading cause of such differences. In RPE degeneration, subconfluent ARPE-19 cells, or in the situation of a breakdown of the blood/retina barrier in uveitis, FoxP3 is permanently localized to the nucleus.

*In vivo* analysis confirmed the role of FoxP3 in the change of the immunogenic phenotype of RPE. The Cx3cr1<sup>GFP/GPF</sup> showed a with age increasing expression and shift into the nucleus after the eighth month, along with a parallel upregulation of the gene expression profiles of IL-1 $\beta$ , MCP-1 (the monocyte attracting

factor), and CXCL1 (the mouse homolog for IL8 rescue factor). Albino rats showed a FoxP3 expression at younger ages that were already prominent at 12 weeks. Similar FoxP3 expression was seen in the uveitis model and laser-induced CNV model. FoxP3 expression was present in the laser scar as well as in the peripheral retina, representing the central immune reaction and cell stress in the periphery. Retinae exposed to cigarette smoke, and human retinae showed FoxP3 expression in both normally looking areas and in areas with RPE atrophy.

*In vivo* studies permitted deeper insights into cellular mechanisms underlying the observations. To study the different *in vivo* situations *in vitro*, we compared non-confluent (CNV and RPE loss in Cx3c1R mice) with confluent ARPE-19 cells; both conditions under the influence of IL-1 $\beta$ , a cytokine that is known to be secreted by invading monocytes. RPE cells reacted to IL-1 $\beta$  by changing their secretory profiles, releasing IL-6 and IL-8 in both confluent and non-confluent cells as well as MCP-1 in non-confluent cells.

The parallel study of the underlying intracellular Ca<sup>2+</sup> change as a second messenger in addition to phosphorylation and mobilization revealed a minimal increase of Ca<sup>2+</sup> in the confluent cells (coinciding with FoxP3 mobilization to the nucleus, which had maximum phosphorylation, but a smaller total amount than in non-confluent-cells). Moreover, intracellular Ca<sup>2+</sup> showed a prevalent increase in the non-confluent cells (which initially had high nuclear FoxP3 that could not be further increased but showed a relatively high increase in its phosphorylation). This release was mediated by coupling ryanodine receptor stimulation with the activation of L-type Ca<sup>2+</sup> channels with release from cytosolic Ca<sup>2+</sup> stores [60].

The study showed some properties of FoxP3 activity regulation. In an earlier study, Busch et al. found that FoxP3-mediated changes in gene expression in ARPE-19 cells correlated with a Ca<sup>2+</sup>-dependent increase in FoxP3 phosphorylation. Similarly, T-Reg showed phosphorylation at Ser-418 correlated to its immune-regulatory function [61]. On the other hand, in cells with FoxP3-rich cytosol, the FoxP3-mediated gene expression was based on the mobilization of the FoxP3 to the nucleus. The increase in the phosphorylation in confluent and non-confluent cells upon stimulation with IL-1 $\beta$  supports combining both mechanisms. However, the initial expression and phosphorylation status of FoxP3 was significant already, indicating a reasonable relation between them. IL-1 $\beta$  is a messenger secreted by active macrophages believed to cause AMD by inducing chronic inflammation [20]. As mentioned earlier, RPE uses IL-1 $\beta$ , in association with other cytokines, as a communication method for talking with players of the immune system to orient them about the ocular system structures (educational barrier)[20]. However, the function of IL-1 $\beta$  receptors in RPE cells has not yet been wholly established [62]. We used it in our experiments as one of the stress inducers and possible secretory phenotype provocateurs.

Previous experiments of mice exposed to intermittent oxidative stress, like cigarette smoke, showed no cell death [54] but gene expression and mitochondrial alterations. In our experiments, they showed high FoxP3 levels. Other stress conditions on ARPE-19 cells, e.g., scratching, demonstrated nuclear localization of FoxP3, mimicking the situation in non-confluent cells. Scarcity of nutrients (e.g., by avoiding medium change for 14 days) mainly caused a relative cytosolic FoxP3 increase. Both scenarios indicated the need for FoxP3 under stress conditions in different ways.

We believe that dysregulated innate immune systems in aging mouse *Cx3cr1<sup>GFP/GFP</sup>* model and already aged retinae are good examples of such stress in animals. In these models, we also detected FoxP3 and FoxP3 nuclear mobilization. Laser-induced choroidal neovascularization is another extreme model where the effect of laser-induced necrosis and destruction of the outer BRB can extend to the other eye, dysregulating its

immune privilege [63]. We correlated the changes of FoxP3 with the secretory profile of ARPE-19 cells in a reaction to IL-1 $\beta$  to learn its possible impact on the local immune system. We found that both confluency levels showed increasing levels of IL-6 and IL-8 at different timing with higher levels in confluent levels. The latter can be attributed to its more stable properties. The non-confluent cells showed, in addition, an increased MCP-1 on the more extended observation. Such observation was similar to the response of degenerating RPE cells under the influence of macrophages, which could initiate positive inflammation feedback by employing monocytes. This appears in line with what was described previously about MCP-1-attracted monocytes in the outer retina [64]. The accumulation of monocytes with IL-1 $\beta$  could induce the secretion of Cxcl1 (in human IL-8), which was lower in 8-month *Cx3cr1<sup>GFP/GFP</sup>* than Wildtype, indicating an underlying immune system process governed by a genetic defect. The scratch injury to the ARPE-19 confluent monolayer triggered the secretion of IL-6, IL-8, MCP-1, and VEGF-A mimicking the profile of geographic atrophy *Cx3cr1<sup>GFP/GFP</sup>* mouse model. The secretion of the VEGF-A is known to be provoked by cytokines, but IL-1 $\beta$  could not further increase it. The RPE may use the IL-8 as a self-protection against degeneration. The FoxP3 activation can be an intermediary step [43]. This picture generally resembles a FoxP3 activation and nuclear mobilization AMD-like pro-inflammatory state similar to that induced by monocytes [65]. In combination with the observed multinuclear phenotype and other structural changes of the RPE that were previously described as a self-regeneration and repair mechanisms [66], Additionally, our observation that remote areas away from the injury site in both mouse models and cell culture reacted to the injury, leading us to think about a state of a widespread inflammatory and self-regenerative reaction [42].

Further studies are required to investigate the above-described FoxP3 changes in the partner eye of patients with degenerative changes [63]. Moreover, the effect of different factors, including lifestyle and environmental exposure, on the expression of FoxP3 and immune mediators present in blood and local ocular environment and the time they require to develop a vision-affecting state should be investigated. Such a study may help discover modifiable factors that decrease the degenerative state. Furthermore, increased knowledge about FoxP3 may also help develop feasible diagnostic imaging and laboratory methods for early detection of AMD and improve the modifiable factors that would help delay or prevent reaching a vision-threatening state and/or the development of new vessels. Moreover, further investigations are required to profile the underlying genetic signature of RPE cells in humans and correlate it with different FoxP3 activity behavior and interaction between RPE and immune system members. Likewise, the cellular and secretory profile associated with different subtypes of AMD should be further assessed in the vitreous, aqueous, and tear film. This should provide insights into new predictive and prognostic markers. Targeting FoxP3 could be one of the RPE-reprogramming mechanisms, helping the cells restore their original function by taking care of the outer retinal layer and reforming the choriocapillaris [67]. The newly introduced surgical techniques of implanting healthy RPE cells (or pluripotent stem cells) in AMD patients [68, 69] can foster the research on RPE by both acquiring living samples correlated with actual disease environment and the possibility of introducing different bioengineered RPE cells and personalization of the treatment that withstand the individual risk factors present in each patient.



## 5. Conclusions

In this study, FoxP3 expression appears to have increased and mobilized to the nucleus in a reaction to stress provokers, including oxidative stress, aging factors, inflammation, and trauma or under the effect of IL-1 $\beta$ . Through this stress, FoxP3 appears vital for the RPE cells to withstand this status. The cell-cell contact was an essential modifier to the reactivity where non-confluent cells could represent an immature status of the cells or mimic the degenerative status leading to FoxP3 nuclear mobilization and phosphorylation.

## Reference list

1. Shechter R, London A, Schwartz M (2013) Orchestrated leukocyte recruitment to immune-privileged sites: absolute barriers versus educational gates. *Nat Rev Immunol* 13:206–18. <https://doi.org/10.1038/nri3391>
2. Strauss O (2005) The retinal pigment epithelium in visual function. *Physiol Rev* 85:845–881. <https://doi.org/10.1152/physrev.00021.2004>
3. Streilein JW (2003) Ocular immune privilege: therapeutic opportunities from an experiment of nature. *Nat Rev Immunol* 3:879–89. <https://doi.org/10.1038/nri1224>
4. Leung R (2006) Back of the eye glossary: Age-related macular degeneration (AMD). *Community Eye Heal J* 19:10
5. Wong WL, Su X, Li X, Cheung CMG, Klein R, Cheng C-Y, Wong TY (2014) Global prevalence of age-related macular degeneration and disease burden projection for 2020 and 2040: a systematic review and meta-analysis. *Lancet Glob Heal* 2:e106–e116. [https://doi.org/10.1016/S2214-109X\(13\)70145-1](https://doi.org/10.1016/S2214-109X(13)70145-1)
6. Rastogi N, Smith RT (2016) Association of age-related macular degeneration and reticular macular disease with cardiovascular disease. *Surv Ophthalmol* 61:422–433. <https://doi.org/10.1016/j.survophthal.2015.10.003>
7. Chakravarthy U, Wong TY, Fletcher A, Piau E, Evans C, Zlateva G, Buggage R, Pleil A, Mitchell P (2010) Clinical risk factors for age-related macular degeneration: a systematic review and meta-analysis. *BMC Ophthalmol* 10:31. <https://doi.org/10.1186/1471-2415-10-31>
8. Choi JK (2011) Diabetes Mellitus and Early Age-related Macular Degeneration. *Arch Ophthalmol* 129:196. <https://doi.org/10.1001/archophthalmol.2010.355>
9. Velilla S, García-Medina JJ, García-Layana A, Dolz-Marco R, Pons-Vázquez S, Pinazo-Durán MD, Gómez-Ulla F, Arévalo JF, Díaz-Llopis M, Gallego-Pinazo R (2013) Smoking and age-related macular degeneration: review and update. *J Ophthalmol* 2013:895147. <https://doi.org/10.1155/2013/895147>
10. Merle BMJ, Silver RE, Rosner B, Seddon JM (2017) Associations Between Vitamin D Intake and Progression to Incident Advanced Age-Related Macular Degeneration. *Investig Ophthalmology Vis Sci* 58:4569. <https://doi.org/10.1167/iovs.17-21673>
11. Swenor BK, Bressler S, Caulfield L, West SK (2010) The Impact of Fish and Shellfish Consumption on Age-Related Macular Degeneration. *Ophthalmology* 117:2395–2401. <https://doi.org/10.1016/j.ophtha.2010.03.058>
12. Evans JR, Lawrenson JG (2017) Antioxidant vitamin and mineral supplements for preventing age-related macular degeneration. *Cochrane database Syst Rev* 7:CD000253. <https://doi.org/10.1002/14651858.CD000253.pub4>

13. Ferreira A, Silva N, Furtado MJ, Carneiro Â, Lume M, Andrade JP Serum vitamin D and age-related macular degeneration: Systematic review and meta-analysis. *Surv Ophthalmol* 66:183–197. <https://doi.org/10.1016/j.survophthal.2020.07.003>
14. Schmidl D, Garhöfer G, Schmetterer L (2015) Nutritional supplements in age-related macular degeneration. *Acta Ophthalmol* 93:105–21. <https://doi.org/10.1111/aos.12650>
15. “European Molecular Biology Laboratory” (2022) GWAS Catalog: age-related macular degeneration. [https://www.ebi.ac.uk/gwas/efotraits/EFO\\_0001365](https://www.ebi.ac.uk/gwas/efotraits/EFO_0001365)
16. Klein RJ, Zeiss C, Chew EY, Tsai J-Y, Sackler RS, Haynes C, Henning AK, SanGiovanni JP, Mane SM, Mayne ST, Bracken MB, Ferris FL, Ott J, Barnstable C, Hoh J (2005) Complement Factor H Polymorphism in Age-Related Macular Degeneration. *Science* (80- ) 308:385–389. <https://doi.org/10.1126/science.1109557>
17. DeWan A, Bracken MB, Hoh J (2007) Two genetic pathways for age-related macular degeneration. *Curr Opin Genet Dev* 17:228–33. <https://doi.org/10.1016/j.gde.2007.04.004>
18. Micklisch S, Lin Y, Jacob S, Karlstetter M, Dannhausen K, Dasari P, von der Heide M, Dahse H-M, Schmözl L, Grassmann F, Alene M, Fauser S, Neumann H, Lorkowski S, Pauly D, Weber BH, Jousen AM, Langmann T, Zipfel PF, Skerka C (2017) Age-related macular degeneration associated polymorphism rs10490924 in ARMS2 results in deficiency of a complement activator. *J Neuroinflammation* 14:4. <https://doi.org/10.1186/s12974-016-0776-3>
19. (2023) Global Burden of Disease. In: *Inst. Heal. Metrics Eval.* <https://www.healthdata.org/gbd>
20. Mathis T, Housset M, Eandi C, Beguier F, Touhami S, Reichman S, Augustin S, Gondouin P, Sahel J-A, Kodjikian L, Goureau O, Guillonneau X, Sennlaub F (2017) Activated monocytes resist elimination by retinal pigment epithelium and downregulate their OTX2 expression via TNF- $\alpha$ . *Aging Cell* 16:173–182. <https://doi.org/10.1111/accel.12540>
21. Touhami S, Beguier F, Augustin S, Charles-Messance H, Vignaud L, Nandrot EF, Reichman S, Forster V, Mathis T, Sahel J-A, Bodaghi B, Guillonneau X, Sennlaub F (2018) Chronic exposure to tumor necrosis factor alpha induces retinal pigment epithelium cell dedifferentiation. *J Neuroinflammation* 15:85. <https://doi.org/10.1186/s12974-018-1106-8>
22. Zamiri P, Masli S, Streilein JW, Taylor AW (2006) Pigment epithelial growth factor suppresses inflammation by modulating macrophage activation. *Invest Ophthalmol Vis Sci* 47:3912–8. <https://doi.org/10.1167/iovs.05-1267>
23. Brandstetter C, Holz FG, Krohne TU (2015) Complement Component C5a Primes Retinal Pigment Epithelial Cells for Inflammasome Activation by Lipofuscin-mediated Photooxidative Damage. *J Biol Chem* 290:31189–98. <https://doi.org/10.1074/jbc.M115.671180>
24. Anderson OA, Finkelstein A, Shima DT (2013) A2E induces IL-1 $\beta$  production in retinal pigment epithelial cells via the NLRP3 inflammasome. *PLoS One* 8:e67263. <https://doi.org/10.1371/journal.pone.0067263>

25. Trakkides T-O, Schäfer N, Reichenthaler M, Kühn K, Brandwijk RJMGE, Toonen EJM, Urban F, Wegener J, Enzmann V, Pauly D (2019) Oxidative Stress Increases Endogenous Complement-Dependent Inflammatory and Angiogenic Responses in Retinal Pigment Epithelial Cells Independently of Exogenous Complement Sources. *Antioxidants (Basel, Switzerland)* 8:. <https://doi.org/10.3390/antiox8110548>
26. Busch C, Annamalai B, Abdusalamova K, Reichhart N, Huber C, Lin Y, Jo EAH, Zipfel PF, Skerka C, Wildner G, Diedrichs-Möhrling M, Rohrer B, Strauß O (2017) Anaphylatoxins Activate Ca<sup>2+</sup>, Akt/PI3-Kinase, and FOXO1/FoxP3 in the Retinal Pigment Epithelium. *Front Immunol* 8:703. <https://doi.org/10.3389/fimmu.2017.00703>
27. Schäfer N, Grosche A, Schmitt SI, Braunger BM, Pauly D (2017) Complement Components Showed a Time-Dependent Local Expression Pattern in Constant and Acute White Light-Induced Photoreceptor Damage. *Front Mol Neurosci* 10:197. <https://doi.org/10.3389/fnmol.2017.00197>
28. Pauly D, Agarwal D, Dana N, Schäfer N, Biber J, Wunderlich KA, Jabri Y, Straub T, Zhang NR, Gautam AK, Weber BHF, Hauck SM, Kim M, Curcio CA, Stambolian D, Li M, Grosche A (2019) Cell-Type-Specific Complement Expression in the Healthy and Diseased Retina. *Cell Rep* 29:2835-2848.e4. <https://doi.org/10.1016/j.celrep.2019.10.084>
29. Hori S, Nomura T, Sakaguchi S (2003) Control of regulatory T cell development by the transcription factor Foxp3. *Science* 299:1057–61. <https://doi.org/10.1126/science.1079490>
30. Kasprawicz DJ, Smallwood PS, Tyznik AJ, Ziegler SF (2003) Scurfin (FoxP3) controls T-dependent immune responses in vivo through regulation of CD4+ T cell effector function. *J Immunol* 171:1216–23. <https://doi.org/10.4049/jimmunol.171.3.1216>
31. Dong Y, Yang C, Pan F (2021) Post-Translational Regulations of Foxp3 in Treg Cells and Their Therapeutic Applications. *Front Immunol* 12:626172. <https://doi.org/10.3389/fimmu.2021.626172>
32. Georgiev P, Charbonnier L-M, Chatila TA (2019) Regulatory T Cells: the Many Faces of Foxp3. *J Clin Immunol* 39:623–640. <https://doi.org/10.1007/s10875-019-00684-7>
33. Wang J, Ioan-Facsinay A, van der Voort EIH, Huizinga TWJ, Toes REM (2007) Transient expression of FOXP3 in human activated nonregulatory CD4+ T cells. *Eur J Immunol* 37:129–38. <https://doi.org/10.1002/eji.200636435>
34. Wildner G (2019) Are rats more human than mice? *Immunobiology* 224:172–176. <https://doi.org/10.1016/j.imbio.2018.09.002>
35. Magg T, Mannert J, Ellwart JW, Schmid I, Albert MH (2012) Subcellular localization of FOXP3 in human regulatory and nonregulatory T cells. *Eur J Immunol* 42:1627–38. <https://doi.org/10.1002/eji.201141838>
36. Wang L, Liu R, Li W, Chen C, Katoh H, Chen G-Y, McNally B, Lin L, Zhou P, Zuo T, Cooney KA, Liu Y, Zheng P (2009) Somatic single hits inactivate the X-linked tumor suppressor FOXP3 in the prostate. *Cancer Cell* 16:336–46. <https://doi.org/10.1016/j.ccr.2009.08.016>

37. Zhang H-Y, Sun H (2010) Up-regulation of Foxp3 inhibits cell proliferation, migration and invasion in epithelial ovarian cancer. *Cancer Lett* 287:91–7. <https://doi.org/10.1016/j.canlet.2009.06.001>
38. Redpath M, Xu B, van Kempen LC, Spatz A (2011) The dual role of the X-linked FoxP3 gene in human cancers. *Mol Oncol* 5:156–63. <https://doi.org/10.1016/j.molonc.2011.03.001>
39. Tan B, Behren A, Anaka M, Vella L, Cebon J, Mariadason JM, Chen W (2012) FOXP3 is not mutated in human melanoma. *Pigment Cell Melanoma Res* 25:398–400. <https://doi.org/10.1111/j.1755-148X.2012.00993.x>
40. Alfaar AS, Stürzbecher L, Diedrichs-Möhrling M, Lam M, Roubéix C, Ritter J, Schumann K, Annamalai B, Pompös I-M, Rohrer B, Sennlaub F, Reichhart N, Wildner G, Strauß O (2022) FoxP3 expression by retinal pigment epithelial cells: transcription factor with potential relevance for the pathology of age-related macular degeneration. *J Neuroinflammation* 19:260. <https://doi.org/10.1186/s12974-022-02620-w>
41. Combadière C, Feumi C, Raoul W, Keller N, Rodéro M, Pézard A, Lavalette S, Houssier M, Jonet L, Picard E, Debré P, Sirinyan M, Deterre P, Ferroukhi T, Cohen S-Y, Chauvaud D, Jeanny J-C, Chemtob S, Behar-Cohen F, Sennlaub F (2007) CX3CR1-dependent subretinal microglia cell accumulation is associated with cardinal features of age-related macular degeneration. *J Clin Invest* 117:2920–8. <https://doi.org/10.1172/JCI31692>
42. Crespo-Garcia S, Corkhill C, Roubéix C, Davids A-M, Kociok N, Strauss O, Jousen AM, Reichhart N (2017) Inhibition of Placenta Growth Factor Reduces Subretinal Mononuclear Phagocyte Accumulation in Choroidal Neovascularization. *Invest Ophthalmol Vis Sci* 58:4997–5006. <https://doi.org/10.1167/iovs.16-21283>
43. Diedrichs-Möhrling M, Niesik S, Priglinger CS, Thurau SR, Obermayr F, Sperl S, Wildner G (2018) Intraocular DHODH-inhibitor PP-001 suppresses relapsing experimental uveitis and cytokine production of human lymphocytes, but not of RPE cells. *J Neuroinflammation* 15:54. <https://doi.org/10.1186/s12974-018-1088-6>
44. Hultquist JF, Schumann K, Woo JM, Manganaro L, McGregor MJ, Doudna J, Simon V, Krogan NJ, Marson A (2016) A Cas9 Ribonucleoprotein Platform for Functional Genetic Studies of HIV-Host Interactions in Primary Human T Cells. *Cell Rep* 17:1438–1452. <https://doi.org/10.1016/j.celrep.2016.09.080>
45. Schumann K, Raju SS, Lauber M, Kolb S, Shifrut E, Cortez JT, Skartsis N, Nguyen VQ, Woo JM, Roth TL, Yu R, Nguyen MLT, Simeonov DR, Nguyen DN, Targ S, Gate RE, Tang Q, Bluestone JA, Spitzer MH, Ye CJ, Marson A (2020) Functional CRISPR dissection of gene networks controlling human regulatory T cell identity. *Nat Immunol* 21:1456–1466. <https://doi.org/10.1038/s41590-020-0784-4>
46. Lingeman E, Jeans C, Corn JE (2017) Production of Purified CasRNPs for Efficacious Genome Editing. *Curr Protoc Mol Biol* 120:31.10.1-31.10.19. <https://doi.org/10.1002/cpmb.43>

47. Kim H, Kim J-S (2014) A guide to genome engineering with programmable nucleases. *Nat Rev Genet* 15:321–334. <https://doi.org/10.1038/nrg3686>
48. Brinkman EK, Chen T, Amendola M, van Steensel B (2014) Easy quantitative assessment of genome editing by sequence trace decomposition. *Nucleic Acids Res* 42:e168. <https://doi.org/10.1093/nar/gku936>
49. Schneider CA, Rasband WS, Eliceiri KW (2012) NIH Image to ImageJ: 25 years of image analysis. *Nat Methods* 9:671–5. <https://doi.org/10.1038/nmeth.2089>
50. Levy O, Calippe B, Lavalette S, Hu SJ, Raoul W, Dominguez E, Housset M, Paques M, Sahel J, Bemelmans A, Combadiere C, Guillonneau X, Sennlaub F (2015) Apolipoprotein E promotes subretinal mononuclear phagocyte survival and chronic inflammation in age-related macular degeneration. *EMBO Mol Med* 7:211–226. <https://doi.org/10.15252/emmm.201404524>
51. Diedrichs-Möhrling M, Nelson PJ, Proudfoot AEI, Thureau SR, Wildner G (2005) The effect of the CC chemokine receptor antagonist Met-RANTES on experimental autoimmune uveitis and oral tolerance. *J Neuroimmunol* 164:22–30. <https://doi.org/10.1016/j.jneuroim.2005.02.023>
52. Thureau SR (2004) The fate of autoreactive, GFP+ T cells in rat models of uveitis analyzed by intravital fluorescence microscopy and FACS. *Int Immunol* 16:1573–1582. <https://doi.org/10.1093/intimm/dxh158>
53. Obert E, Strauss R, Brandon C, Grek C, Ghatnekar G, Gourdie R, Rohrer B (2017) Targeting the tight junction protein, zonula occludens-1, with the connexin43 mimetic peptide,  $\alpha$ CT1, reduces VEGF-dependent RPE pathophysiology. *J Mol Med* 95:535–552. <https://doi.org/10.1007/s00109-017-1506-8>
54. Woodell A, Coughlin B, Kunchithapautham K, Casey S, Williamson T, Ferrell WD, Atkinson C, Jones BW, Rohrer B (2013) Alternative Complement Pathway Deficiency Ameliorates Chronic Smoke-Induced Functional and Morphological Ocular Injury. *PLoS One* 8:e67894. <https://doi.org/10.1371/journal.pone.0067894>
55. Bozic CR, Gerard NP, von Uexkull-Guldenband C, Kolakowski LF, Conklyn MJ, Breslow R, Showell HJ, Gerard C (1994) The murine interleukin 8 type B receptor homologue and its ligands. Expression and biological characterization. *J Biol Chem* 269:29355–29358. [https://doi.org/10.1016/S0021-9258\(18\)43882-3](https://doi.org/10.1016/S0021-9258(18)43882-3)
56. Tian J, Ishibashi K, Honda S, Boylan SA, Hjelmeland LM, Handa JT (2005) The expression of native and cultured human retinal pigment epithelial cells grown in different culture conditions. *Br J Ophthalmol* 89:1510–7. <https://doi.org/10.1136/bjo.2005.072108>
57. Samuel W, Jaworski C, Postnikova OA, Kutty RK, Duncan T, Tan LX, Poliakov E, Lakkaraju A, Redmond TM (2017) Appropriately differentiated ARPE-19 cells regain phenotype and gene expression profiles similar to those of native RPE cells. *Mol Vis* 23:60–89
58. Chen M, Hombrebueno JR, Luo C, Penalva R, Zhao J, Colhoun L, Pandi SPS, Forrester J V., Xu

- H (2013) Age- and Light-Dependent Development of Localised Retinal Atrophy in CCL2<sup>-/-</sup>CX3CR1GFP/GFP Mice. *PLoS One* 8:e61381.  
<https://doi.org/10.1371/journal.pone.0061381>
59. Klettner A, Brinkmann A, Winkelmann K, Käckenmeister T, Hildebrandt J, Roider J (2020) Effect of long-term inflammation on viability and function of RPE cells. *Exp Eye Res* 200:108214.  
<https://doi.org/10.1016/j.exer.2020.108214>
60. Beskina O, Miller A, Mazzocco-Spezia A, Pulina M V, Golovina VA (2007) Mechanisms of interleukin-1 $\beta$ -induced Ca<sup>2+</sup> signals in mouse cortical astrocytes: roles of store- and receptor-operated Ca<sup>2+</sup> entry. *Am J Physiol Cell Physiol* 293:C1103-11.  
<https://doi.org/10.1152/ajpcell.00249.2007>
61. Deng G, Song X, Fujimoto S, Piccirillo CA, Nagai Y, Greene MI (2019) Foxp3 Post-translational Modifications and Treg Suppressive Activity. *Front Immunol* 10:2486.  
<https://doi.org/10.3389/fimmu.2019.02486>
62. Lavalette S, Raoul W, Houssier M, Camelo S, Levy O, Calippe B, Jonet L, Behar-Cohen F, Chemtob S, Guillonneau X, Combadière C, Sennlaub F (2011) Interleukin-1 $\beta$  inhibition prevents choroidal neovascularization and does not exacerbate photoreceptor degeneration. *Am J Pathol* 178:2416–23. <https://doi.org/10.1016/j.ajpath.2011.01.013>
63. Lucas K, Karamichos D, Mathew R, Zieske JD, Stein-Streilein J (2012) Retinal laser burn-induced neuropathy leads to substance P-dependent loss of ocular immune privilege. *J Immunol* 189:1237–42. <https://doi.org/10.4049/jimmunol.1103264>
64. Sennlaub F, Auvynet C, Calippe B, Lavalette S, Poupel L, Hu SJ, Dominguez E, Camelo S, Levy O, Guyon E, Saederup N, Charo IF, Rooijen N Van, Nandrot E, Bourges J-L, Behar-Cohen F, Sahel J-A, Guillonneau X, Raoul W, Combadiere C (2013) CCR2(+) monocytes infiltrate atrophic lesions in age-related macular disease and mediate photoreceptor degeneration in experimental subretinal inflammation in Cx3cr1 deficient mice. *EMBO Mol Med* 5:1775–93.  
<https://doi.org/10.1002/emmm.201302692>
65. Dietrich L, Lucius R, Roider J, Klettner A (2020) Interaction of inflammatorily activated retinal pigment epithelium with retinal microglia and neuronal cells. *Exp Eye Res* 199:108167.  
<https://doi.org/10.1016/j.exer.2020.108167>
66. Chen M, Rajapakse D, Fraczek M, Luo C, Forrester J V., Xu H (2016) Retinal pigment epithelial cell multinucleation in the aging eye - a mechanism to repair damage and maintain homeostasis. *Aging Cell* 15:436–445. <https://doi.org/10.1111/accel.12447>
67. Colamatteo A, Carbone F, Bruzzaniti S, Galgani M, Fusco C, Maniscalco GT, Di Rella F, de Candia P, De Rosa V (2020) Molecular Mechanisms Controlling Foxp3 Expression in Health and Autoimmunity: From Epigenetic to Post-translational Regulation. *Front Immunol* 10:.  
<https://doi.org/10.3389/fimmu.2019.03136>

68. Kashani AH, Uang J, Mert M, Rahhal F, Chan C, Avery RL, Dugel P, Chen S, Lebkowski J, Clegg DO, Hinton DR, Humayun MS (2020) Surgical Method for Implantation of a Biosynthetic Retinal Pigment Epithelium Monolayer for Geographic Atrophy: Experience from a Phase 1/2a Study. *Ophthalmol Retin* 4:264–273. <https://doi.org/10.1016/j.oret.2019.09.017>
69. da Cruz L, Fynes K, Georgiadis O, Kerby J, Luo YH, Ahmado A, Vernon A, Daniels JT, Nommiste B, Hasan SM, Gooljar SB, Carr A-JF, Vugler A, Ramsden CM, Bictash M, Fenster M, Steer J, Harbinson T, Wilbrey A, Tufail A, Feng G, Whitlock M, Robson AG, Holder GE, Sagoo MS, Loudon PT, Whiting P, Coffey PJ (2018) Phase 1 clinical study of an embryonic stem cell-derived retinal pigment epithelium patch in age-related macular degeneration. *Nat Biotechnol* 36:328–337. <https://doi.org/10.1038/nbt.4114>



# Statutory Declaration

"I, Ahmed Alfaar, by personally signing this document in lieu of an oath, hereby affirm that I prepared the submitted dissertation on the topic (Die Rolle von FoxP3 bei der altersbedingten Makuladegeneration.) - (The role of FoxP3 in Age-related macular degeneration.), independently and without the support of third parties, and that I used no other sources and aids than those stated.

All parts which are based on the publications or presentations of other authors, either in letter or in spirit, are specified as such in accordance with the citing guidelines. The sections on methodology (in particular regarding practical work, laboratory regulations, statistical processing) and results (in particular regarding figures, charts and tables) are exclusively my responsibility.

Furthermore, I declare that I have correctly marked all of the data, the analyses, and the conclusions generated from data obtained in collaboration with other persons, and that I have correctly marked my own contribution and the contributions of other persons (cf. declaration of contribution). I have correctly marked all texts or parts of texts that were generated in collaboration with other persons.

My contributions to any publications to this dissertation correspond to those stated in the below joint declaration made together with the supervisor. All publications created within the scope of the dissertation comply with the guidelines of the ICMJE (International Committee of Medical Journal Editors; <http://www.icmje.org>) on authorship. In addition, I declare that I shall comply with the regulations of Charité – Universitätsmedizin Berlin on ensuring good scientific practice.

I declare that I have not yet submitted this dissertation in identical or similar form to another Faculty.

The significance of this statutory declaration and the consequences of a false statutory declaration under criminal law (Sections 156, 161 of the German Criminal Code) are known to me."

Date

Signature

09.06.2023

# Declaration of your own contribution to the publications

**Ahmed Samir Alfaar** contributed the following to the below listed publications:

**Alfaar AS\***, Stürzbecher L, Diedrichs-Möhring M, Lam M, Roubeix C, Ritter J, Schumann K, Annamalai B, Pompös I-M, Rohrer B, Sennlaub F, Reichhart N, Wildner G, Strauß O (2022) FoxP3 expression by retinal pigment epithelial cells: transcription factor with potential relevance for the pathology of age-related macular degeneration. *J Neuroinflammation* 19:260. <https://doi.org/10.1186/s12974-022-02620-w>.

## Planning and design of the experiments:

- Co-development of the research question (together with the supervisor).
- Planning the animal experiments (not carried out due to a lack of license).

## Performance of the experiments:

- Conducting the "founder experiment," which provided the proof-of-principle for the justification of all other experiments; without it, this paper would not have been possible.
- Methodological implementation: cell culture, in vitro data including calcium imaging, conducting/analyzing histological data after animal experiments.
- Full-time data collection/analysis (Figures 1A-D; 4A-D; 6 completely; 7 completely).
- Our research group does not have the expertise for the other data (smoker data, Crisp/Cas9, secretion analysis, uveitis, scratch assay), or access to the material (human retinas).
- Critical interpretation was done in conjunction with the collaboration partners.

## Writing and editing the publication:

- Contribution to the initial draft of the manuscript (methods and results as a subject-specific interpretation were contributed by the collaboration partners; the first full version was created by the supervisor from all the contributions received).
- Revision during the "maturation" of the manuscript.

**Further related publications that I published on the topic during the Ph.D. period:**

1. Cordes M, Bucichowski P, Alfaar AS, Tsang SH, Almedawar S, Reichhart N, Strauß O (2020) Inhibition of Ca<sup>2+</sup> channel surface expression by mutant bestrophin-1 in RPE cells. *FASEB J* 34:4055–4071.

doi:10.1096/fj.201901202RR iF(2021): 5.834 iF(2020): 5.192 iF(2019):4.966 (Q1)

1. Reichhart N, Schöberl S, Keckeis S, Alfaar AS, Roubex C, Cordes M, Crespo-Garcia S, Haeckel A, Kociok N, Föckler R, Fels G, Mataruga A, Rauh R, Milenkovic VM, Zühlke K, Klusmann E, Schellenberger E, Strauß O (2019) Anoctamin-4 is a bona fide Ca<sup>2+</sup>-dependent non-selective cation channel. *Sci Rep* 9:2257.

doi: 10.1038/s41598-018-37287-y iF(2021): 4.122 iF(2019): 3.998 iF(2018): 4.011 (Q2)

## Excerpt from Journal Summary List

Journal Data Filtered By: **Selected JCR Year: 2020** Selected Editions: SCIE,SSCI  
 Selected Categories: **"NEUROSCIENCES"** Selected Category Scheme: WoS  
**Gesamtanzahl: 273 Journale**

Rank	Full Journal Title	Total Cites	Journal Impact Factor	Eigenfactor Score
1	NATURE REVIEWS NEUROSCIENCE	49,897	34.870	0.048890
2	NATURE NEUROSCIENCE	73,709	24.884	0.128020
3	TRENDS IN COGNITIVE SCIENCES	33,482	20.229	0.036270
4	NEURON	111,115	17.173	0.175220
5	ACTA NEUROPATHOLOGICA	28,031	17.088	0.036970
6	MOLECULAR PSYCHIATRY	28,622	15.992	0.046220
7	Molecular Neurodegeneration	6,772	14.195	0.011650
8	TRENDS IN NEUROSCIENCES	22,858	13.837	0.019470
9	Nature Human Behaviour	5,549	13.663	0.023120
10	BRAIN	64,627	13.501	0.061550
11	BIOLOGICAL PSYCHIATRY	50,155	13.382	0.045540
12	JOURNAL OF PINEAL RESEARCH	12,492	13.007	0.008170
13	BEHAVIORAL AND BRAIN SCIENCES	11,610	12.579	0.007760
14	Annual Review of Neuroscience	14,699	12.449	0.010490
15	PROGRESS IN NEUROBIOLOGY	15,161	11.685	0.010300
16	SLEEP MEDICINE REVIEWS	11,218	11.609	0.014840
17	ANNALS OF NEUROLOGY	43,728	10.422	0.039960
18	NEUROSCIENCE AND BIOBEHAVIORAL REVIEWS	36,525	8.989	0.048970
19	Brain Stimulation	9,206	8.955	0.015960
20	npj Parkinsons Disease	1,093	8.651	0.003040
21	FRONTIERS IN NEUROENDOCRINOLOGY	5,338	8.606	0.005050
22	Neurology-Neuroimmunology & Neuroinflammation	3,863	8.485	0.008390
23	Journal of Neuroinflammation	19,657	8.322	0.027070

## Printing copy(s) of the publication(s)

The online version can be found on:

<https://doi.org/10.1186%2Fs12974-022-02620-w>

## RESEARCH

## Open Access



# FoxP3 expression by retinal pigment epithelial cells: transcription factor with potential relevance for the pathology of age-related macular degeneration

Ahmad Samir Alfaar<sup>1,2</sup>, Lucas Stürzbecher<sup>1</sup>, Maria Diedrichs-Möhning<sup>3</sup>, Marion Lam<sup>4</sup>, Christophe Roubeix<sup>4</sup>, Julia Ritter<sup>5</sup>, Kathrin Schumann<sup>5</sup>, Balasubramaniam Annamalai<sup>6</sup>, Inga-Marie Pompös<sup>1</sup>, Bärbel Rohrer<sup>6</sup>, Florian Sennlaub<sup>4</sup>, Nadine Reichhart<sup>1†</sup>, Gerhild Wildner<sup>3\*†</sup> and Olaf Strauß<sup>1\*†</sup>

## Abstract

**Background:** Forkhead-Box-Protein P3 (FoxP3) is a transcription factor and marker of regulatory T cells, converting naive T cells into Tregs that can downregulate the effector function of other T cells. We previously detected the expression of FoxP3 in retinal pigment epithelial (RPE) cells, forming the outer blood–retina barrier of the immune privileged eye.

**Methods:** We investigated the expression, subcellular localization, and phosphorylation of FoxP3 in RPE cells in vivo and in vitro after treatment with various stressors including age, retinal laser burn, autoimmune inflammation, exposure to cigarette smoke, in addition of IL-1 $\beta$  and mechanical cell monolayer destruction. Eye tissue from humans, mouse models of retinal degeneration and rats, and ARPE-19, a human RPE cell line for in vitro experiments, underwent immunohistochemical, immunofluorescence staining, and PCR or immunoblot analysis to determine the intracellular localization and phosphorylation of FoxP3. Cytokine expression of stressed cultured RPE cells was investigated by multiplex bead analysis. Depletion of the FoxP3 gene was performed with CRISPR/Cas9 editing.

**Results:** RPE in vivo displayed increased nuclear FoxP3-expression with increases in age and inflammation, long-term exposure of mice to cigarette smoke, or after laser burn injury. The human RPE cell line ARPE-19 constitutively expressed nuclear FoxP3 under non-confluent culture conditions, representing a regulatory phenotype under chronic stress. Confluently grown cells expressed cytosolic FoxP3 that was translocated to the nucleus after treatment with

<sup>†</sup>Nadine Reichhart (njreichhart@gmail.com), Gerhild Wildner (gerhild.wildner@med.uni-muenchen.de) and Olaf Strauß are shared corresponding authors.

\*Correspondence: Gerhild.Wildner@med.uni-muenchen.de; Olaf.strauss@charite.de

<sup>1</sup> Experimental Ophthalmology, Department of Ophthalmology, Charité - Universitätsmedizin Berlin, Corporate Member of Freie Universität, Berlin Institute of Health, Humboldt-University, 10117 Berlin, Germany

<sup>3</sup> Section of Immunobiology, Department of Ophthalmology, University Hospital, LMU Munich, 80336 Munich, Germany

Full list of author information is available at the end of the article



© The Author(s) 2022. **Open Access** This article is licensed under a Creative Commons Attribution 4.0 International License, which permits use, sharing, adaptation, distribution and reproduction in any medium or format, as long as you give appropriate credit to the original author(s) and the source, provide a link to the Creative Commons licence, and indicate if changes were made. The images or other third party material in this article are included in the article's Creative Commons licence, unless indicated otherwise in a credit line to the material. If material is not included in the article's Creative Commons licence and your intended use is not permitted by statutory regulation or exceeds the permitted use, you will need to obtain permission directly from the copyright holder. To view a copy of this licence, visit <http://creativecommons.org/licenses/by/4.0/>. The Creative Commons Public Domain Dedication waiver (<http://creativecommons.org/publicdomain/zero/1.0/>) applies to the data made available in this article, unless otherwise stated in a credit line to the data.

IL-1 $\beta$  to imitate activated macrophages or after mechanical destruction of the monolayer. Moreover, with depletion of FoxP3, but not of a control gene, by CRISPR/Cas9 gene editing decreased stress resistance of RPE cells.

**Conclusion:** Our data suggest that FoxP3 is upregulated by age and under cellular stress and might be important for RPE function.

**Keywords:** IL-1 $\beta$ , Ca-channels, CRISPR/Cas9, Phosphorylation, RPE, Age-related macular degeneration, FoxP3, Immune barrier, Immune privilege of the retina

## Background

The immune privilege of the eye, by which inflammatory responses are limited, is maintained by different mechanisms, including multiple blood–eye barriers [1–4]. Three different blood–eye barriers exclude non-activated immune cells from the entry of the eye or educate the invading immune cells to switch to a tolerant/repairing phenotype. Shechter et al. [4] further classified these barriers into two types: “true blood barriers” or “blood–aqueous barriers”. The so-called “true blood barrier”, the inner retinal barrier, is formed by the retinal blood vessels equipped with tight junctions of the endothelial cells and surrounded by pericytes and Müller cells, which aim at sealing the retina against invasion from the bloodstream. The two other barriers are the blood–aqueous barrier of the non-pigmented ciliary body epithelium and the outer blood–retina barrier, or the retinal pigment epithelium (RPE) [5–8]. These barriers are called “educational” or “regulating gates” and consist of fenestrated endothelia that face the ocular epithelia with tight junctions. Those epithelia interact with invading cells of the immune system by secreting immunosuppressive or immunoregulatory factors and expressing surface molecules with immunoregulatory or cytotoxic functions like FasL and PDL1. Potentially destructive effector cells of both the innate and the adaptive arm of the immune system are converted to a regulatory or repairing phenotype when they pass these barriers [4].

When activated cells of the immune system interact with or pass through the RPE, its phenotype changes from maintaining tolerance to immune stimulation [9–15]. To efficiently interact with the immune system, the RPE expresses many immune surface receptors/ligands, including anaphylatoxin receptors [16–26], Toll-like receptors [27–32], and receptors for cytokines like IL-1 $\beta$  receptor [17, 33–35] or TNF- $\alpha$  receptor [12, 14, 28, 36–44]. Furthermore, the RPE can secrete immune-relevant cytokines and chemokines like MCP-1/CCL2 [15, 16, 45–49], IL-6 [27–29, 31, 47, 49, 50] or IL-12, IFN- $\gamma$ , IL-8/CXCL8 and IP-10/CXCL10 [49], as well as complement factors such as C3, C5 and CFH [16, 19, 21, 39, 51–58]. Interestingly, cytokines and chemokines released from macrophages or T cells can induce the secretion of VEGF-A in RPE cells, indicating that an interaction with

the immune system might also promote an angiogenic phenotype [12–14, 33, 35, 57]. Studies from both animal and in vitro models provide examples of the dynamic interplay between the RPE and immune cells. Invading mononuclear phagocytes secrete TNF- $\alpha$ , IL-6, and IL-1 $\beta$ , which in turn provoke pro-inflammatory reactions by the RPE [12, 14, 37–41]. The RPE secretes MCP-1/CCL2 and complement factors that attract monocytes and activate the monocyte pro-inflammatory phenotype M1. The first step towards the shift to immune activation might be monocytes that escape control by the RPE [12], activation of inflammasomes in stressed RPE, and the RPE’s interaction with an overactive complement system [17, 36, 59], explaining the association of the risk for the development of age-related macular degeneration (AMD) with polymorphisms in complement genes [16, 23, 53, 59]. The detailed mechanisms that induce the switch in the RPE-phenotype from immune inhibitory to inflammatory and/or angiogenic are so far unknown, but represent major targets in therapy development.

Surprisingly, we have found that the RPE can express the transcription factor FoxP3 (forkhead box P3), which was previously thought to be specifically expressed by regulatory T cells [16, 60, 61]. Human and rat effector T cells transiently express FoxP3 after activation. FoxP3 expression is maintained when those cells differentiate into regulatory cells (Tregs) but is downregulated if the cells keep their effector phenotype [62, 63]. While FoxP3 is localized in the cytoplasm of activated effector cells, in Tregs it is translocated to the nucleus [64]. FoxP3-positive Treg cells can suppress inflammation and promote regeneration and tissue homeostasis [65–67]. The phenotypes of the FoxP3-positive regulatory cells depend on the level of FoxP3 expression: resting Tregs express lower levels, while effector Tregs have higher levels of FoxP3. Furthermore, the impact of FoxP3 on cell function depends on splicing variants and several post-translational modifications like methylation, acetylation, prenylation, ubiquitination, glycosylation, and phosphorylation that modify and regulate the function of FoxP3 [65].

Cell types other than Tregs that can express FoxP3 have been identified, such as epithelial cells of the prostate [68], ovary [69], and mammary glands [70], as well as a variety of cancer cells [71–73]. While prostate, ovary,

and mammary glands are important for reproduction and are thus immune privileged, cancer cells often take advantage of tolerance-inducing mechanisms to protect themselves from immune attacks. Several observations in an earlier study indicate a role of FoxP3 expression in the RPE that is associated with local immune reactions. Normally, the RPE does not express FoxP3 but rather initiates its expression under conditions of stress, as occurs in experimental uveitis [16]. Furthermore, stimulation of RPE cells with anaphylatoxins leads to increased expression of complement factors/receptors as well as the secretion of cytokines such as MCP-1/CCL2, VEGF-A, and IL-6 that are associated with increased FoxP3 phosphorylation [16]. Oxidative stress, one of the risk factors promoting AMD, also induces FoxP3 expression in the RPE [59]. Thus, FoxP3 could be regarded as a general immune regulatory transcription factor in the RPE and might therefore play an essential role in the development of diseases such as AMD.

While the role of FoxP3 in T lymphocyte function and regulation has been extensively investigated, its role in the RPE function remains unexplored. By analogy to FoxP3+ Tregs that play a critical role in immune tolerance and chronic stress, which promotes a pro-inflammatory phenotype, we propose that FoxP3 induces regulatory functions of the RPE as a part of its role in maintaining the outer blood–retina barrier function. FoxP3 thus might play a major role for RPE function, as prior evidence demonstrates that its expression in the RPE is stress- and disease-related. The aim of this study was to test this hypothesis by analyzing the FoxP3 expression both in vivo and in vitro AMD models, including human and animal tissue, and in RPE cell cultures by application of IL-1 $\beta$ .

## Material and methods

### Animals

All animal experiments were conducted in accordance with the ARVO statement for the use of animals in ophthalmic and vision research. Mouse experiments were approved by the LaGeSo under G0039/19, except for the smoke exposure experiment which was approved by the IACUC at MUSC under institutional approval number 00399. We used C57BL/6J mice for laser-induced choroidal neovascularization (CNV) and as controls for the *Cx3cr1<sup>GFP/GFP</sup>* mice that are on the C57BL/6 J genetic background. *Cx3cr1<sup>GFP/GFP</sup>* mice older than 10 months are hyperinflammatory and develop age-dependent sub-retinal inflammation, a hallmark of AMD [74]. The animals were kept under a 12-h light–dark cycle, standard environmental conditions, and food and water were provided ad libitum.

The laser-induction of CNV was performed as previously described [75]. In brief, four laser burns were applied around the optic nerve using an Argon laser (120 mW, 100 ms, 50  $\mu$ m), under anesthesia with 1% ketamine hydrochloride (Actavis, Munich, Germany) and 0.1% xylazine (Rompun; Bayer Vital GmbH, Leverkusen, Germany), and dilated pupils (2.5% phenylephrine-hydrochloride and 0.5% tropicamide (Charité Apotheke, Berlin, Germany)). Retinal bleeding after laser burn led to exclusion of the eye.

Experimental autoimmune uveitis was induced in Lewis rats as previously described [49] and was approved by the government of Upper Bavaria (ROB-55.2–1-2532. Vet\_02-15–225). In brief, Lewis rats were subcutaneously immunized with retinal S-antigen peptide PDSAg (Polypeptide Laboratories, Strasbourg, France) in CFA (BD Biosciences, Heidelberg, Germany), the experiment was terminated 30 days later, and eyes were collected for cryosections.

### Immunohistochemistry of RPE/choroid flatmounts

RPE/choroid flatmounts from mouse eyes were prepared as previously described [75]. In short, eyes were enucleated, fixed in 4% paraformaldehyde for 12 min at room temperature, and sectioned at the limbus; the retinas were removed from the RPE/choroid/sclera and 6–8 radial sections were made. After incubation of the RPE/choroid/sclera tissue in 5% Triton X-100 in TBS overnight at 4 °C, the samples were incubated in blocking buffer for 1 h (5% BSA in TBS). Subsequently, an incubation with rabbit polyclonal anti-FoxP3 (Novus, 1:200) antibody and ActiStain555-conjugated phalloidin (Biomol, Hamburg, Germany, 1:500) followed for 48 h. Rat anti-mouse CD102 (BD-Pharmingen, Heidelberg, Germany, 1:200) was used to visualize the laser scars. After a few washes, the samples were incubated for 1 h at room temperature with the appropriate Alexa Fluor<sup>®</sup>-conjugated secondary antibodies (Thermo Fisher Scientific; 1:1000). Tissues were embedded in DAKO fluorescence mounting medium (Agilent, Ratingen, Germany) and images were taken using a LSM 510 confocal laser-scanning microscope (Zeiss, Jena, Germany) and digitalized using ZEN 3.1 Blue Edition software (Zeiss, Oberkochen, Germany).

### Immunohistochemistry of sagittal sections

#### Human AMD samples

Eyes from donors with a known history of AMD and age-matched controls were collected from the Minnetonka Lions Eye Bank. We examined 4 eyes of the group “Non-Geographic Atrophy” (Non-GA) and 3 eyes with “Geographic Atrophy” (GA). The group of Non-GA included three males and one female, the mean age was 85.75  $\pm$  1 years, and the time of death-to enucleation was



193.75 ± 9 min (3:14 h). The death causes in the Non-GA were intracerebral hemorrhage, cardiac arrest, lung cancer, and dementia. The group of GA included two females and one male, the mean age was 85 ± 2.6 years, and the death-to-enucleation time was 278.5 ± 60 min (4:38 h). The death causes in the GA group were breast cancer, congestive heart failure, and an acute cardiac event. When reported, the death-to-cooling times in both groups were between 1 and 2:25 h. The posterior segment was fixed for 4 h in 4% PFA, dissected, embedded in paraffin, and sectioned. Slides were generously sent to us for further processing. Horse serum was used to block unspecific binding. The primary antibody, rabbit polyclonal FoxP3 (1:200, Novus Biologicals; the same antibody as used for ARPE-19 staining below) was incubated with the sections at 4 °C overnight. A secondary AP-coupled anti-rabbit antibody was incubated for 1 h at RT and a Fast Red substrate kit (Sigmafast Fast Red TR/Naphthol AS-MX, Sigma/Merck) was used to visualize positive staining under brightfield microscopy using a DM5500 microscope (Leica, Nanterre, France).

#### Rat eyes

Eyes from killed animals were embedded in Tissue Tec OCT compound (Paesel and Lorey, Frankfurt/Main, Germany) and immediately snap frozen in methyl butane (Merck, Darmstadt Germany) at -70 °C to avoid shrinking of the tissue. Air-dried cryosections (8 µm, performed with a CryoStat Microm HM560 Microtom, Thermo Scientific, Dreieich, Germany) were fixed in ice-cold acetone for 10 min and then dried, and the sections were incubated with rabbit anti-rat FoxP3 antibody (Novus Biologicals, Abingdon, UK) diluted 1:100 in PBS/3% donkey serum overnight at 4 °C in a humid chamber. After washing 3 × with PBS, Cy3-conjugated affininpure donkey anti-rabbit IgG(H+L) (Jackson Laboratories, Dianova, Hamburg, Germany) was added as a secondary antibody at a dilution of 1:100 in PBS and incubated for 1 h at RT in the dark. Then the slides were washed 3 × with PBS and mounted with Vectashield HardSet with DAPI H-1500 (Biozol, Eching, Germany). Pictures were taken with an Axio Observer 7 with ApoTome (Zeiss, Oberkochen, Germany).

#### Cell culture

The research team of Prof. Marius Ader (Center of Regenerative Medicine, Dresden Germany) provided human RPE cells differentiated from inducible stem cells (iPS-RPE). iPS-RPE cells (differentiated from the iPS cell line CRTDi004-A; CTRD Dresden registered under <https://hpscreg.eu/cell-line/CRTDi004-A>) were grown on filter inserts and reached transepithelial

resistance at 600 Ωcm<sup>2</sup>. The cells were maintained in mTeSR™ plus medium (Stemcell Technologies, Cologne Germany) at 37 °C and 5% CO<sub>2</sub>. The local Ethics Committee approved the use of human material under the registration number EA1/024/17.

ARPE-19 cells were cultured in DMEM/F12 (Thermo Fisher, Darmstadt, Germany) with Glutamax (stable glutamine) supplemented with 10% FCS and 50 U penicillin/50 mg streptomycin at 37 °C and 5% CO<sub>2</sub>. The cell density differed between confluent and non-confluent (50–70% confluency), with confluent cells forming a closed monolayer. Before any treatment, medium was exchanged with serum-free medium for 24 h. ARPE-19 cells were then incubated with 100 ng/ml IL-1β (Sigma Aldrich/Merck, Darmstadt, Germany) for 6 min, 1 h, and 2 h, respectively, at 37 °C and 5% CO<sub>2</sub>, supernatants were collected, and cells immediately harvested. Confluent cells had a density of 30.000 cells per cm<sup>2</sup>, non-confluent cultures 20.000 cells per cm<sup>2</sup>.

#### Generation and characterization of APRE-19 KO cells

Electroporation of ARPE-19 cells was performed using the SF Cell Line EP Kit (Lonza) and 4D-Nucleofector (Lonza; nucleofection code: DN-100). Each reaction contained 5 × 10<sup>5</sup> ARPE-19 cells, (grown confluent or non-confluent and trypsinized immediately prior to electroporation) 4 µl of the respective Cas9 RNP and 1 µl of electroporation enhancer (IDT). Cas9 RNPs were assembled with 100 µM crRNA (IDT) and 100 µM tracrRNA (IDT) mixed in a 1:1 ratio and incubated for 5 min at 96 °C to generate 50 µM crRNA–tracrRNA duplexes. Then, 40 µM *S. pyogenes* Cas9-NLS (purified using published protocols [76]; Cas9 expression plasmid: pMJ915; Addgene #69090, Watertown, MA, USA) was slowly added to the crRNA–tracrRNA duplexes and incubated for 15 min at room temperature. The crRNAs targeting CXCR4 and FoxP3 have been functionally validated in human T cells before with editing efficiencies of 60–90% or 60–80%, respectively [77, 78]; protospacer sequences: FoxP3: TCATGGCTGGGCTCTCCAGG; CXCR4: GAA GCGTGATGACAAAGAGG; non-targeting control: GGTTCTTGACTACCGTAATT. After nucleofection, 80 µl pre-warmed DMEM + 10% FCS was added and cells rested for 10 min at 37 °C. Transfected ARPE-19 cells were seeded again to grow to either 100% or 50% confluency in 6 well plates. 1, 3 and 10 days after nucleofection DNA was isolated from all conditions using QuickExtract (Epicenter) according to the manufacturer's recommendation. The editing efficiencies were determined by amplicon sequencing followed by Sanger sequencing. Each PCR reaction contained 12.5 µl of 2 × iProof HF master mix (Bio-Rad), 1.25 µl of 10 µM forward primer

(Sigma), 1.25  $\mu$ l of 10  $\mu$ M reverse primer (Sigma), and 9  $\mu$ l of H<sub>2</sub>O (primer sequences: CXCR4 fwd: AGAGGA GTTAGCCAAGATGTGACTTTG, CXCR4 rev: GGA CAGGATGACAATACCAGG CAGGATAAGGCC, FoxP3 fwd2: AGCTCTGCAACTTATTAGCTG, FoxP3 rev: GCTTAAAGACGGCCATTC). The thermocycler setting consisted of one step at 95 °C for 3 min, followed by 35 cycles at 94 °C for 20 s, 65 °C for 20 s, and 72 °C for 1 min (wherein the annealing temperature was decreased by 0.5 °C per cycle); followed by 25 cycles at 98 °C for 20 s, 58 °C for 20 s, and 72 °C for 1 min. Sanger sequencing was performed by Microsynth AG (Balgach, Switzerland). Sequencing traces were analyzed with the TIDE webtool (<http://tide.nki.nl>; [79]).

### Calcium imaging

ARPE-19 cells grown on 15 mm glass cover slips ( $8.5 \times 10^3$  cells  $\cdot$  cm<sup>-2</sup>) were kept under serum-free conditions overnight. Calcium imaging was carried out as previously described in [16]. In short, after incubation for 40 min with fura-2/AM (2  $\mu$ M, Invitrogen), the cover slips were placed in a custom-made recording chamber (bath solution consisting of (in mM): 138 NaCl, 5.8 KCl, 0.41 MgSO<sub>4</sub>, 0.48 MgCl<sub>2</sub>, 0.95 CaCl<sub>2</sub>, 4.17 NaHCO<sub>3</sub>, 1.1 NaH<sub>2</sub>PO<sub>4</sub>, 25 HEPES) and imaged using a Zeiss Axiovert 40 CFL inverted microscope (Carl Zeiss AG) equipped with a 40 $\times$  oil immersion objective, a Visichrome High Speed Polychromator System (Visitron Systems), and a high-resolution CCD camera (CoolSNAP EZ, Photometrics). IL-1 $\beta$  (100 ng/ml) was added in the presence of the following agonists/blockers: (R)-(+)-BayK 8644 (10  $\mu$ M, Tocris, Wiesbaden, Germany), Thapsigargin (1  $\mu$ M, Acros, Schwerte, Germany), Ruthenium Red (1  $\mu$ M, Alomone, Jerusalem, Israel), and Dantrolene (1  $\mu$ M, LY294002 (50  $\mu$ M; Cayman Chemical Tallinn, Estonia). Fura-2/AM signal was acquired using the MetaFluor Fluorescence Ratio Imaging Software (Visitron Systems). Fluorescence intensity of Fura-2 was detected at an emission wavelength of 505 nm, while the excitation wavelengths were set to 340/380 nm. Changes in intracellular free Ca<sup>2+</sup> are presented as changes of the ratios of the fluorescence of the two excitation wavelengths (dF/F) in relation to the baseline (ddF/F).

### Immunofluorescence staining of ARPE-19 cells after stimulation with IL-1 $\beta$

Cells grown on 15-mm-diameter cover slips to confluence or non-confluence were fixed in 4% PFA for 10 min and permeabilized in 5% Triton X-100 in TBS for 10 min, or alternatively fixed for 15 min with ice-cold methanol. After blocking in 5% BSA in TBS for 30 min, the primary antibody (rabbit polyclonal FoxP3, Novus Biologicals, 1:200) was applied overnight at 4 °C. After incubation

with an appropriate secondary antibody conjugated with AF647 or Cy3 for 1 h at RT, nuclei were counterstained with DAPI (according to supplier; Sigma, Taufkirchen, Germany). Coverslips were mounted in fluorescent mounting Medium (DAKO, Glastrup, Denmark) or Entellan (Merck, Darmstadt, Germany) and visualized using an LSM 510 confocal laser-scanning microscope (Zeiss, Jena, Germany) and ZEN software 3.1 Blue Edition (Zeiss, Oberkochen, Germany) or a Zeiss Axioskop 2plus an Axio Observer 7 with ApoTome (Zeiss, Oberkochen, Germany) or imaged with a Zeiss Axioskop 2plus (Carl Zeiss, Jena, Germany), and photographs were taken with a Sony CyberShot DSC-S70 3.3 mp digital camera. (Carl Zeiss, Jena, Germany). The integrated density of pixels in the nucleus was determined using ImageJ software [80].

### Dot blotting

ARPE-19 cells were grown on Transwell plates as 4-week-old monolayers or as subconfluent cells (80% confluency) on regular plates. The cultures of each plate were switched to serum-free medium overnight prior to the experiment. Cells were stimulated with 100 ng/ml IL-1 $\beta$  (Sigma Aldrich) or equal amounts of vehicle (PBS) for 1 h, followed by careful washing with ice-cold PBS 3 times and harvesting in sucrose isolation buffer (250 mM sucrose, 1 mM EGTA, 10 mM HEPES, and 1 mg/ml fatty acid-free BSA; pH of 7.4). Cells were homogenized using a Dounce homogenizer and centrifuged at 700g for 5 min to obtain supernatant (cytosol) and pellet (nuclear fraction). The supernatant was collected in phosphatase inhibitors (1:100), 1 mM sodium orthovanadate, 1 mM sodium fluoride, Triton X-100 and 4% SDS. The pellet was washed twice with isolation buffer and centrifuged at 1000g for 5 min. The pellet/nuclear fraction was resuspended in RIPA buffer containing 50 mM Tris-HCl, 150 mM NaCl, 0.1% SDS, 0.5% sodium deoxycholate, and 1% Triton X-100 (pH 7.4) with phosphatase inhibitors (1:100), 1 mM sodium orthovanadate, and 1 mM sodium fluoride. Dot blotting was performed as described by us previously [81]. In short, equal amounts of protein (1.5  $\mu$ g) were loaded per fraction on a 96-well plate (Bio-Dot<sup>®</sup> Microfiltration Apparatus; Bio-Rad Laboratories Inc.) and vacuum transferred onto nitrocellulose membranes. Membranes were incubated with primary antibodies (1:1000) against Phospho-FoxP3 (Ser 418; Abgent Biotech) or FoxP3 (Cell Signaling Technologies) overnight. Antibodies against GAPDH (cytoplasm; Cell Signaling Technologies) and histone H3 (nuclear fraction; Cell Signaling Technologies) were used for normalization. Proteins were visualized with horseradish peroxidase-conjugated secondary antibodies (Santa Cruz Biotechnology) followed by incubation with Clarity<sup>™</sup>

Western ECL Blotting Substrate (Bio-Rad Laboratories, Inc.) and chemiluminescent detection. Protein dots were scanned and densities quantified using ImageJ software [80].

#### RNA isolation, cDNA synthesis and RT-PCR

For murine samples retina and RPE were harvested and immediately stored in liquid N<sub>2</sub>. The preparation technique yields RPE and choroid. The tissue was homogenized with Qiazol Lysis Reagent (Qiagen) and Precellys ceramic beads (Peqlab Biotechnology, Erlangen, Germany). Total RNA was isolated using a RNeasy Mini Kit (Qiagen). After reverse transcription with the High-Capacity cDNA Reverse Transcription Kit (Applied Biosystems, Waltham, USA), RT-qPCR was performed using the QuantStudio 3 Real-Time PCR System (Applied Biosystems) with TaqMan Fast Universal PCR Master Mix (Scientific, Waltham, MA, USA). Primer and probes were purchased from Thermo Fisher (Schwerte, Germany) or designed using Primer Express 3.0 and synthesized by BioTez (Germany) (see Table 1). The target mRNA expression was quantitatively analyzed with the standard curve method. All expression values were normalized to the housekeeping gene 18S rRNA.

#### Cytokine/chemokine secretion

Supernatants from confluent and subconfluent ARPE-19 cell cultures, without exchange of medium (DMEM with 5% FCS and stable glutamine) for 2 weeks were tested. In some experiments, a pipet scratch 24 h prior to the experiment induced further mechanical stress to cells. Cytokine secretion after treatment with 100 ng recombinant human IL-1 $\beta$ /ml medium (OriGene, Rockville, USA) was measured in supernatants collected and frozen after 6 min, 1 h and 2 h of incubation with IL-1 $\beta$ , at which point the cells were harvested and immediately shock frozen at -80 °C. Immediately after thawing, the supernatants were tested by human Bio-Plex bead analysis (Bio-Rad Laboratories Inc., Hercules, USA) according to the manufacturer's instruction. Tested analytes were IL-1 $\alpha$

IL-1 $\beta$ , IL-1ra, IL-6, IL-8/CXCL8, IL-10, IL-12 (p70 and p40), IFN- $\gamma$ , MCP-1/CCL2, MCP-3/CCL7, PDGF, IL-17, IL-13, and VEGF, but only those that were secreted by the ARPE-19 cells are shown. The final values obtained in the bioplex analysis were calculated from the median value of fluorescence of at least 50 measured beads per analyte and sample.

#### Data analysis

All data are presented as mean values  $\pm$  SEM. Statistical significance was calculated using the Mann-Whitney U test for Ca<sup>2+</sup>-Imaging analyses and protein secretion analyses. For immunocytochemistry, western blot, and gene expression analyses, Student's t-test was used (p values \* $p < 0.05$ , \*\* $p < 0.01$ , and \*\*\* $p < 0.001$ ). All calculations were performed in Graph Pad Prism (Version 9.3.1), Sigma Plot 14.0 (Systat, San Jose, USA), and Excel 2016.

#### Results

Our previously published work showed that under normal conditions in vivo the RPE does not express FoxP3, while it does upregulate FoxP3-expression in uveitis [16], suggesting a correlation with stress situations like ocular inflammation. To test this hypothesis, we investigated FoxP3-expression in the context of AMD, a retinal disease that combines the risk factors of age and polymorphisms in genes of the innate immune system, and which is proposed to be caused by oxidative stress and chronic, low-grade inflammation as major pathomechanisms. Thus, we investigated RPE cells for FoxP3 expression under the conditions of age and AMD-relevant pathologic scenarios in various species, including humans.

In the first set of experiments, we investigated the expression of FoxP3 in the RPE of rodent models (Fig. 1). The *Cx3cr1*<sup>GFP/GFP</sup> mouse lacks the expression of the fractalkine receptor Cx3cr1, which causes a subsequent hyperinflammatory phenotype. These mice develop age-dependent subretinal inflammation, a hallmark for AMD [11, 15, 74]. The model combines aging, an inflammatory response with invading monocytes, and loss of RPE cells.

**Table 1** Mouse PCR primers

Gene	Company	Assay ID	Forward (5'- 3')	Reverse (5'- 3')	Probe
CXCL1	BioTeZ Berlin-Buch GmbH		CTG CAC CCA AAC CGA AGT C	AGC TTC AGG GTC AAG GCA AG	
MCP-1	BioTeZ Berlin-Buch GmbH		GGC TCA GCC AGA TGC AGT TAA	CCT ACT CAT TGG GAT CAT CTT GCT	CCC CAC TCA CCT GCT GCT ACT CAT TCA
IL-1 $\beta$	Thermo Fisher	Mm00434288			
18S	BioTeZ Berlin-Buch GmbH		ACA TCC AAG GAA GGC AGC AG	TTT TCG TCA CTA CCT CCC CG	CGC GCA AAT TAC CCA CTC CCG AC

(See figure on next page.)

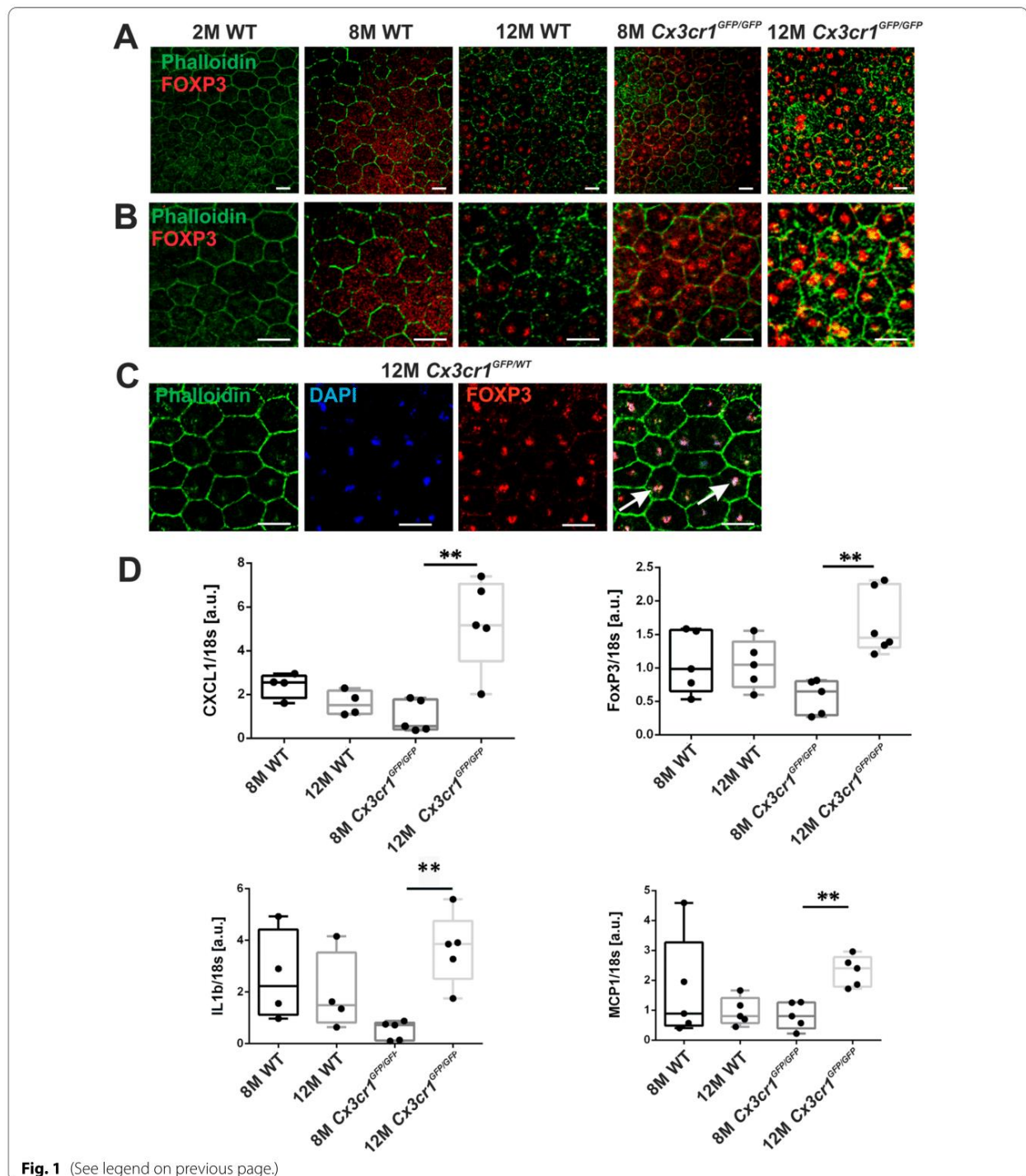
**Fig. 1** FoxP3 and cytokine expression in *Cx3cr1<sup>GFP/GFP</sup>* mice. **A** RPE flatmount preparations from transgenic mice that display features of geographic atrophy (*Cx3cr1<sup>GFP/GFP</sup>* mice and their wild-type littermates) stained with phalloidin (green) and for FoxP3 (red) at different ages: panels from left to right: 2, 8, 12 month wild type (WT) and 8 and 12 month *Cx3cr1<sup>GFP/GFP</sup>* mice. Scale bar represents 20  $\mu$ m. **B** Same as A, but at higher magnification to highlight the subcellular localization of FoxP3. Scale bar represents 20  $\mu$ m. **C** Verification of FoxP3 localization in the nucleus: RPE flatmounts from 12-month *Cx3cr1<sup>GFP/WT</sup>* mice were stained (from left to right) with phalloidin (green), with DAPI (blue) and for FoxP3 (red); the red dots clearly indicate the presence of FoxP3 in nucleus. Scale bar represents 20  $\mu$ m. **D** Changes in gene expression of the cytokines IL-1 $\beta$ , MCP-1, CXCL1 and the transcription factor FoxP3 in the RPE/choroid of *Cx3cr1<sup>GFP/GFP</sup>* mice and their wildtypes in arbitrary units (a.u.), graphs arranged to compare the progression from the ages 8 months to 12 months (normalized to 18S RNA). (CXCL1 = chemokine (CXC-motif) ligand-1; IL-1 $\beta$  (or IL1b) = interleukin-1 $\beta$ ; FoxP3 = forkhead box protein P3; MCP-1 = monocyte chemoattractant protein). Student's t-test was performed, p values  $**p < 0.01$ ;  $N = 5$

We stained the RPE of RPE/choroidal flatmount preparations from *Cx3cr1<sup>GFP/GFP</sup>* mice and their wild-type (WT) littermates for FoxP3 together with phalloidin, a marker for polymerized actin, to outline the RPE cells (Fig. 1). At the age of 2 months, WT mice displayed a regular cobblestone pattern of RPE cells with no FoxP3 expression (Fig. 1A, left panel, and 1B at higher magnification). The pattern of the RPE morphology remained stable when analyzed at the age of 8 months in WT mice (Fig. 1A, B, second panel from left) but with patchy FoxP3 expression and localization restricted to the cytosol (Fig. 1B, second panel from left). In 8-month-old *Cx3cr1<sup>GFP/GFP</sup>* mice, which still possess a regular hexagonal pattern of RPE cells, a more homogenous FoxP3 expression was observed, with localization shifted predominantly to the nucleus. (Fig. 1A, B, fourth panels from left showing two different magnifications). At 12 months of age, *Cx3cr1<sup>GFP/GFP</sup>* mice showed enlarged, irregularly shaped RPE cells containing up to three nuclei, with an intense, homogeneous, and exclusively nuclear localization of FoxP3 (Fig. 1A, B, right panels). The structural changes correspond to those reported by Chen et al. [82] and might indicate ongoing repair activities for defects that occurred to the epithelium. The WT mice of the same age showed very mild signs of RPE degeneration, mainly in isolated cells displaying two nuclei (Fig. 1A/B; second panels from the right). While FoxP3 expression in WT mice does not appear to be increased beyond the levels observed at 8 months, at 12 months FoxP3 was exclusively localized in the nuclei. A combined DAPI/FoxP3 staining in *Cx3cr1<sup>GFP/WT</sup>* retinas at the age of 12 months confirmed the localization of FoxP3 to the nucleus (Fig. 1C). Thus, although after 8 months of age, cytosolic FoxP3 expression was induced in the RPE, progressive degeneration of the RPE resulted in FoxP3 translocation to the nucleus.

As FoxP3 is a transcription factor, we proposed that its upregulation and localization to the nucleus promote changes in the expression of pro-inflammatory cytokine genes in the RPE. Therefore, we investigated mRNA expression of FoxP3, IL-1 $\beta$ , MCP-1 and Cxcl1

at 8 and 12 months in RPE/choroid mRNA probes [the time points when FoxP3 expression was enhanced in both, WT and *Cx3cr1<sup>GFP/GFP</sup>* mice (Fig. 1D)]. We compared the expression levels between WT and *Cx3cr1<sup>GFP/GFP</sup>* mice at different time points (Additional file 1: Figure S1) and between the two genotypes at the different time points (Fig. 1D). These data show that at the stage of RPE degeneration and nuclear FoxP3 localization in 12-month-old *Cx3cr1<sup>GFP/GFP</sup>* mice, expression of FoxP3 and the pro-inflammatory factors IL-1 $\beta$ , MCP-1 and CXCL1 (the mouse equivalent to human IL-8; [83, 84]) was significantly increased compared to WT mice. Additionally, while the expression of IL-1 $\beta$ , MCP-1 and CXCL1 remained stable over time in WT mice, a significant upregulation was observed in *Cx3cr1<sup>GFP/GFP</sup>* mice between 8 to 12 months of age. The other factors of our panel did not reach significance in the comparison of WT with *Cx3cr1<sup>GFP/GFP</sup>* mice, as the WT mice also showed increased FoxP3 and cytokine expression levels with age. A comparison between the genotypes revealed an increased expression of FoxP3 and all cytokines at the age of 12 months (Additional file 1: Figure S1) in *Cx3cr1<sup>GFP/GFP</sup>* mice compared to wild-type controls.

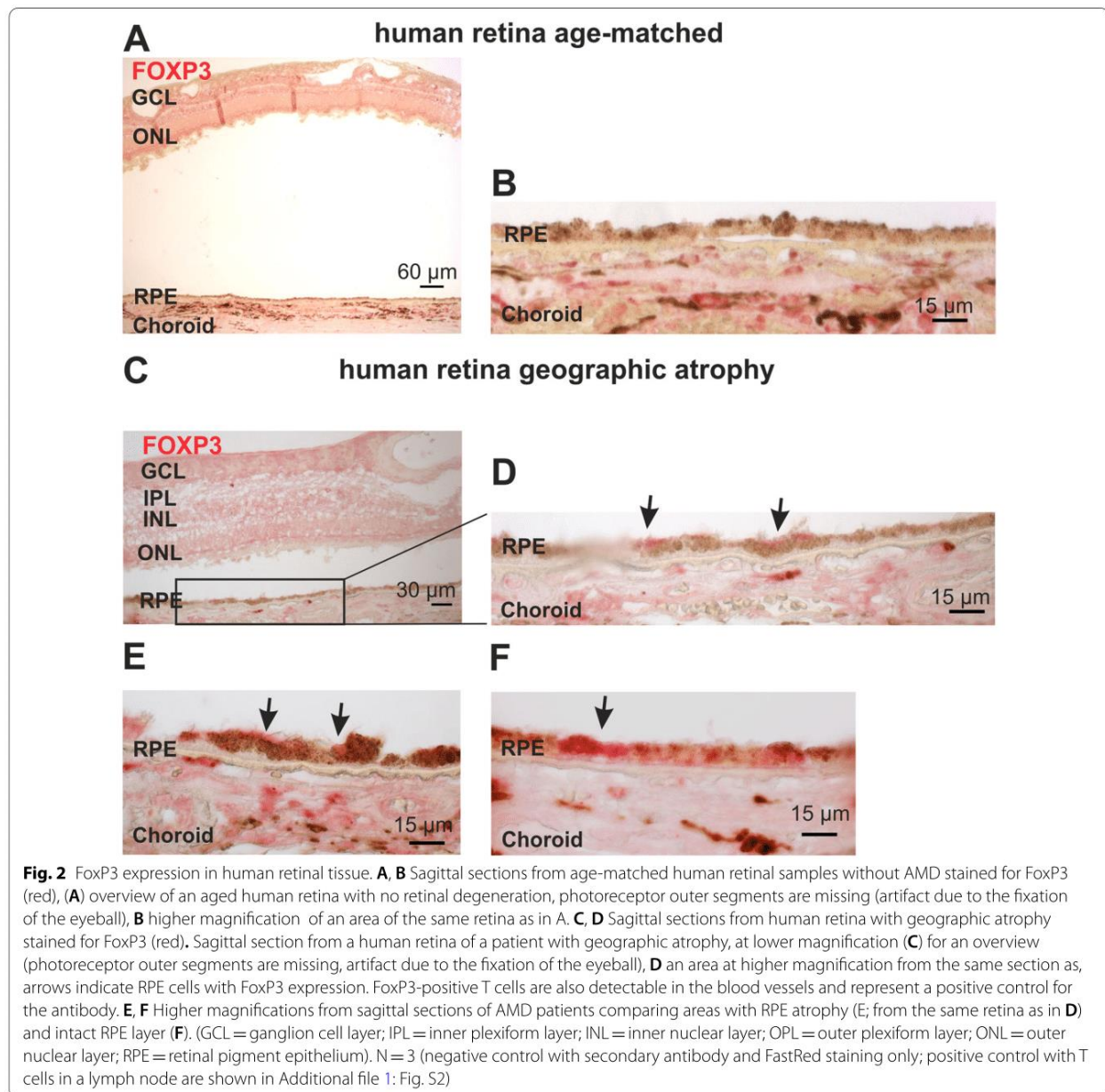
Since this mouse model with subretinal inflammation, one of the hallmarks for dry AMD, demonstrated heightened FoxP3 expression and nuclear localization in conjunction with pro-inflammatory cytokine expression, we analyzed retinal sagittal sections from human donors with dry AMD and healthy, age-matched donors using immunohistochemical staining for FoxP3 expression (Fig. 2). In healthy aged human retinas ( $n = 4$ ) we found no FoxP3 expression in the RPE (Fig. 2A, B; examples from four eyes). In contrast, in all human sagittal sections from AMD patients ( $n = 3$ ), FoxP3 was expressed in an area with still intact RPE (Fig. 2D, E). These observations are in conjunction with our findings in the RPE of 8-month-old wild type and *Cx3cr1<sup>GFP/GFP</sup>* mice (Fig. 1A, B). In addition, we found FoxP3 expression in the RPE of AMD donor eyes in an area with partial destruction of the RPE layer (Fig. 2E, F; examples from two eyes), which corresponds to our observations from 12-month-old



*Cx3cr1*<sup>GFP/GFP</sup> mice (Fig. 1A, B). Our antibodies and staining methods were verified in a tissue sample from a human lymph node as a positive control, and the staining

with the secondary antibody only as a negative control (Additional file 1: Fig. S2).

As the WT mice appeared to show de novo FoxP3-expression followed by translocation into the nucleus



with age, we investigated FoxP3-expression in the RPE from retinal sections of albino rats (Lewis rats) between the ages of 10 weeks to 11 months (Fig. 3). Interestingly, in albino rats, FoxP3 expression was already apparent by 10 weeks. The lack of pigment might cause enhanced stress for the RPE of these animals that had developed retinal degeneration in the past when they were not yet housed in transparent shaded cages (our own unpublished observations). In Fig. 3C, E, and G, cells with cytosolic expression of FoxP3 can be detected in the choroid, indicating the presence of effector T lymphocytes. In

addition, this model verifies the specificity of the primary antibody used. Figure 3G shows cytosolic and nuclear FoxP3-positive cells invading the layer of photoreceptor outer segments, accompanied by a strong upregulation of FoxP3 in the RPE. In previous studies, these invading cells have been identified as regulatory T cells with nuclear FoxP3 localization and effector T cells with cytosolic FoxP3 [85, 86].

The quantification of FoxP3 expression by RPE cells in rat retinas was determined as % overlay of DAPI and FoxP3 staining of the nuclei ( $n=15$ ) using ImageJ

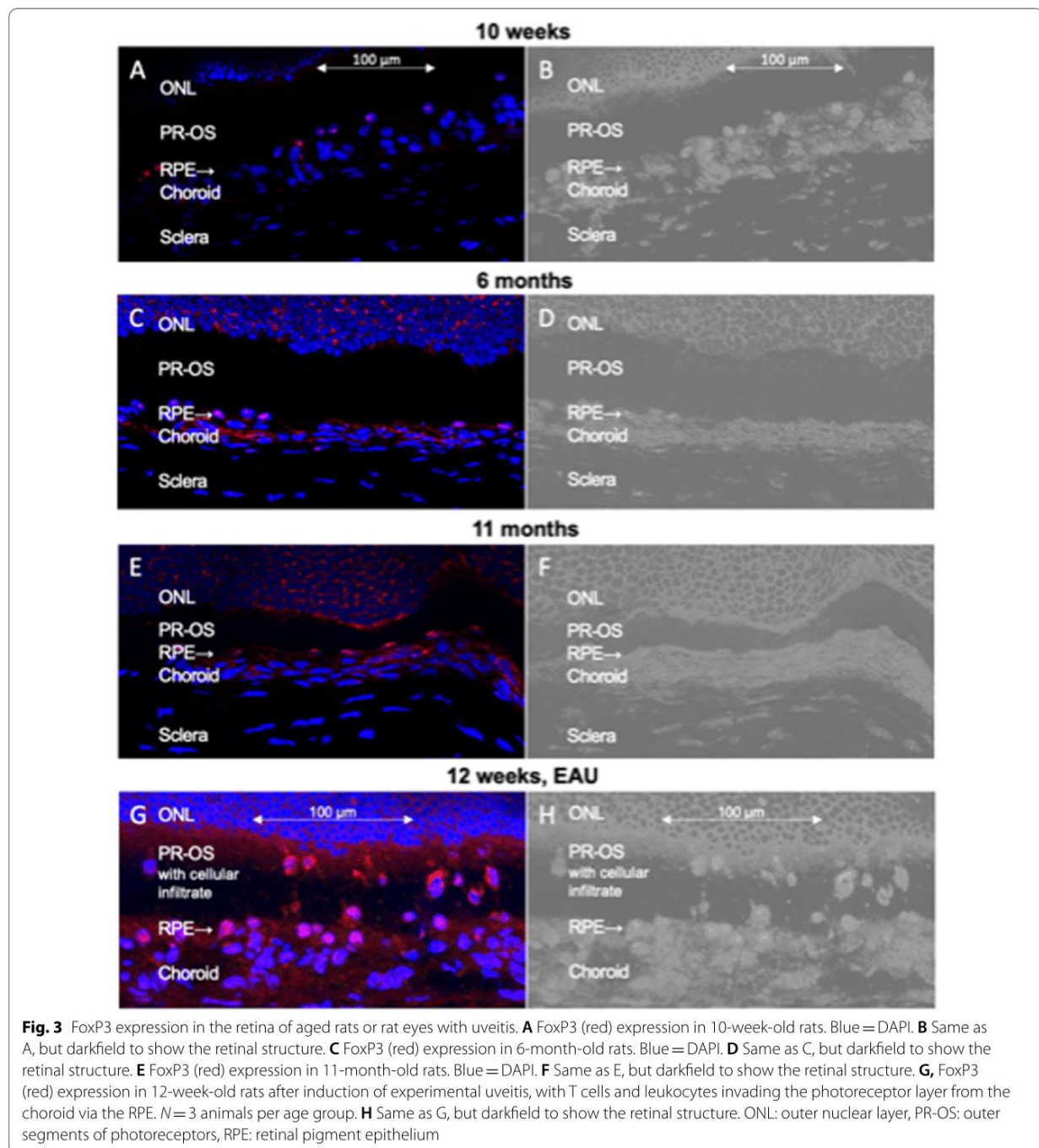
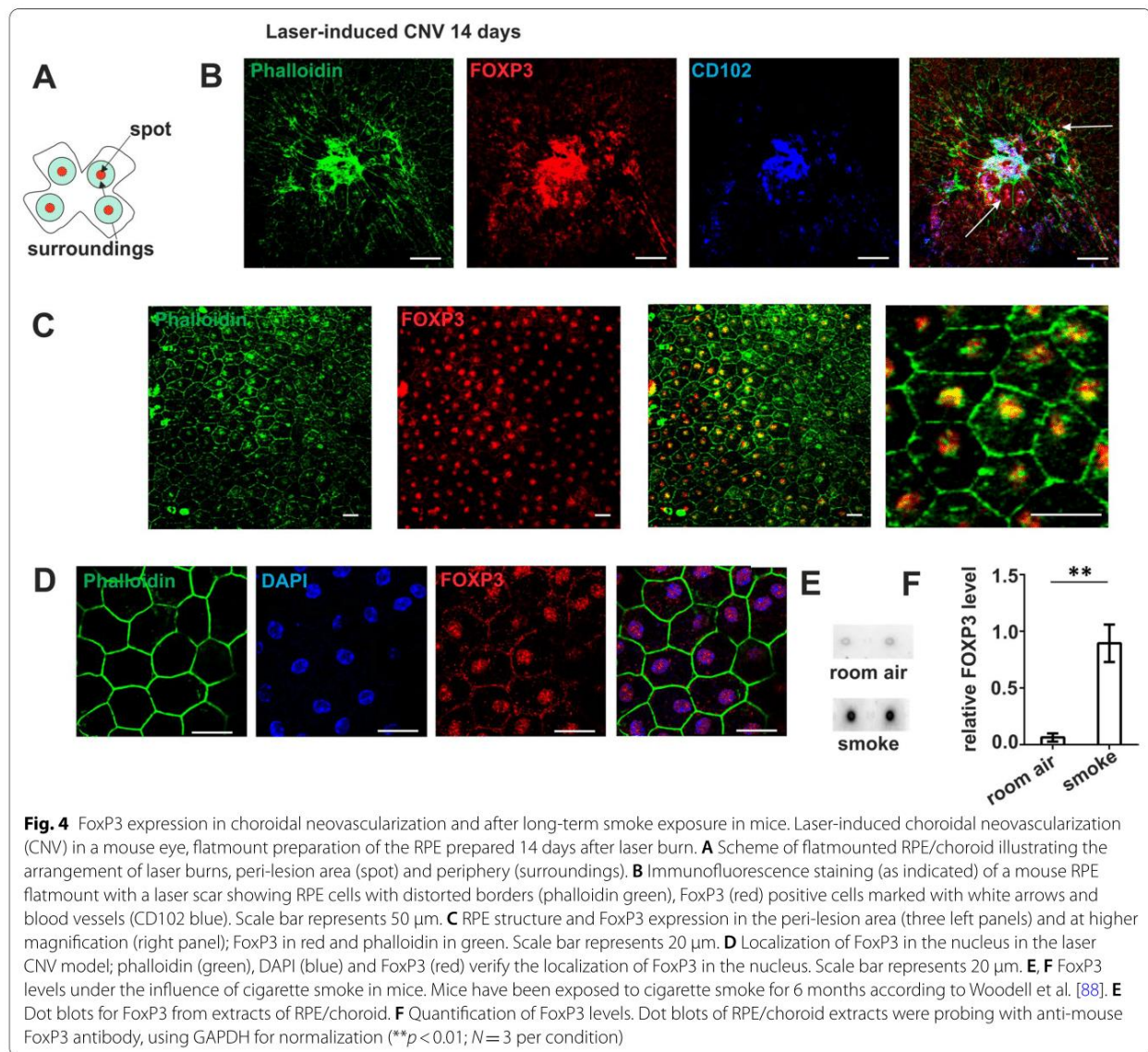


**Fig. 3** FoxP3 expression in the retina of aged rats or rat eyes with uveitis. **A** FoxP3 (red) expression in 10-week-old rats. Blue = DAPI. **B** Same as A, but darkfield to show the retinal structure. **C** FoxP3 (red) expression in 6-month-old rats. Blue = DAPI. **D** Same as C, but darkfield to show the retinal structure. **E** FoxP3 (red) expression in 11-month-old rats. Blue = DAPI. **F** Same as E, but darkfield to show the retinal structure. **G**, FoxP3 (red) expression in 12-week-old rats after induction of experimental uveitis, with T cells and leukocytes invading the photoreceptor layer from the choroid via the RPE.  $N = 3$  animals per age group. **H** Same as G, but darkfield to show the retinal structure. ONL: outer nuclear layer, PR-OS: outer segments of photoreceptors, RPE: retinal pigment epithelium

software [80]. The levels of FoxP3 expression in RPE cells were found similar in 10-week-old (32.4%,  $n = 19$ ) and 6-month-old (28.4%,  $n = 15$ ) rat retinas and significantly increased to the age of 11 months (63.5%,  $n = 6$ ), with  $p = 0.0011$  for 10 weeks to 11 months, and  $p < 0.0001$  for 6 months to 11 months. Interestingly, in 12-week-old

eyes with experimental autoimmune uveitis FoxP3 expression in RPE cells was comparable to 11-month-old untreated rats (62.6%,  $n = 10$ , Fig. 3G).

Another mouse model with relevance for AMD is one with laser burn-induced choroidal neovascularization (CNV) that shows features of wet AMD in humans. It



combines a strong inflammatory response with the formation of new blood vessels from the choroid. In contrast to the *Cx3cr1<sup>GFP/GFP</sup>* mouse model, the laser-induced CNV model includes a stronger inflammatory reaction. To induce neovascularization, four laser spots that break the RPE barrier were placed around the optic nerve head (Fig. 4A). Fourteen days later, flatmount preparations of the outer retina were stained with phalloidin (green) to indicate the cell borders, anti-CD102 (blue) to visualize newly developed blood vessels, and anti-FoxP3 (red) (Fig. 4A, B). An overview of the lasered area (Fig. 4B) shows the newly developed blood vessels in white due to the overlay of the three different fluorophores (right), and FoxP3-positive RPE cells (red staining) at the border of

the CNV as well as in more peripheral areas. At a greater distance to the laser spot (Fig. 4C), the RPE cells were uniformly FoxP3-positive and, as in the *Cx3cr1<sup>GFP/GFP</sup>* mouse model, FoxP3 was localized to the nuclei (Fig. 4D). We have previously characterized this area as a perilesion around the CNV, containing cells that have lost junctional markers and/or their normal hexagonal shape [87]; hence, it was not surprising that FoxP3 expression and nuclear localization was induced in these RPE cells. Thus, in mouse models, we found that both, aging and age-dependent degeneration of RPE cells, as well as laser burn-induced RPE injury followed by neovascularization, induced FoxP3 expression in RPE cells with a major localization in the nucleus.

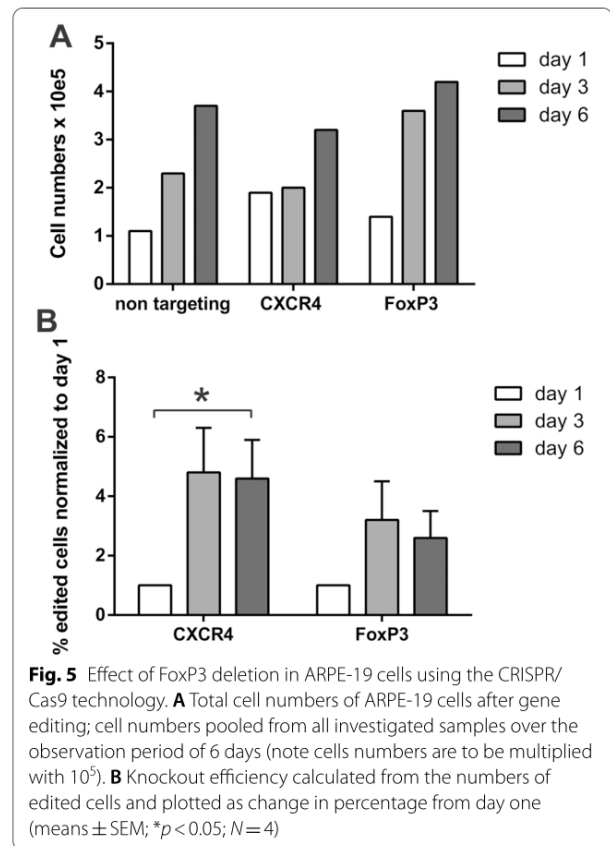


As a final mouse model of AMD-like pathology, we investigated FoxP3 expression in RPE of mice exposed to constant cigarette smoke. In these mice, we have reported RPE alterations, which include changes in RPE signature gene expression as well as mitochondrial changes indicative of oxidative damage [88]. We found eightfold increased levels of FoxP3 in extracts of RPE/choroid from mice that have been exposed to cigarette smoke ("passive smokers") for 6 months when compared to room air-maintained animals (Fig. 4E, F).

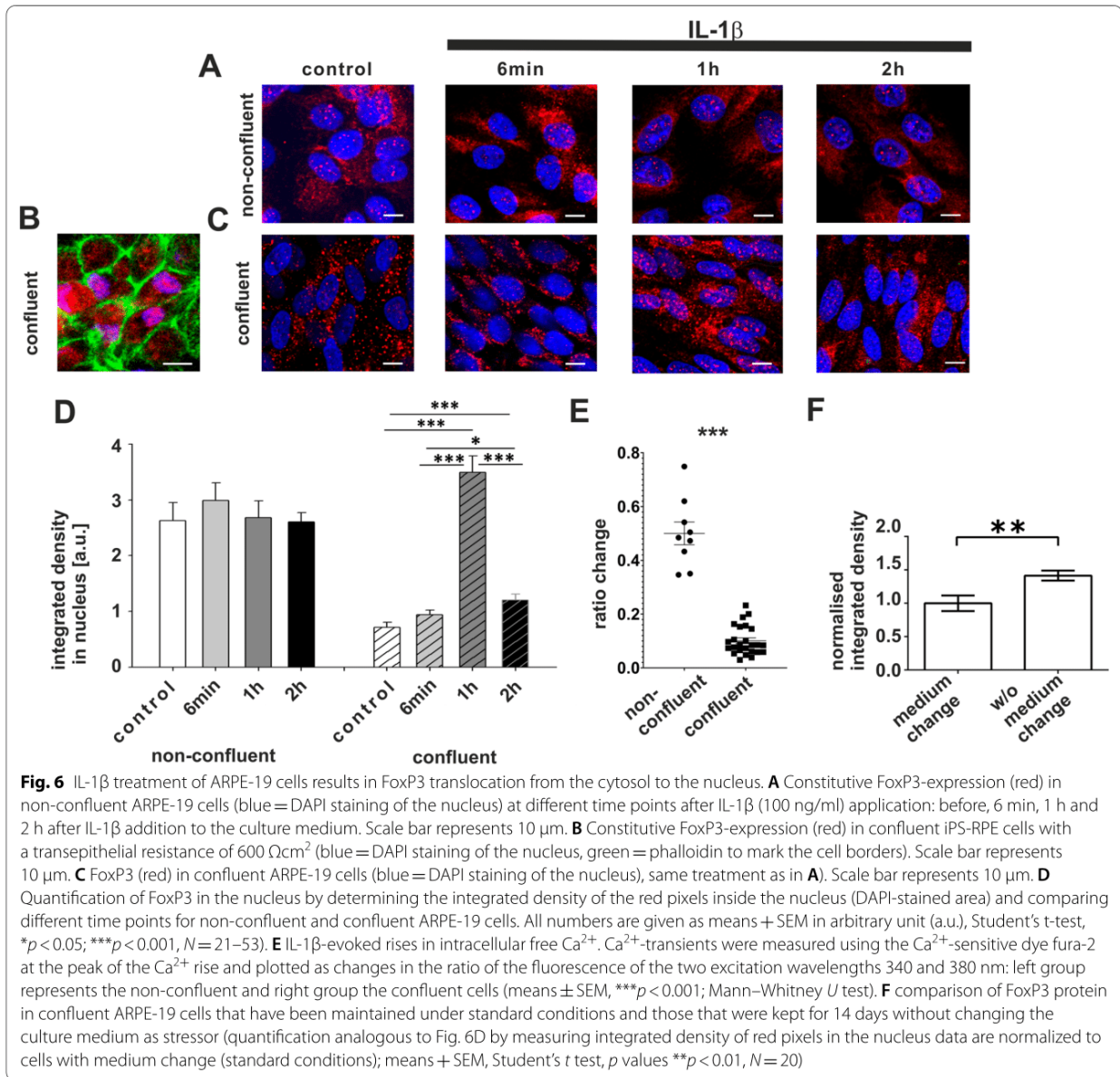
In this manuscript, we also compared confluent grown with non-confluent ARPE-19 cells, assuming that non-confluent RPE cells would represent a more stressed condition. This assumption is based on data published by others, showing that ARPE-19 cells grown as a stable monolayer exhibit gene expression profiles more comparable to those of native primary RPE cells, while the non-confluent cells represent a destabilized condition that leads to rapid changes of the phenotype and loss of RPE differentiation [89, 90].

To investigate the function of FoxP3 expression in ARPE-19 cells, we used CRISPR/Cas9 editing to abolish the FoxP3 gene and, as a control, we knocked out the CXCR4 receptor using the recently established method [91] (Fig. 5). After genome editing, the cells were further cultured and the editing efficiencies as well as the numbers of viable cells were monitored at day 1, 3 and 6 after CRISPR editing and compared to cells electroporated with non-targeting control Cas9 RNPs (Fig. 5A). The total number of viable cells was comparable in non-targeting, CXCR4 KO and FoxP3 KO cell cultures. For comparison, the proliferation rate of untreated ARPE-19 cells over 6 days was determined and is now shown as Additional file 1: Figure S3. Importantly, since Cas9 RNPs remain in the cells for up to 72 h and can introduce further mutations within this time window [92] CRISPR/Cas9 editing of the FoxP3 gene resulted in a peak of 18% edited cells at day 3 and then declined again. Measuring the KO efficiency in percent compared to day one, there is no significant change in the FoxP3 KO group. In contrast, CXCR4 KO cells reached their peak of editing efficiency at day 3 and remained stable with subsequent significantly increased KO efficiency normalized to day one (Fig. 5B). The reason for the reduced frequency of FoxP3-knockout cells over time could be that the non-edited cells within this condition have a cell growth or survival advantage compared to FoxP3 KO cells, thereby outcompeting the FoxP3 KO cells. Overall, our results suggest that FoxP3 expression is beneficial for cell growth in RPE cells.

Taken together, thus far, we have shown that FoxP3 expression and localization to the nucleus is induced in RPE cells in mouse models of AMD, as well as in donor



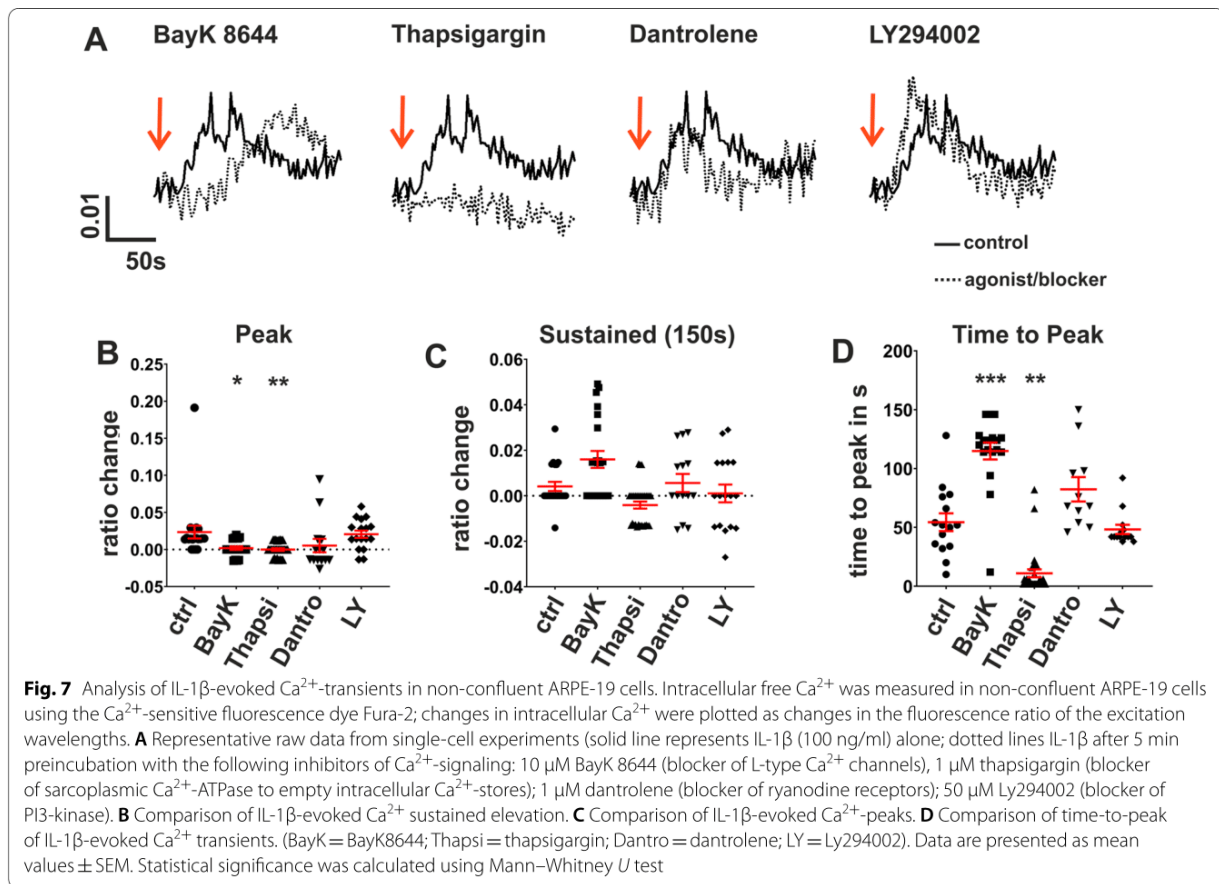
retinas from AMD patients, and that FoxP3 is required for growth of cultured ARPE-19 cells. To further investigate the importance of FoxP3 expression for RPE cells, we used cultured RPE cells. Human RPE cells differentiated from inducible stem cells of healthy donors (iPS-RPE), as well as cells of the established ARPE-19 cell line, showed constitutive expression of FoxP3 with cytosolic and/or nuclear localization (Fig. 6A–C). We selected the ARPE-19 cell line as a model system to study the regulation of FoxP3 in response to AMD-like stressors, as we have previously shown that the anaphylatoxins C3a and C5a modulate FoxP3 phosphorylation in these cells [16]. In order to elucidate a possible link between FoxP3 expression/localization and AMD pathology, we investigated the effects of IL-1 $\beta$ , a major macrophage-derived pro-inflammatory cytokine. A recent hypothesis postulates that a chronic, local presence of monocytes compromises the immune regulatory capacity of the RPE, potentially shifting the phenotype of the RPE from a regulatory type to an immune stimulating effector type [12]. IL-1 $\beta$  is one of the monokines that might lead to the loss of the immune regulatory phenotype of the RPE and has been detected in many AMD-relevant models [38, 50, 93, 94]. Thus, we treated confluent and non-confluent



ARPE-19 cells, which, respectively, simulate the stages of stable and destabilized RPE, with IL-1 $\beta$  and investigated its impact on FoxP3 expression/localization and subsequent cytokine/chemokine secretion.

To evaluate the shift of constitutively expressed FoxP3 from the cytosol to the nucleus in response to IL-1 $\beta$ , we analyzed the percentage of FoxP3 in the nucleus of ARPE-19 cells. For that purpose, confluent and non-confluent cells were exposed to IL-1 $\beta$  (100 ng/ml), and the localization of FoxP3 was investigated by immunofluorescence staining and counting pixels of FoxP3 staining (Fig. 6D). Even under untreated control conditions, confluent and

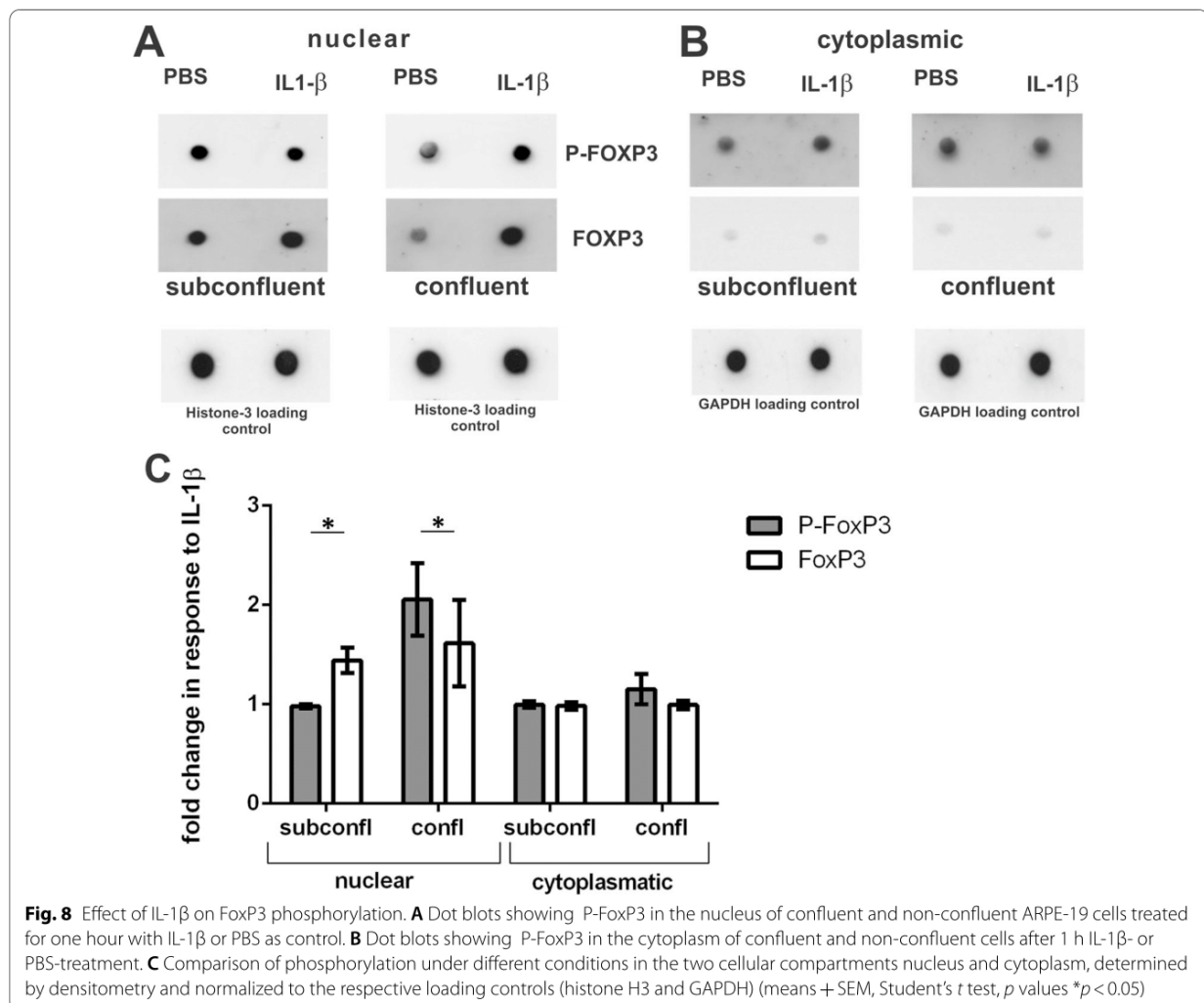
non-confluent cells showed differences in FoxP3 localization (Fig. 6A, C). While in both confluent and non-confluent culture conditions, a significant amount of FoxP3 expression was observed, confluent cells showed predominant FoxP3 localization in the cytosol with a minor fraction in the nuclei (Figs. 6C, 10A). In contrast, non-confluent cells had a larger proportion of FoxP3 in the nuclei (Figs. 6G, 10A). Stimulation with IL-1 $\beta$  also had different effects on cells in these two stages. In non-confluent cells, FoxP3 localization in the nuclei remained unchanged after IL-1 $\beta$  application (Fig. 6A, D). In contrast, in confluent cells IL-1 $\beta$  application led to a transient



increase in nuclear localization of FoxP3 that returned to baseline levels after 2 h, even though IL-1 $\beta$  was still present in the culture media (Fig. 6C, D). Thus, confluent cells seem to represent a baseline state that can become activated after a 1 h exposure to IL-1 $\beta$ , whereas stressed, non-confluent cells already appear to be maximally activated. To rule out the possibility that non-confluent cells might fail to express IL-1 $\beta$  receptors and are thus unable to respond to IL-1 $\beta$ , we measured changes in intracellular free Ca<sup>2+</sup> as a second messenger by fluorescence microscopy-based cell imaging with the Ca<sup>2+</sup>-sensitive fluorescence dye fura-2 as the probe. Interestingly, while all non-confluent cells responded to stimulation with IL-1 $\beta$  with a strong increase in intracellular free Ca<sup>2+</sup>, only a very small proportion of confluent cells were IL-1 $\beta$ -reactive and showed significantly smaller Ca<sup>2+</sup> peaks (Fig. 6E). Taken together, this set of experiments showed that IL-1 $\beta$  induced a transient shift of FoxP3 from the cytosol into the nucleus in confluent RPE cells, whereas the non-confluent cells that displayed a permanent high FoxP3-expression in the nucleus did not experience increased nuclear FoxP3 expression, even

though responded with a strong Ca<sup>2+</sup> signal to only 40 s contact with IL-1 $\beta$ . As another stressor, we kept monolayers of ARPE-19 cells for 14 days without changing the FCS-containing medium. These confluent cells without medium exchange also had increased FoxP3 expression in the nucleus after 14 days (Fig. 6F).

Considering that the non-confluent cells might reflect the stage at which RPE cell loss occurs in AMD [95], we hypothesized that IL-1 $\beta$ -dependent increase of intracellular free Ca<sup>2+</sup> as a second messenger is essential for RPE cells that are more close to die. Thus, we investigated the underlying signaling mechanisms in detail. We studied Ca<sup>2+</sup> signaling in non-confluent ARPE-19 cells using blockers for ion channels and intracellular Ca<sup>2+</sup> stores to investigate whether RPE cells with a predominant nuclear FoxP3 expression display the specialized molecular mechanisms needed of signal transduction. IL-1 $\beta$ -induced Ca<sup>2+</sup> increase was dependent on the activation of L-type Ca<sup>2+</sup> channels through release of Ca<sup>2+</sup> from cytosolic Ca<sup>2+</sup> stores and coupling via ryanodine receptors (Fig. 7A–D). The peak of the IL-1 $\beta$ -evoked Ca<sup>2+</sup>-rise was significantly reduced by either the L-type channel



blocker BayK8644 (10  $\mu$ M), after preincubation with the blocker of sarcoplasmic Ca<sup>2+</sup>-ATPase (SERCA) thapsigargin (1  $\mu$ M) or with dantrolene (1  $\mu$ M), the blocker of ryanodine receptors. The latter one couples release of Ca<sup>2+</sup> from cytoplasmic Ca<sup>2+</sup>-stores with activation of L-type channels. L-type Ca<sup>2+</sup> channel blockade with BayK8644 or ryanodine receptor blockade by dantrolene also slowed down the time-to-peak, indicating that L-Type channels coupling with ryanodine receptors are responsible for the raising phase of the Ca<sup>2+</sup> signal. The blocker of PI3-kinase Ly294002 (50  $\mu$ M) had no effect. In summary, both confluent and non-confluent ARPE-19 cells respond to IL-1 $\beta$  but do so in different ways. IL-1 $\beta$  receptor activation leads to nuclear translocation of FoxP3 in confluent cells but to a Ca<sup>2+</sup> shift in non-confluent cells.

FoxP3 localization in cells is one simple marker for its activity and has already been correlated with substantial

changes in the functional phenotype in both this study and others. Another marker of its activity is the phosphorylation status of FoxP3, that we have previously described in the context of anaphylatoxin-dependent regulation of secretion in RPE cells [16]. Therefore, we measured the proportion of phosphorylated FoxP3 over total FoxP3 from the cytosol and the nuclei and compared these values between confluent and non-confluent cells stimulated with IL-1 $\beta$ . Protein levels were measured in dot blots stained for FoxP3 and phosphorylated (P-)FoxP3, normalized to GAPDH (cytosolic fraction) or Histone 3 (nuclear fraction) (Fig. 8A, B). Using densitometry, we estimated the protein content of P-FoxP3 and total FoxP3 and calculated the ratios (Fig. 8C). In confluent, untreated ARPE-19 cells the amount of P-FoxP3 in the nucleus was higher than in the cytosol. Moreover, confluent ARPE-19 cells showed a higher proportion of P-FoxP3 in the nucleus compared to non-confluent

cells (Fig. 8C), even though the confluent cells display less overall FoxP3 localization in the nucleus (Fig. 6). After application of IL-1 $\beta$ , we found a slight decrease of P-FoxP3 in the nuclear fraction of confluent cells, whereas the amount in the cytosol remained unchanged. Again, the non-confluent cells behaved differently. In untreated cells, the proportion of P-FoxP3 in the nucleus was equal to that in the cytosol (Fig. 8C). However, following stimulation with IL-1 $\beta$ , we found a significant increase in the proportion of P-FoxP3 in the nucleus (Fig. 8C), although the amount of total FoxP3 remained unchanged (Fig. 6).

To assess whether the corresponding cellular response might contribute to an AMD-relevant RPE cell behavior, we investigated the secretory phenotype of ARPE-19 cells under conditions for which we can correlate the potential impact of FoxP3 by its localization in the nucleus or cytosol. Again, we used confluent and non-confluent cells that were stimulated with IL-1 $\beta$ , and the supernatants were collected at the end of the incubation time and profiles of secreted factors generated (Fig. 9). In general, both confluent and non-confluent showed comparable spectra of secreted factors that were changed by IL-1 $\beta$  stimulation over time (Fig. 9A, B). However, the confluent cells produced much higher amounts (2.5 times up to 20 times higher) of the identified factors at baseline and at the early time points (6 min and 1 h) compared to the non-confluent cells, while the maximal secretion after 2 h of IL-1 $\beta$ -stimulation was similar. Under both culture conditions, IL-1 $\beta$  led to a selected increase in the secretion of IL-8 and IL-6 among the 14 investigated cytokines and chemokines measured as increasing concentrations in the culture medium. However, MCP-1 was only enhanced in non-confluent cells.

In addition to the IL-1 $\beta$ -dependent changes in FoxP3 localization and secretion profiles, we also observed IL-1 $\beta$ -independent stimulation of FoxP3 activity by translocation from cytoplasm to nucleus. After a scratch through the confluent monolayer of ARPE-19 cells, we found a translocation of FoxP3 into the nucleus in cells of the injured culture 24 h later, as well as a secretion profile that compares to the one induced by IL-1 $\beta$  stimulation. In contrast to IL-1 $\beta$ -stimulation, the scratch disrupting the cell monolayer induced VEGF-A secretion in addition to MCP-1, IL-8 and IL-6 in ARPE-19 cells (Fig. 10A, B). Although the cells had been in culture without change of their medium (containing 5% FCS and stable glutamine) for 2 weeks, they secreted high amounts of cytokines and responded differentially to IL-1 $\beta$ -stimulation and scratch. The cytokine concentrations in culture medium were comparable to those from APRE-19 cell cultures only challenged with IL-1 $\beta$

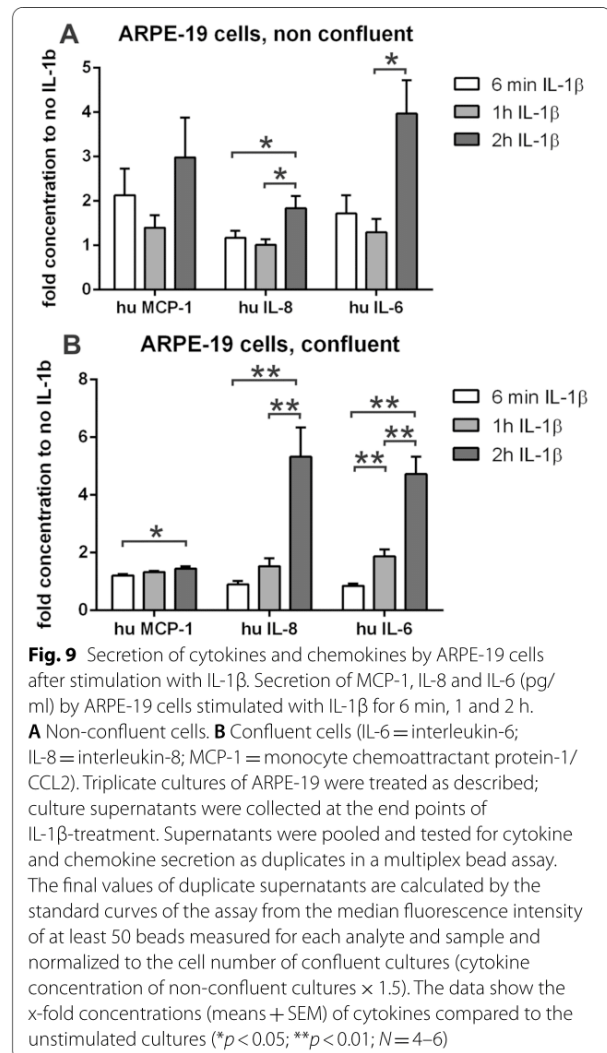
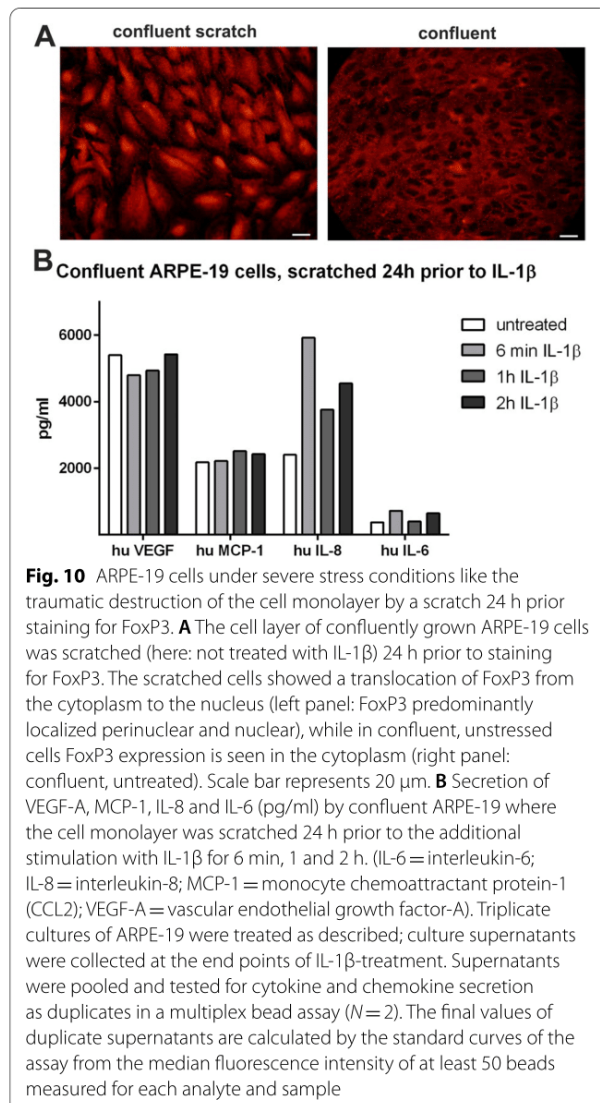


(Fig. 9), while the cytokine expression pattern was changed.

In summary, we showed that FoxP3 activity is differentially regulated under varying conditions that mimic cellular stress of the RPE and local inflammation in AMD (Figs. 9, 10).

## Conclusions

Here we have shown that FoxP3 is expressed in the aged retina and under circumstances of retinal degeneration as well as in acute and chronic inflammation in various species including humans. FoxP3 seems to be an important transcription factor of RPE cells under stress conditions. It is under regulatory control, in part, by oxidative stress, loss of cell–cell contact, or the pro-inflammatory cytokine IL-1 $\beta$ . Oxidative stress (cigarette smoke) and IL-1 $\beta$  can affect the translocation of FoxP3 between the



cytosol and the nucleus, as well as its phosphorylation status. As IL-1 $\beta$  changed the FoxP3 activation status, resulting in changed secretory profiles of RPE cells, we conclude that changed secretions (namely MCP-1 and IL-8) are important target genes of that transcription factor. A correlation between cellular confluence and non-confluence in *in vivo* and *in vitro* models indicated that cells in intact monolayers, such as those in pre-disease states, or cells even localized at a far distance to areas of degeneration, express FoxP3. However, this expression is mostly localized to the cytoplasm, with weak abundance in the nucleus. In contrast, cells in diseased areas, which possess disrupted monolayers, showed uniformly high localization of FoxP3 to the nucleus. Our data suggest

that these differences in the cellular distribution of FoxP3 influence the reactivity of RPE cells to the pro-inflammatory cytokine IL-1 $\beta$  and might represent a basis for the immunologic switch in RPE cells from healthy to a diseased state. Our data further suggested that in cells with abundant nuclear FoxP3, FoxP3-mediated gene expression might be regulated by Ca<sup>2+</sup>-dependent phosphorylation of FoxP3. In cells with a major proportion of FoxP3 present in the cytosol, regulation of FoxP3-mediated gene expression primarily depended on the translocation from cytosol to the nucleus.

We recently reported that FoxP3 protein is not detected in the RPE of young animals. Here we report that with aging, murine RPE cells started to express FoxP3, which was predominantly localized in the cytosol. However, in disease conditions such as experimental uveitis or laser-induced CNV, FoxP3 abundantly localized to the nucleus, which is suggestive of an increased activity of the transcription factor on gene expression in the RPE. Moreover, in the laser CNV model, we documented abundant nuclear FoxP3 in the neovascular areas or zones with loss of RPE cells as well as neighboring RPE peri-lesion areas. Importantly, we also confirmed FoxP3-expression in human RPE from geographic atrophy lesions, which was not detected in age-matched healthy retinas. The time between FoxP3 expression in the RPE and onset of clinical signs of geographic atrophy is currently not known in humans, but is expected to be individually variable due to the differences in lifestyle and genetic background, which could explain the lack of FoxP3 in aged, but healthy human eyes. Thus, FoxP3 appears as a pivotal transcription factor for the RPE associated with aging and conditions of stress. This is further reflected by our investigations of the ARPE-19 cell line, in which we report constitutive FoxP3 expression. We speculate that under culture conditions this human RPE cell line does not reach its final differentiation state that would permit a shut-down of FoxP3 expression, but instead remains at a certain level of permanent cell stress (i.e., similar to the aged RPE in rodents). The observation that the localization of FoxP3 varied with the status of the cell culture supports this hypothesis. In non-confluent (i.e., more stressed) cells, FoxP3 localized predominantly to the nucleus, whereas in cells forming an intact monolayer (i.e., healthy) for more than 2 weeks the majority of FoxP3 was found in the cytosol. ARPE-19 cells can regain a phenotype and transcriptome like native RPE after culture in confluence for months, while we maintained the cells as confluent cultures for up to 3 weeks only [89, 90]. Thus, the not yet terminally differentiated cells may still require FoxP3 expression to retain cellular integrity. The deletion experiments targeting the FoxP3 gene in ARPE-19 support the importance of FoxP3 expression for the

resistance of these cells to the stress of CRISPR/Cas9 gene editing by electroporation. Since ARPE-19 cells are of male origin they are hemizygous for the FoxP3 gene encoded on the X-chromosome, resulting in a complete knockout of FoxP3 by CRISPR/Cas9-gene editing in an efficiently targeted cell and reduced recovery of FoxP3-deficient cells. Based on these observations, we propose that FoxP3 expression and its translocation to the nucleus in situations of enhanced stress is essential for the resistance against age-dependent changes or RPE damage, or acute or chronic inflammation like in uveitis.

Co-culturing of RPE cells and lymphocytes results in the induction of regulatory, FoxP3-expressing T cells that support the maintenance of the ocular immune privilege, which requires TGF- $\beta$ -production by the RPE and helps for the induction of peripheral Tregs [96, 97]. Since TGF- $\beta$  plays major roles in the immune privilege of the eye and is also produced by RPE cells, FoxP3 expression in the RPE might be induced by autocrine activation with TGF- $\beta$  [98]. FoxP3 expression of the RPE cells themselves was not yet known when these RPE-lymphocyte co-culture experiments were originally performed. Interestingly, in human and rat T cells, FoxP3 is transiently localized to the cytoplasm of activated effector T cells, and only when they have differentiated to regulatory cells is FoxP3 found in the nucleus [63, 99–103].

The shift to nuclear localization of FoxP3 in RPE cells under stress conditions might reflect the gain of a regulatory, immunosuppressive phenotype of the RPE, necessary to maintain the ocular immune privilege once the outer blood–retina barrier is endangered. We do not yet know whether we can immediately transfer the knowledge of FoxP3 in regulatory T lymphocytes to the RPE, but so far, our findings support this hypothesis. In Tregs, phosphorylation of FoxP3 at Ser-418 supports their regulatory/suppressive function. Here we have shown that in RPE cells the nuclear FoxP3 is also phosphorylated at Ser-418, likely indicating a highly immune-suppressive RPE-phenotype [104, 105]. In general, we observed a shift of intracellular FoxP3 localization upon IL-1 $\beta$  stimulation. On one hand, we found an increase of FoxP3 in the nucleus in confluent cultures that seemed to be accompanied by a decrease of nuclear phosphorylated FoxP3. On the other hand, in subconfluent cultures we observed no changes of cellular FoxP3 localization but an increase of phosphorylated FoxP3 in the nucleus.

Here, these differences might be related to the different cell culture conditions of ARPE-19 cells grown in transwells (confluent) versus glass cover slips (non-confluent). However, it is worthwhile to mention that under both conditions we see a robust expression of FoxP3. The analysis of the dot blots from transwell-grown cells showed a significant amount of phosphorylated FoxP3

under baseline conditions already. Thus, the strongly increased FoxP3 expression goes along with a large proportion of already phosphorylated FoxP3.

To imitate stress, we further investigated factors that lead to FoxP3 activation and the resulting changes in the secretory activity of RPE cells. Since the RPE forms the border between the immune system and the inner eye as an "educational barrier", RPE cells need to communicate with the cells of the immune system using a common set of cytokines and receptors [4, 49]. Activated macrophages release IL-1 $\beta$  and are thought to be drivers of chronic inflammation leading to AMD [12, 27, 38]; and although expression of the IL-1 $\beta$  receptor on RPE cells was postulated, it was never proven at a functional level [106, 107].

IL-1 $\beta$ -mediated signaling in the RPE was examined in confluent and non-confluent ARPE-19 cells by investigating the intracellular Ca<sup>2+</sup> increase along with FoxP3 translocation to the nucleus. Confluent cells reacted to IL-1 $\beta$  stimulation with very small Ca<sup>2+</sup> peaks in only a small subset of cells. In contrast, in response to IL-1 $\beta$  stimulation, non-confluent cells showed a widespread increase in free cytosolic Ca<sup>2+</sup> as a second messenger that was driven by the release of Ca<sup>2+</sup> from cytosolic Ca<sup>2+</sup> stores as well as ryanodine receptor-dependent activation of L-type Ca<sup>2+</sup> channels [108]. When analyzing FoxP3 localization, confluent ARPE-19 displayed a transient increase of FoxP3 translocation to the nucleus, whereas non-confluent cells with already "constitutive" nuclear FoxP3 did not respond with altered FoxP3 localization. Phosphorylation of FoxP3 at Ser-418 was found to be increased in non-confluent cells and IL-1 $\beta$  stimulation resulted in an increase of phosphorylated nuclear FoxP3, whereas confluent cells already showed maximal levels of nuclear P-FoxP3 that could not be further elevated although the total Foxp3 is lower than in non-confluent cells. Finally, we investigated the effect of risk factors of AMD that induce oxidative stress, like cigarette smoke, on FoxP3 expression/localization in animal models. Mice exposed to intermittent cigarette smoke for 6 months [88], exhibit changes in gene expression in the RPE as well as mitochondrial alteration, but no apparent cell death [88]. In smoke exposed mice, levels of FoxP3 in the RPE were significantly elevated when compared to room air-maintained mice. In an in vitro assay with scratched confluent cell monolayers of ARPE-19 cells, FoxP3 localization was predominantly in the nucleus compared to the non-injured, confluent monolayer cultures. These collective data indicate that damage of the RPE cell monolayer leads to a phenotype of FoxP3 expression that is resembling non-confluent cells. Furthermore, culturing ARPE-19 cells for 14 days without medium change increased the FoxP3 expression, however, with expression in the

cytosol. Thus, this pattern of stress-induced FoxP3 activation indicates that RPE cells might need FoxP3 expression in situations of oxidative stress, inflammation and trauma for their function and probably also for their survival.

We hypothesize that these events are also represented by the animal models with AMD relevance, where we could identify FoxP3 expression and translocation into the nucleus. The aged retina with increased oxidative stress and the *Cx3cr1<sup>GFP/GFP</sup>* mouse are both models with a decreased innate immune regulation and function, which leads to a loss of RPE cells with increasing age. The laser-induced choroidal neovascularization model is driven by a strong local inflammatory response caused by cell necrosis and the break of the outer blood–retina barrier. Moreover, retinal laser burn causes a breakdown of the ocular immune privilege even in the non-treated partner eye [109]. In each of these models, the stressor leads to loss in RPE integrity, which is accompanied by translocation of FoxP3 into the nucleus.

To answer the question of whether FoxP3-dependent regulation of gene expression is required for the RPE to control local immune responses, we investigated changes in the secretory profile of ARPE-19 cells under conditions correlated with FoxP3 activation. First, we found that confluent ARPE-19 cells showed much stronger reactions of secretory activity compared to non-confluent cells, which is suggestive of a more stable phenotype when cells have reached confluence. Under stimulation with IL-1 $\beta$ , both confluent and non-confluent cells increased the secretion of IL-6 and IL-8, while non-confluent cells only showed increased MCP-1 after 2 h of IL-1 $\beta$  exposure. In physiologically relevant conditions, the secretion of MCP-1 by already damaged/stressed RPE cells in response to IL-1 $\beta$  released from macrophages could in turn further attract and stimulate monocytes and thus create a feedback loop perpetuating inflammation. The changes of mRNA expression in RPE/choroid samples with age in *Cx3cr1<sup>GFP/GFP</sup>* mice support this conclusion. Here, increased levels of FoxP3 coincide with increased levels of IL-1 $\beta$ . Indeed, Sennlaub et al. [15] had previously demonstrated that increased levels of MCP-1 lead to increased numbers of monocytes in the outer retina. Increased numbers of monocytes, along with increased IL-1 $\beta$  expression, might in turn enhance Cxcl1 expression, the mouse analogue of human IL-8, in concordance with our data shown here. Interestingly, when compared with wild-type mice, the Cxcl1 expression is lower in the *Cx3cr1<sup>GFP/GFP</sup>* mice at 8 months of age. We interpret this effect as an early onset of interaction of the RPE with immune cells in the *Cx3cr1<sup>GFP/GFP</sup>* mouse model, where both, monocytes and T cells, are dysregulated by the gene deficiency.

Another way to stress ARPE-19 cells is the destruction of the confluent monolayer of cells by a scratch, which disrupts the contact between the cells, creating an injury comparable to laser burn in animal models. The damage induced the secretion of high levels of MCP-1, IL-8, IL-6 and especially VEGF-A that could not be further increased by addition of IL-1 $\beta$ . VEGF-A was only induced by the scratch-mediated cell destruction, and not solely by IL-1 $\beta$  application. The expression of this panel of genes also occurred in the retina of the *Cx3cr1<sup>GFP/GFP</sup>* mouse model with relevance for geographic atrophy. In the degenerative state of the retina, the cytokines MCP-1, IL-8 (the mouse homologue is Cxcl1), and IL-1 $\beta$ , were significantly increased. As IL-8 is known to play a role in autocrine self-protection of the RPE against degenerative impacts, the FoxP3-driven reaction likely represents a rescue mechanism [49, 110].

The secretion profile indicates a pro-inflammatory phenotype of the RPE when FoxP3 is active. As IL-1 $\beta$  is a driver towards that phenotype and is secreted by monocytes that invade the outer retina in AMD-like inflammatory scenarios [27, 107], it is likely that the secretion activity of monocytes drives FoxP3 translocation into the nucleus. The cell morphology of the aged RPE implies regenerating activities in response to defects in the monolayer [82]. Thus, IL-1 $\beta$  secreted by monocytes establishes a combined self-regenerating and pro-inflammatory phenotype in the RPE. This would explain why RPE cells in the aged, but healthy retina showed only weak FoxP3 expression in the nucleus since monocytes are lacking in the healthy situation. However, we found that also RPE cells that are in a far distance to laser injuries showed FoxP3 expression, suggesting a spread of information about a dangerous situation over the RPE. This was also observed in cultured ARPE-19 cells after scratching the monolayer, where the information of the injury and the nuclear FoxP3 translocation was spreading over the entire culture. This might be in correlation with a previously published observation of our group that not only the laser site contains activated monocytes and likely microglia cells [75], but there is a pan-retinal activation of microglia that might induce the FoxP3 translocation to the nucleus.

In summary, we found that RPE cells induce FoxP3 expression and nuclear localization under both stress conditions and in pre-degenerative states. FoxP3 expression during RPE cell stress seems essential for cell survival, as suggested by the reduced resistance of ARPE-19 cells to stress after FoxP3-knockout. Cell degeneration or strong local inflammation enhanced FoxP3 phosphorylation and/or translocation into the nucleus, which was also dependent on the cellular status (confluent or not).



## The consequences of FoxP3 expression and its subcellular localization in RPE cells require further investigation.

### Abbreviations

AMD: Age-related macular degeneration; BSA: Bovine serum albumin; DAPI: 4',6-Diamidino-2-phenylindole; EGTA: Ethylene glycol-bis(aminoethylether)-N,N,N',N'-tetraacetate; GAPDH: Glycerin aldehyde-3-phosphate-dehydrogenase; GFP: Green fluorescent protein; C3, C3a, C5a: Complement factor 3, -3a, -5; Ca: Calcium; CFH: Complement factor H; CNV: Choroidal neovascularization; CRISPR/Cas9: **C**lustered **R**egularly **I**nterspaced **S**hort **P**alindromic **R**epeats/CRISPR-associated 9; CXCR4: CX-chemokine receptor 4; CX3CR1: CX3-chemokine receptor 1; FoxP3: Forkhead-box-protein P3; IFN- $\gamma$ : Interferon- $\gamma$ ; IL-1 $\beta$ : Interleukin-1 $\beta$ ; MCP-1: Monocyte chemoattractant protein-1; PBS: Phosphate-buffered saline; RPE: Retinal pigment epithelium; TBS: TRIS-buffered saline; TGF- $\beta$ : Transforming growth factor- $\beta$ ; Treg: Regulatory T cell; VEGF-A: Vascular endothelial growth factor-A; WT: Wild type.

### Supplementary Information

The online version contains supplementary material available at <https://doi.org/10.1186/s12974-022-02620-w>.

**Additional file 1.** The additional file provides statistical comparison of gene expression between wildtype and *Cx3cr1<sup>GFP/GFP</sup>* mice at the different time points, control data for human FoxP3 staining, the growth rate of ARPE-19 to compare with Crisp/Cas treated ARPE-19 cells and uncropped dot plots.

### Acknowledgements

The authors greatly acknowledge the contributions of PD Dr. Andreas Ohlmann and Prof. Dr. Stephan Thurau in microscope technique. We thank Dr. Norbert Kociok for the help with qPCR calculations, Prof. Marius Adler and Susanne Luft (CRTD Dresden, Germany) for providing iPS-RPE. We thank Shahryar Khattak and the Facility ("Stem Cell Engineering Facility at Center for Regenerative Therapies Dresden (CRTD), Technische Universität Dresden") for providing the iPS cell line. We are very thankful to Kyrie Wilson and R.J. Lambert for text editing that greatly improved our manuscript. The proliferation of untreated RPE cells was measured by Andjela Sekulic—it is greatly acknowledged.

### Author contributions

ASA: investigation, formal analysis, writing editing, data curation; LS: investigation, formal analysis, data curation, visualization; MD-M: investigation, formal analysis; ML: investigation, formal analysis; CR: investigation, formal analysis; JR: investigation, methodology, formal analysis, visualization; KS: data curation, supervision, validation, writing review and editing; BA: investigation, formal analysis, visualization; I-MP: investigation, formal analysis, visualization; BR: supervision, data curation, validation, writing review and editing; FS: supervision, data curation, writing review and editing; NR: investigation, formal analysis, conceptualization, supervision, visualization; validation GW: conceptualization, investigation, data curation, visualization, writing original draft, validation, project administration, supervision; OS: project administration, conceptualization, data curation, funding acquisition, supervision, validation, visualization, writing original draft. All authors read and approved the final manuscript.

### Funding

Open Access funding enabled and organized by Projekt DEAL. We are very thankful for the financial support by the Dr. Werner Jackstaedt-Stiftung and by the Einstein Foundation/BIH Visiting Fellow Program. There is no role of the funding institutions in the study design, data collection/analysis, interpretation and writing of the manuscript.

### Availability of data and materials

The datasets used and/or analyzed during the current study are available from the corresponding author on reasonable request.

### Declarations

#### Ethics approval and consent to participate

Not applicable.

#### Consent for publication

Not applicable.

#### Competing interests

All authors declare no competing interests to this study.

#### Author details

<sup>1</sup>Experimental Ophthalmology, Department of Ophthalmology, Charité - Universitätsmedizin Berlin, Corporate Member of Freie Universität, Berlin Institute of Health, Humboldt-University, 10117 Berlin, Germany. <sup>2</sup>Department of Ophthalmology, University Hospital of Ulm, 89075 Ulm, Germany. <sup>3</sup>Section of Immunobiology, Department of Ophthalmology, University Hospital, LMU Munich, 80336 Munich, Germany. <sup>4</sup>Institut de La Vision, Sorbonne Université, INSERM, CNRS, 75012 Paris, France. <sup>5</sup>Institut Für Med. Mikrobiologie, Immunologie Und Hygiene, TU München, 81675 Munich, Germany. <sup>6</sup>Department of Ophthalmology, College of Medicine, Medical University South Carolina, Charleston, SC 29425, USA.

Received: 12 May 2022 Accepted: 9 October 2022

Published online: 22 October 2022

### References

- Streilein JW. Regional immunity and ocular immune privilege. *Chem Immunol.* 1999;73:11–38.
- Streilein JW. Immunoregulatory mechanisms of the eye. *Prog Retin Eye Res.* 1999;18(3):357–70.
- Streilein JW. Ocular immune privilege: therapeutic opportunities from an experiment of nature. *Nat Rev Immunol.* 2003;3(11):879–89.
- Shechter R, London A, Schwartz M. Orchestrated leukocyte recruitment to immune-privileged sites: absolute barriers versus educational gates. *Nat Rev Immunol.* 2013;13(3):206–18.
- Strauss O. Pharmacology of the retinal pigment epithelium, the interface between retina and body system. *Eur J Pharmacol.* 2016;787:84–93.
- Strauss O. The retinal pigment epithelium in visual function. *Physiol Rev.* 2005;85(3):845–81.
- Lakkaraju A, Umapathy A, Tan LX, Daniele L, Philp NJ, Boesze-Battaglia K, et al. The cell biology of the retinal pigment epithelium. *Prog Retin Eye Res.* 2020;78:100846.
- Sparrow JR, Hicks D, Hamel CP. The retinal pigment epithelium in health and disease. *Curr Mol Med.* 2010;10(9):802–23.
- Camelo S, Calippe B, Lavalette S, Dominguez E, Hur J, Devevre E, et al. Thinning of the RPE and choroid associated with T lymphocyte recruitment in aged and light-challenged mice. *Mol Vis.* 2015;21:1051–9.
- Houssot M, Sennlaub F. Thrombospondin-1 and pathogenesis of age-related macular degeneration. *J Ocul Pharmacol Ther.* 2015;31(7):406–12.
- Levy O, Calippe B, Lavalette S, Hu SJ, Raoul W, Dominguez E, et al. Apolipoprotein E promotes subretinal mononuclear phagocyte survival and chronic inflammation in age-related macular degeneration. *EMBO Mol Med.* 2015;7(2):211–26.
- Mathis T, Houssot M, Eandi C, Beguier F, Touhami S, Reichman S, et al. Activated monocytes resist elimination by retinal pigment epithelium and downregulate their OTX2 expression via TNF-alpha. *Aging Cell.* 2017;16(1):173–82.
- Omri S, Behar-Cohen F, de Kozak Y, Sennlaub F, Verissimo LM, Jonet L, et al. Microglia/macrophages migrate through retinal epithelium barrier by a transcellular route in diabetic retinopathy: role of PKCzeta in the Goto Kakizaki rat model. *Am J Pathol.* 2011;179(2):942–53.
- Touhami S, Beguier F, Augustin S, Charles-Messance H, Vignaud L, Nandrot EF, et al. Chronic exposure to tumor necrosis factor alpha induces retinal pigment epithelium cell dedifferentiation. *J Neuroinflammation.* 2018;15(1):85.

15. Sennlaub F, Auvynet C, Calippe B, Lavalette S, Poupel L, Hu SJ, et al. CCR2(+) monocytes infiltrate atrophic lesions in age-related macular disease and mediate photoreceptor degeneration in experimental subretinal inflammation in Cx3cr1 deficient mice. *EMBO Mol Med*. 2013;5(11):1775–93.
16. Busch C, Annamalai B, Abduslamova K, Reichhart N, Huber C, Lin Y, et al. Anaphylatoxins Activate Ca(2+), Akt/P13-Kinase, and FOXO1/FoxP3 in the Retinal Pigment Epithelium. *Front Immunol*. 2017;8:703.
17. Brandstetter C, Holz FG, Krohne TU. Complement Component C5a primes retinal pigment epithelial cells for inflammasome activation by lipofuscin-mediated photooxidative damage. *J Biol Chem*. 2015;290(52):31189–98.
18. Fernandez-Godino R, Garland DL, Pierce EA. A local complement response by RPE causes early-stage macular degeneration. *Hum Mol Genet*. 2015;24(19):5555–69.
19. Fernandez-Godino R, Pierce EA. C3a triggers formation of sub-retinal pigment epithelium deposits via the ubiquitin proteasome pathway. *Sci Rep*. 2018;8(1):9679.
20. Hu M, Liu B, Jawad S, Ling D, Casady M, Wei L, et al. C5a contributes to intraocular inflammation by affecting retinal pigment epithelial cells and immune cells. *Br J Ophthalmol*. 2011;95(12):1738–44.
21. Long Q, Cao X, Bian A, Li Y. C3a Increases VEGF and Decreases PEDF mRNA levels in human retinal pigment epithelial cells. *Biomed Res Int*. 2016;2016:6958752.
22. Ramos de Carvalho JE, Klaassen I, Vogels IM, Schipper-Krom S, van Noorden CJ, Reits E, et al. Complement factor C3a alters proteasome function in human RPE cells and in an animal model of age-related RPE degeneration. *Invest Ophthalmol Vis Sci*. 2013;54(10):6489–501.
23. Schafer N, Grosche A, Schmitt SI, Braunger BM, Pauly D. Complement components showed a time-dependent local expression pattern in constant and acute white light-induced photoreceptor damage. *Front Mol Neurosci*. 2017;10:197.
24. Skeie JM, Fingert JH, Russell SR, Stone EM, Mullins RF. Complement component C5a activates ICAM-1 expression on human choroidal endothelial cells. *Invest Ophthalmol Vis Sci*. 2010;51(10):5336–42.
25. Vogt SD, Barnum SR, Curcio CA, Read RW. Distribution of complement anaphylatoxin receptors and membrane-bound regulators in normal human retina. *Exp Eye Res*. 2006;83(4):834–40.
26. Wang YP, Hui YN, Wang YS, Wang HY. Detection of C5a receptor expressions on human epiretinal membranes and cultured RPE cells by immunohistochemical staining. *Xi Bao Yu Fen Zi Mian Yi Xue Za Zhi*. 2003;19(3):221–2.
27. Dietrich L, Lucius R, Roeder J, Klettner A. Interaction of inflammationally activated retinal pigment epithelium with retinal microglia and neuronal cells. *Exp Eye Res*. 2020;199:108167.
28. Klettner A, Hamann T, Schluter K, Lucius R, Roeder J. Retinal pigment epithelium cells alter the pro-inflammatory response of retinal microglia to TLR-3 stimulation. *Acta Ophthalmol*. 2014;92(8):e621–9.
29. Kumar MV, Nagineni CN, Chin MS, Hooks JJ, Detrick B. Innate immunity in the retina: Toll-like receptor (TLR) signaling in human retinal pigment epithelial cells. *J Neuroimmunol*. 2004;153(1–2):7–15.
30. Tarallo V, Hirano Y, Gelfand BD, Dridi S, Kerur N, Kim Y, et al. DICER1 loss and Alu RNA induce age-related macular degeneration via the NLRP3 inflammasome and MyD88. *Cell*. 2012;149(4):847–59.
31. Terheyden L, Roeder J, Klettner A. Basolateral activation with TLR agonists induces polarized cytokine release and reduces barrier function in RPE in vitro. *Graefes Arch Clin Exp Ophthalmol*. 2021;259(2):413–24.
32. Zhu Y, Dai B, Li Y, Peng H. C5a and toll-like receptor 4 crosstalk in retinal pigment epithelial cells. *Mol Vis*. 2015;21:1122–9.
33. Sun Q, Gong L, Qi R, Qing W, Zou M, Ke Q, et al. Oxidative stress-induced KLF4 activates inflammatory response through IL17RA and its downstream targets in retinal pigment epithelial cells. *Free Radic Biol Med*. 2020;147:271–81.
34. Zhang J, Bai Y, Huang L, Qi Y, Zhang Q, Li S, et al. Protective effect of autophagy on human retinal pigment epithelial cells against lipofuscin fluorophore A2E: implications for age-related macular degeneration. *Cell Death Dis*. 2015;6: e1972.
35. Zamiri P, Masli S, Streilein JW, Taylor AW. Pigment epithelial growth factor suppresses inflammation by modulating macrophage activation. *Invest Ophthalmol Vis Sci*. 2006;47(9):3912–8.
36. Anderson OA, Finkelstein A, Shima DT. A2E induces IL-1 $\alpha$  production in retinal pigment epithelial cells via the NLRP3 inflammasome. *PLoS ONE*. 2013;8(6): e67263.
37. Catalioto RM, Valenti C, Maggi CA, Giuliani S. Enhanced Ca(2+) response and stimulation of prostaglandin release by the bradykinin B2 receptor in human retinal pigment epithelial cells primed with proinflammatory cytokines. *Biochem Pharmacol*. 2015;97(2):189–202.
38. Chen M, Hombrebueno JR, Luo C, Penalva R, Zhao J, Colhoun L, et al. Age- and light-dependent development of localized retinal atrophy in CCL2(-/-)CX3CR1(GFP/GFP) mice. *PLoS ONE*. 2013;8(4): e61381.
39. Efstathiou NE, Moustafa GA, Maidana DE, Konstantinou EK, Notomi S, Barbisan PRT, et al. Acadesine suppresses TNF-alpha induced complement component 3 (C3), in retinal pigment epithelial (RPE) cells. *PLoS ONE*. 2020;15(12): e0244307.
40. Huang H, Liu Y, Wang L, Li W. Age-related macular degeneration phenotypes are associated with increased tumor necrosis-alpha and subretinal immune cells in aged Cxcr5 knockout mice. *PLoS ONE*. 2017;12(3): e0173716.
41. Jasielska M, Semkova I, Shi X, Schmidt K, Karagiannis D, Kokkinou D, et al. Differential role of tumor necrosis factor (TNF)-alpha receptors in the development of choroidal neovascularization. *Invest Ophthalmol Vis Sci*. 2010;51(8):3874–83.
42. Li W, Ma N, Liu MX, Ye BJ, Li YJ, Hu HY, et al. C1q/TNF-related protein-9 attenuates retinal inflammation and protects blood-retinal barrier in db/db mice. *Eur J Pharmacol*. 2019;853:289–98.
43. van Bilsen K, van Hagen PM, Bastiaans J, van Meurs JC, Missotten T, Kuijpers RW, et al. The neonatal Fc receptor is expressed by human retinal pigment epithelial cells and is downregulated by tumour necrosis factor-alpha. *Br J Ophthalmol*. 2011;95(6):864–8.
44. Zhang SX, Wang JJ, Gao G, Shao C, Mott R, Ma JX. Pigment epithelium-derived factor (PEDF) is an endogenous antiinflammatory factor. *FASEB J*. 2006;20(2):323–5.
45. Ando Y, Sato Y, Kudo A, Watanabe T, Hirakata A, Okada AA, et al. Anti-inflammatory effects of the NFkappaB inhibitor dehydroxymethylepox-yquinomicin on ARPE19 cells. *Mol Med Rep*. 2020;22(1):582–90.
46. Ehlken C, Grundel B, Michels D, Junker B, Stahl A, Schlunck G, et al. Increased expression of angiogenic and inflammatory proteins in the vitreous of patients with ischemic central retinal vein occlusion. *PLoS ONE*. 2015;10(5): e0126859.
47. Jo DH, Yun JH, Cho CS, Kim JH, Kim JH, Cho CH. Interaction between microglia and retinal pigment epithelial cells determines the integrity of outer blood-retinal barrier in diabetic retinopathy. *Glia*. 2019;67(2):321–31.
48. Lin T, Walker GB, Kurji K, Fang E, Law G, Prasad SS, et al. Parainflammation associated with advanced glycation endproduct stimulation of RPE in vitro: implications for age-related degenerative diseases of the eye. *Cytokine*. 2013;62(3):369–81.
49. Diedrichs-Möhrling M, Niesik S, Priglinger CS, Thureau SR, Obermayr F, Sperl S, et al. Intraocular DHODH-inhibitor PP-001 suppresses relapsing experimental uveitis and cytokine production of human lymphocytes, but not of RPE cells. *J Neuroinflammation*. 2018;15(1):54.
50. Klettner A, Brinkmann A, Winkelmann K, Kackenmeister T, Hildebrandt J, Roeder J. Effect of long-term inflammation on viability and function of RPE cells. *Exp Eye Res*. 2020;200: 108214.
51. Amadi-Obi A, Yu CR, Dambuzza I, Kim SH, Marrero B, Ekwuagu CE. Interleukin 27 induces the expression of complement factor H (CFH) in the retina. *PLoS ONE*. 2012;7(9): e45801.
52. Marazita MC, Dugour A, Marquioni-Ramella MD, Figueroa JM, Suburo AM. Oxidative stress-induced premature senescence dysregulates VEGF and CFH expression in retinal pigment epithelial cells: implications for age-related macular degeneration. *Redox Biol*. 2016;7:78–87.
53. Pauly D, Agarwal D, Dana N, Schafer N, Biber J, Wunderlich KA, et al. Cell-type-specific complement expression in the healthy and diseased retina. *Cell Rep*. 2019;29(9):2835–48.
54. Weinberger AW, Eddahabi C, Carstesen D, Zipfel PF, Walter P, Skerka C. Human complement factor H and factor H-like protein 1 are expressed in human retinal pigment epithelial cells. *Ophthalmic Res*. 2014;51(2):59–66.
55. Zhang Y, Huang Q, Tang M, Zhang J, Fan W. Complement Factor H expressed by retinal pigment epithelium cells can suppress

- neovascularization of human umbilical vein endothelial cells: an in vitro study. *PLoS ONE*. 2015;10(6): e0129945.
56. Mulfaul K, Ozaki E, Fernando N, Brennan K, Chirco KR, Connolly E, et al. Toll-like receptor 2 facilitates oxidative damage-induced retinal degeneration. *Cell Rep*. 2020;30(7):2209–24.
  57. Luo C, Zhao J, Madden A, Chen M, Xu H. Complement expression in retinal pigment epithelial cells is modulated by activated macrophages. *Exp Eye Res*. 2013;112:93–101.
  58. Rohrer B, Coughlin B, Kunchithapautham K, Long Q, Tomlinson S, Takahashi K, et al. The alternative pathway is required, but not alone sufficient, for retinal pathology in mouse laser-induced choroidal neovascularization. *Mol Immunol*. 2011;48(6–7):e1–8.
  59. Trakkides TO, Schafer N, Reichenthaler M, Kuhn K, Brandwijk R, Toonen EJM, et al. Oxidative Stress increases endogenous complement-dependent inflammatory and angiogenic responses in retinal pigment epithelial cells independently of exogenous complement sources. *Antioxidants (Basel)*. 2019;8:11.
  60. Hori S, Nomura T, Sakaguchi S. Control of regulatory T cell development by the transcription factor Foxp3. *Science*. 2003;299(5609):1057–61.
  61. Kasprovicz DJ, Smallwood PS, Tyznik AJ, Ziegler SF, Scurfin (FoxP3) controls T-dependent immune responses in vivo through regulation of CD4+ T cell effector function. *J Immunol*. 2003;171(3):1216–23.
  62. Wang J, Ioan-Facsinay A, Voort E, Huizinga T, Toes R. Transient expression of FOXP3 in human activated nonregulatory CD4+ T cells. *Eur J Immunol*. 2007;37:129–38.
  63. Wildner G. Are rats more human than mice? *Immunobiology*. 2019;224(1):172–6.
  64. Magg T, Mannert J, Ellwart JW, Schmid I, Albert MH. Subcellular localization of FOXP3 in human regulatory and nonregulatory T cells. *Eur J Immunol*. 2012;42(6):1627–38.
  65. Dong Y, Yang C, Pan F. Post-translational regulations of Foxp3 in treg cells and their therapeutic applications. *Front Immunol*. 2021;12: 626172.
  66. Munoz-Rojas AR, Mathis D. Tissue regulatory T cells: regulatory chameleons. *Nat Rev Immunol*. 2021;78:89.
  67. Georgiev P, Charbonnier LM, Chatila TA. Regulatory T Cells: the Many Faces of Foxp3. *J Clin Immunol*. 2019;39(7):623–40.
  68. Wang L, Liu R, Li W, Chen C, Katoh H, Chen GY, et al. Somatic single hits inactivate the X-linked tumor suppressor FOXP3 in the prostate. *Cancer Cell*. 2009;16(4):336–46.
  69. Zhang HY, Sun H. Up-regulation of Foxp3 inhibits cell proliferation, migration and invasion in epithelial ovarian cancer. *Cancer Lett*. 2010;287(1):91–7.
  70. Zuo T, Wang L, Morrison C, Chang X, Zhang H, Li W, et al. FOXP3 is an X-linked breast cancer suppressor gene and an important repressor of the HER-2/ErbB2 oncogene. *Cell*. 2007;129(7):1275–86.
  71. Redpath M, Xu B, van Kempen LC, Spatz A. The dual role of the X-linked FoxP3 gene in human cancers. *Mol Oncol*. 2011;5(2):156–63.
  72. Tallon B, Bhawan J. FoxP3 expression is increased in cutaneous squamous cell carcinoma with perineural invasion. *J Cutan Pathol*. 2010;37(11):1184–5.
  73. Tan B, Behren A, Anaka M, Vella L, Cebon J, Mariadason JM, et al. FOXP3 is not mutated in human melanoma. *Pigment Cell Melanoma Res*. 2012;25(3):398–400.
  74. Combadiere C, Feumi C, Raoul W, Keller N, Rodero M, Pezard A, et al. CX3CR1-dependent subretinal microglia cell accumulation is associated with cardinal features of age-related macular degeneration. *J Clin Invest*. 2007;117(10):2920–8.
  75. Crespo-Garcia S, Corkhill C, Roubeix C, Davids AM, Kociok N, Strauss O, et al. Inhibition of Placenta Growth Factor Reduces Subretinal Mononuclear Phagocyte Accumulation in Choroidal Neovascularization. *Invest Ophthalmol Vis Sci*. 2017;58(12):4997–5006.
  76. Lingeman E, Jeans C, Corn JE. Production of Purified CasRNPs for Efficient Genome Editing. *Curr Protoc Mol Biol*. 2017;120:31101–9.
  77. Hultquist JF, Schumann K, Woo JM, Manganaro L, McGregor MJ, Doudna J, et al. A Cas9 ribonucleoprotein platform for functional genetic studies of HIV-host interactions in primary human T Cells. *Cell Rep*. 2016;17(5):1438–52.
  78. Schumann K, Raju SS, Lauber M, Kolb S, Shifrut E, Cortez JT, et al. Functional CRISPR dissection of gene networks controlling human regulatory T cell identity. *Nat Immunol*. 2020;21(11):1456–66.
  79. Brinkman EK, Chen T, Amendola M, van Steensel B. Easy quantitative assessment of genome editing by sequence trace decomposition. *Nucleic Acids Res*. 2014;42(22): e168.
  80. Schneider CA, Rasband WS, Eliceiri KW. NIH Image to ImageJ: 25 years of image analysis. *Nat Methods*. 2012;9(7):671–5.
  81. Busch C, Annamalai B, Abduslamova K, Reichhart N, Huber C, Lin Y, et al. Anaphylatoxins Activate Ca2+, Akt/PI3-Kinase, and FOXO1/FoxP3 in the retinal pigment epithelium. *Front Immunol*. 2017;8:703.
  82. Chen M, Rajapakse D, Fraczek M, Luo C, Forrester JV, Xu H. Retinal pigment epithelial cell multinucleation in the aging eye - a mechanism to repair damage and maintain homeostasis. *Aging Cell*. 2016;15(3):436–45.
  83. Bozic CR, Gerard NP, von Uexkull-Guldenband C, Kolakowski LF Jr, Conklyn MJ, Breslow R, et al. The murine interleukin 8 type B receptor homologue and its ligands. Expression and biological characterization. *J Biol Chem*. 1994;269(47):29355–8.
  84. Rovai LE, Herschman HR, Smith JB. The murine neutrophil-chemoattractant chemokines LIX, KC, and MIP-2 have distinct induction kinetics, tissue distributions, and tissue-specific sensitivities to glucocorticoid regulation in endotoxemia. *J Leukoc Biol*. 1998;64(4):494–502.
  85. Diedrichs-Mohring M, Nelson PJ, Proudfoot AE, Thureau SR, Wildner G. The effect of the CC chemokine receptor antagonist Met-RANTES on experimental autoimmune uveitis and oral tolerance. *J Neuroimmunol*. 2005;164(1–2):22–30.
  86. Thureau SR, Mempel TR, Flugel A, Diedrichs-Mohring M, Krombach F, Kawakami N, et al. The fate of autoreactive, GFP+ T cells in rat models of uveitis analyzed by intravitreal fluorescence microscopy and FACS. *Int Immunol*. 2004;16(11):1573–82.
  87. Obert E, Strauss R, Brandon C, Grek C, Ghatnekar G, Gourdie R, et al. Targeting the tight junction protein, zonula occludens-1, with the connexin43 mimetic peptide, alphaCT1, reduces VEGF-dependent RPE pathophysiology. *J Mol Med (Berl)*. 2017;95(5):535–52.
  88. Woodell A, Coughlin B, Kunchithapautham K, Casey S, Williamson T, Ferrell WD, et al. Alternative complement pathway deficiency ameliorates chronic smoke-induced functional and morphological ocular injury. *PLoS ONE*. 2013;8(6): e67894.
  89. Tian J, Ishibashi K, Honda S, Boylan SA, Hjelmeland LM, Handa JT. The expression of native and cultured human retinal pigment epithelial cells grown in different culture conditions. *Br J Ophthalmol*. 2005;89(11):1510–7.
  90. Samuel W, Jaworski C, Postnikova OA, Kutty RK, Duncan T, Tan LX, et al. Appropriately differentiated ARPE-19 cells regain phenotype and gene expression profiles similar to those of native RPE cells. *Mol Vis*. 2017;23:60–89.
  91. Schumann K, Lin S, Boyer E, Simeonov DR, Subramaniam M, Gate RE, et al. Generation of knock-in primary human T cells using Cas9 ribonucleoproteins. *Proc Natl Acad Sci U S A*. 2015;112(33):10437–42.
  92. Kim H, Kim JS. A guide to genome engineering with programmable nucleases. *Nat Rev Genet*. 2014;15(5):321–34.
  93. Wooff Y, Man SM, Aggio-Bruce R, Natoli R, Fernando N. IL-1 Family Members Mediate Cell Death, Inflammation and Angiogenesis in Retinal Degenerative Diseases. *Frontiers in Immunology*. 2019;10.
  94. Dabouz R, Cheng CWH, Abram P, Omri S, Cagnone G, Sawmy KV, et al. An allosteric interleukin-1 receptor modulator mitigates inflammation and photoreceptor toxicity in a model of retinal degeneration. *J Neuroinflammation*. 2020;17(1):359.
  95. Zanzottera EC, Ach T, Huisingh C, Messinger JD, Spaide RF, Curcio CA. Visualizing retinal pigment epithelium phenotypes in the transition to geographic atrophy in age-related macular degeneration. *Retina*. 2016;36(Suppl 1):S12–25.
  96. Imai A, Sugita S, Kawazoe Y, Horie S, Yamada Y, Keino H, et al. Immunosuppressive properties of regulatory T cells generated by incubation of peripheral blood mononuclear cells with supernatants of human RPE cells. *Invest Ophthalmol Vis Sci*. 2012;53(11):7299–309.
  97. Vega JL, Saban D, Carrier Y, Masli S, Weiner HL. Retinal pigment epithelial cells induce foxp3(+) regulatory T cells via membrane-bound TGF-beta. *Ocul Immunol Inflamm*. 2010;18(6):459–69.
  98. Tran DQ. TGF-beta: the sword, the wand, and the shield of FOXP3(+) regulatory T cells. *J Mol Cell Biol*. 2012;4(1):29–37.

99. Allan SE, Crome SQ, Crellin NK, Passerini L, Steiner TS, Bacchetta R, et al. Activation-induced FOXP3 in human T effector cells does not suppress proliferation or cytokine production. *Int Immunol*. 2007;19(4):345–54.
100. Gavin MA, Torgerson TR, Houston E, DeRoos P, Ho WY, Stray-Pedersen A, et al. Single-cell analysis of normal and FOXP3-mutant human T cells: FOXP3 expression without regulatory T cell development. *Proc Natl Acad Sci U S A*. 2006;103(17):6659–64.
101. Kmieciak M, Gowda M, Graham L, Godder K, Bear HD, Marincola FM, et al. Human T cells express CD25 and Foxp3 upon activation and exhibit effector/memory phenotypes without any regulatory/suppressor function. *J Transl Med*. 2009;7:89.
102. Pillai V, Ortega SB, Wang CK, Karandikar NJ. Transient regulatory T-cells: a state attained by all activated human T-cells. *Clin Immunol*. 2007;123(1):18–29.
103. Wang J, Ioan-Facsinay A, van der Voort EI, Huizinga TW, Toes RE. Transient expression of FOXP3 in human activated nonregulatory CD4+ T cells. *Eur J Immunol*. 2007;37(1):129–38.
104. Deng G, Song X, Fujimoto S, Piccirillo CA, Nagai Y, Greene MI. Foxp3 Post-translational Modifications and Treg Suppressive Activity. *Front Immunol*. 2019;10:2486.
105. Nie H, Zheng Y, Li R, Guo TB, He D, Fang L, et al. Phosphorylation of FOXP3 controls regulatory T cell function and is inhibited by TNF-alpha in rheumatoid arthritis. *Nat Med*. 2013;19(3):322–8.
106. Jaffe GJ, Van Le L, Valea F, Haskill S, Roberts W, Arend WP, et al. Expression of interleukin-1 alpha, interleukin-1 beta, and an interleukin-1 receptor antagonist in human retinal pigment epithelial cells. *Exp Eye Res*. 1992;55(2):325–35.
107. Lavalette S, Raoul W, Houssier M, Camelo S, Levy O, Calippe B, et al. Interleukin-1beta inhibition prevents choroidal neovascularization and does not exacerbate photoreceptor degeneration. *Am J Pathol*. 2011;178(5):2416–23.
108. Beskina O, Miller A, Mazzocco-Spezia A, Pulina MV, Golovina VA. Mechanisms of interleukin-1beta-induced Ca2+ signals in mouse cortical astrocytes: roles of store- and receptor-operated Ca2+ entry. *Am J Physiol Cell Physiol*. 2007;293(3):C1103–11.
109. Lucas K, Karamichos D, Mathew R, Zieske JD, Stein-Streilein J. Retinal laser burn-induced neuropathy leads to substance P-dependent loss of ocular immune privilege. *J Immunol*. 2012;189(3):1237–42.
110. Rossi O, Karczewski J, Stolte EH, Brummer RJ, van Nieuwenhoven MA, Meijerink M, et al. Vectorial secretion of interleukin-8 mediates autocrine signalling in intestinal epithelial cells via apically located CXCR1. *BMC Res Notes*. 2013;6:431.

### Publisher's Note

Springer Nature remains neutral with regard to jurisdictional claims in published maps and institutional affiliations.

Ready to submit your research? Choose BMC and benefit from:

- fast, convenient online submission
- thorough peer review by experienced researchers in your field
- rapid publication on acceptance
- support for research data, including large and complex data types
- gold Open Access which fosters wider collaboration and increased citations
- maximum visibility for your research: over 100M website views per year

At BMC, research is always in progress.

Learn more [biomedcentral.com/submissions](https://biomedcentral.com/submissions)



## Curriculum Vitae

Ahmed Samir Ahmed Alfaar,

MBBCh, Dip Inf., MSc<sup>Ophthalmology</sup>, MSc<sup>Oncology</sup>, Dr. med., FEBO

Mein Lebenslauf wird aus datenschutzrechtlichen Gründen in der elektronischen Version meiner Arbeit nicht veröffentlicht

---

## Publication list

### Journal articles:

\*; Corresponding author, **Underlined**; First Author/Shared first author; **Gray**; Not indexed in Pubmed, IF: Impact factor

#### 2022

Abdelazeem B, Abbas KS, Shehata J, El-Shahat NA, Eltaras MM, Qaddoumi I, **Alfaar AS** (2022) Survival trends for patients with retinoblastoma between 2000 and 2018: What has changed? *Cancer Med* Accepted Online.

doi: 10.1002/cam4.5406 **Q2 IF: 4.711**

**Alfaar AS**, Stürzbecher L, Diedrichs-Möhrling M, Lam M, Roubéix C, Ritter J, Schumann K, Annamalai B, Pompös I-M, Rohrer B, Sennlaub F, Reichhart N, Wildner G, Strauß O (2022) FoxP3 expression by retinal pigment epithelial cells: transcription factor with potential relevance for the pathology of age-related macular degeneration. *J Neuroinflammation* 19:260.

doi: 10.1186/s12974-022-02620-w **Q1 IF: 9.587**

**Alfaar AS**, Saad AM, KhalafAllah MT, Elsherif OE, Osman MH, Strauß O (2021) Second primary malignancies of eye and ocular adnexa after a first primary elsewhere in the body. *Graefes Arch Clin Exp Ophthalmol* 259:515–526.

doi:10.1016/j.jid.2022.04.013 **Q1 IF: 7.590** **IF(2020): 3.117** **IF(2019): 2.396**

**Alfaar AS**, Suckert CN, Rehak M, Girbardt C (2022) The epidemiology of adults' eyelid malignancies in Germany between 2009 and 2015; An analysis of 42,710 patients' data. *Eur J Ophthalmol* 33:11206721221125018.

doi:10.1177/11206721221125018 **Q4 IF: 1.922**

**Alfaar A**, Saad A, Chlad P, Elsherif OE, Elshami M, Busch C, Rehak M (2022) Uveal melanoma and marital status: a relationship that affects survival. *Int Ophthalmol* 42:3857–3867.

doi: 10.1007/s10792-022-02406-2 **Q3 IF: 2.029**

#### 2021

**Alfaar AS**, Saad A, Wiedemann P, Rehak M (2022) The epidemiology of uveal melanoma in Germany: a nationwide report of incidence and survival between 2009 and 2015. *Graefes Arch Clin Exp Ophthalmol* 260:1723–1731.

doi:10.1007/s00417-021-05317-7 **Q2 IF: 3.535** **IF(2020): 3.117** **IF(2019): 2.396**

GBD 2019 Blindness and Vision Impairment Collaborators, Vision Loss Expert Group of the Global Burden of Disease Study (2021) Trends in prevalence of blindness and distance and near vision impairment over 30 years: an analysis for the Global Burden of Disease Study. *Lancet Glob Heal* 9:e130–e143.

doi:10.1016/S2214-109X(20)30425-3 **Q1 IF: 38.927** **IF(2020): 26.763** **IF(2019): 21.597**

GBD 2019 Blindness and Vision Impairment Collaborators, Vision Loss Expert Group of the Global Burden of Disease Study (2021) Causes of blindness and vision impairment in 2020 and trends over 30 years, and prevalence of avoidable blindness in relation to VISION 2020: the Right to Sight: an analysis for the Global Burden of Disease Study. *Lancet Glob Heal* 9:e144–e160.

doi:10.1016/S2214-109X(20)30489-7 **Q1 IF: 38.927** **IF(2020): 26.763** **IF(2019): 21.597**

#### 2020

**Alfaar AS**, Saad A, Elzouki S, Abdel-Rahman MH, Strauss O, Rehak M (2020) Uveal melanoma-associated cancers revisited. *ESMO open* 5:e000990.

doi:10.1136/esmoopen-2020-000990 **Q1 IF: 6.883** **IF(2020): 6.540** **IF(2019): 5.329**

El Zomor H, Nour R, Saad A, Taha H, Shelil AE, Aleieldin A, Saad Zaghloul M, **Alfaar AS** (2021) Unilateral retinoblastoma; natural history and an age-based protocol in 248 patients. *Eye (Lond)* 35:2564–2572.

[doi:10.1038/s41433-020-01275-2](https://doi.org/10.1038/s41433-020-01275-2) [Q1 IF: 4.456](#) [IF\(2020\): 3.775](#) [IF\(2019\): 2.455](#)

**Alfaar AS**, Saad AM, KhalafAllah MT, Elsherif OE, Osman MH, Strauß O (2021) Second primary malignancies of eye and ocular adnexa after a first primary elsewhere in the body. *Graefes Arch Clin Exp Ophthalmol* 259:515–526.

[doi:10.1007/s00417-020-04896-1](https://doi.org/10.1007/s00417-020-04896-1) [Q2 IF: 3.535](#) [IF\(2020\): 3.117](#) [IF\(2019\): 2.396](#) [IF\(2018\): 2.250](#)

Hammad M, Hosny M, Khalil EM, **Alfaar AS**, Fawzy M (2021) Pediatric ependymoma: A single-center experience from a developing country. *Indian J Cancer* 58:378–386.

[doi: 10.4103/ijc.IJC\\_373\\_19](https://doi.org/10.4103/ijc.IJC_373_19) [Q4 IF: 1.397](#) [IF\(2020\): 1.224](#) [IF\(2019\): 0.765](#)

Saad AM, Elmatboly AM, Gad MM, Al-Husseini MJ, Jazieh KA, Alzuabi MA, **Alfaar AS** (2020) Association of Brain Cancer With Risk of Suicide. *JAMA Netw open* 3:e203862.

[doi:10.1001/jamanetworkopen.2020.3862](https://doi.org/10.1001/jamanetworkopen.2020.3862) [Q1 IF: 13.353](#) [IF\(2020\): 8.485](#) [IF\(2019\): 5.032](#)

Zekri W, Hammad M, Rashed WM, Ahmed G, Elshafie M, Adly MH, Elborai Y, Abdalla B, Taha H, Elkinae N, Refaat A, Younis A, **Alfaar AS** (2020) The outcome of childhood adrenocortical carcinoma in Egypt: A model from developing countries. *Pediatr Hematol Oncol* 37:198–210.

[doi:10.1080/08880018.2019.1710309](https://doi.org/10.1080/08880018.2019.1710309) [Q3 IF: 2.070](#) [IF\(2020\): 1.969](#) [IF\(2019\): 1.232](#) [IF\(2018\): 1.041](#)

Cordes M, Bucichowski P, Alfaar AS, Tsang SH, Almedawar S, Reichhart N, Strauß O (2020) Inhibition of Ca<sup>2+</sup> channel surface expression by mutant bestrophin-1 in RPE cells. *FASEB J* 34:4055–4071.

[doi:10.1096/fj.201901202RR](https://doi.org/10.1096/fj.201901202RR) [Q1 IF: 5.834](#) [IF\(2020\): 5.192](#) [IF\(2019\): 4.966](#)

## 2019

Reichhart N, Schöberl S, Keckeis S, **Alfaar AS**, Roubeix C, Cordes M, Crespo-Garcia S, Haeckel A, Kociok N, Föckler R, Fels G, Mataruga A, Rauh R, Milenkovic VM, Zühlke K, Klussmann E, Schellenberger E, Strauß O (2019) Anoctamin-4 is a bona fide Ca<sup>2+</sup>-dependent non-selective cation channel. *Sci Rep* 9:2257.

[doi: 10.1038/s41598-018-37287-y](https://doi.org/10.1038/s41598-018-37287-y) [Q2 IF: 4.122](#) [IF\(2019\): 3.998](#) [IF\(2018\): 4.011](#)

Saad AM, Gad MM, Al-Husseini MJ, AlKhayat MA, Rachid A, **Alfaar AS**, Hamoda HM (2019) Suicidal death within a year of a cancer diagnosis: A population-based study. *Cancer* 125:972–979.

[doi:10.1002/cncr.31876](https://doi.org/10.1002/cncr.31876) [Q1 IF: 6.537](#) [IF\(2019\): 5.772](#) [IF\(2018\): 6.102](#)

*\*\*This article was well received. It was in the top 5% of all research outputs scored by Altmetric. It was mentioned by many news outlets, including Reuters, as newsworthy and was selected for a news story.*

Al-Husseini MJ, Saad AM, El-Shewy KM, Nissan NE, Gad MM, Alzuabi MA, Samir Alfaar A (2019) Prior malignancy impact on survival outcomes of glioblastoma multiforme; population-based study. *Int J Neurosci* 129:447–454.

[doi:10.1080/00207454.2018.1538989](https://doi.org/10.1080/00207454.2018.1538989) [IF: 1.848](#) [IF\(2019\): 2.107](#) [IF\(2018\): 1.852](#)

## 2018

Rashed WM, Saad AM, Al-Husseini MJ, Galal AM, Ismael AM, Al-Tayep AM, El Shafie A, Ali MA, **Alfaar AS** (2018) Incidence of adrenal gland tumor as a second primary malignancy: SEER-based study. *Endocr Connect* 7:1040–8.

[doi:10.1530/EC-18-0304](https://doi.org/10.1530/EC-18-0304) [IF: 3.041](#) [IF\(2018\): 2.474](#) [IF\(2017\): 3.041](#)

Adly MH, Sobhy M, Rezk MA, Ishak M, Afifi MA, Shafie A El, Ali MA, Zekri W, **Alfaar AS**, Rashed WM (2018) Risk of second malignancies among survivors of pediatric thyroid cancer. *Int J Clin Oncol* 23:625–633.

[doi:10.1007/s10147-018-1256-9](https://doi.org/10.1007/s10147-018-1256-9) [IF: 2.610](#) [IF\(2018\): 2.503](#) [IF\(2017\): 2.610](#)

1. Chamdine O, Elhawary GAS, Alfaar AS, Qaddoumi I (2018) The incidence of brainstem primitive neuroectodermal tumors of childhood based on SEER data. *Child's Nerv Syst* 34:431–439.

[doi:10.1007/s00381-017-3687-4](https://doi.org/10.1007/s00381-017-3687-4) [IF: 1.235](#) [IF\(2018\): 1.327](#) [IF\(2017\): 1.235](#)

## 2017

**Alfaar AS, Hassan WM, Bakry MS, Qaddoumi I (2017)** Neonates with cancer and causes of death; lessons from 615 cases in the SEER databases. *Cancer Med* 6:1817–1826.

doi:10.1002/cam4.1122 | IF: 3.362 | IF(2017): 3.202 | IF(2016): 3.362

**Alfaar AS, Chantada G, Qaddoumi I (2018)** Survivin is high in retinoblastoma, but what lies beneath? *J Am Assoc Pediatr Ophthalmol Strabismus*.

doi:10.1016/j.jaapos.2017.02.021 | Q4 IF: 1.325 | IF(2017): 0.916 | IF(2016): 0.997

**Rashed WM, Zekri W, Awad M, Taha H, Abdalla B, Alfaar AS (2017)** Nonfunctioning Adrenocortical Carcinoma in Pediatric Acute Lymphoblastic Leukemia. *J Pediatr Hematol Oncol* 39:150–152.

doi:10.1097/MPH.0000000000000699 | Q4 IF: 1.170 | IF(2017): 1.060 | IF(2016): 1.076

**Elzomor H, Taha H, Nour R, Aleieldin A, Zaghloul MS, Qaddoumi I, Alfaar AS (2017)** A multidisciplinary approach to improving the care and outcomes of patients with retinoblastoma at a pediatric cancer hospital in Egypt. *Ophthalmic Genet* 38:345–351.

doi: 10.1080/13816810.2016.1227995 | Q4 IF: 1.27 | IF(2017): 1.574 | IF(2016): 1.277

## 2016

**Hassan WM, Bakry MS, Hassan HM, Alfaar AS (2016)** Incidence of orbital, conjunctival and lacrimal gland malignant tumors in USA from Surveillance, Epidemiology and End Results, 1973-2009. *Int J Ophthalmol* 9:1808–1813.

doi:10.18240/ijjo.2016.12.18 | Q4 IF: 1.645 | IF(2016): 1.177 | IF(2015): 0.939

**Alfaar AS, Nour R, Bakry MS, Kamal M, Hassanain O, Labib RM, Rashed WM, Elzomor H, Alieldin A, Taha H, Zaghloul MS, Ezzat S, AboElnaga S, others (2017)** A change roadmap towards research paradigm in low-resource countries: retinoblastoma model in Egypt. *Int Ophthalmol* 37:111–118.

doi:10.1007/s10792-016-0233-4 | Q3 IF: 2.029 | IF(2016): 1.077 | IF(2015): 0.959

**Alfaar AS, Hassan WM, Bakry MS, Ezzat S (2017)** Clinical Research Recession: Training Needs Perception Among Medical Students. *J Cancer Educ* 32:728–733.

doi:10.1007/s13187-016-0995-4 | Q3 IF: 1.771 | IF(2016): 1.329 | IF(2015): 1.368

**Elzomor H, Taha H, Nour R, Aleieldin A, Zaghloul MS, Qaddoumi I, Alfaar AS (2017)** A multidisciplinary approach to improving the care and outcomes of patients with retinoblastoma at a pediatric cancer hospital in Egypt. *Ophthalmic Genet* 38:345–351.

doi: 10.1089/bio.2015.0004 | Q3 IF: 1.274 | IF(2016): 1.277 | IF(2015): 1.886

## 2015

**El Zomor H, Nour R, Alieldin A, Taha H, Montasr MM, Moussa E, El Nadi E, Ezzat S, Alfaar AS (2015)** Clinical presentation of intraocular retinoblastoma; 5-year hospital-based registry in Egypt. *J Egypt Natl Canc Inst* 27:195–203.

doi:10.1016/j.jnci.2015.09.002 | No IF yet

**ElZomor H, Taha H, Aleieldin A, Nour R, Zaghloul MS, Fawzi M, Kamel A, Alfaar AS (2015)** High Risk Retinoblastoma: Prevalence and Success of Treatment in Developing Countries. *Ophthalmic Genet* 36:287–9.

doi:10.3109/13816810.2015.1016241 | Q4 IF: 1.274 | IF(2015): 1.886 | IF(2014): 1.455

**Taha H, Amer HZ, El-Zomor H, Alieldin A, Nour R, Konsowa R, Zekri W, El Nadi E, Alfaar AS (2015)** Phthisis bulbi: clinical and pathologic findings in retinoblastoma. *Fetal Pediatr Pathol* 34:176–84.

doi: 10.3109/15513815.2015.1014951 | Q4 IF: 1.412 | IF(2015): 0.514 | IF(2014): 0.481

**Alfaar AS, Zamzam M, Abdalla B, Magdi R, El-Kinaai N (2015)** Childhood Ewing Sarcoma of the Orbit. *J Pediatr Hematol Oncol* 37:433–7.

doi: 10.1097/MPH.0000000000000346 | Q4 IF: 1.170 | IF(2015): 1.146 | IF(2014): 0.902



Zekri W, Yehia D, Elshafie MM, Zaghloul MS, El-Kinaai N, Taha H, Refaat A, Younes AA, **Alfaar AS** (2015) Bilateral clear cell sarcoma of the kidney. J Egypt Natl Canc Inst 27:97–100.

doi: 10.1016/j.jnci.2015.03.002

No IF yet

Hassan WM, Mehanna M, Nour R, Yehia D, Atta N, **Alfaar AS** (2015) Association between quality of clinical trials and human development index in heart failure using JADAD scale. Princ Pract Clin Res 1:40–46.

doi: 10.21801/ppcrj.2015.12.2

No IF yet

## 2014

El-Nadi E, Elzomor H, Labib RM, **Alfaar AS**, Zaghloul MS, Taha H, Elwakeel M, Younes A, Elwakeel M (2015) Childhood orbital rhabdomyosarcoma: Report from Children's Cancer Hospital-57357-Egypt. J Solid Tumors 2:94.

doi: 10.5430/jst.v5n2p94

No IF yet

Hassan WM, **Alfaar AS**, Bakry MS, Ezzat S (2014) Orbital tumors in USA: Difference in survival patterns. Cancer Epidemiol 38:515–522.

doi: 10.1016/j.canep.2014.07.001

Q3 IF: 2.890

IF(2014): 2.771

IF(2013): 2.558

Zekri W, **Alfaar AS**, Yehia D, Elshafie MM, Zaghloul MS, El-Kinaai N, Taha H, Refaat A, Younes AA (2014) Clear cell sarcoma of the kidney: patients' characteristics and improved outcome in developing countries. Pediatr Blood Cancer 61:2185–90.

doi: 10.1002/pbc.25192

Q1 IF: 3.838

IF(2014): 2.562

IF(2013): 2.562

**Alfaar AS**, Nour R, others (2014) What a reference manager can add for a physician in web 2.0 era. Egypt J Cardiothorac Anesth 8:55.

doi: 10.4103/1687-9090.143253

No IF yet

Amgad M, **Alfaar AS** (2014) Integrating web 2.0 in clinical research education in a developing country. J Cancer Educ 29:536–40.

doi: 10.1007/s13187-013-0595-5

IF (Now): 1.77

IF(2014) 1.23

IF(2013): 1.054

## 2013

Shohdy KS, **Alfaar AS** (2013) Nanoparticles targeting mechanisms in cancer therapy; great efforts, less implementations. Ther Deliv 04:1197–1209.

doi: 10.4155/tde.13.75

No IF yet

## 2012

**Alfaar AS**, Kamal S, Abouelnaga S, Greene WL, Quintana Y, Ribeiro RC, Qaddoumi I a (2012) International telepharmacy education: another venue to improve cancer care in the developing world. Telemed J E Health 18:470–4.

doi: 10.1089/tmj.2011.0182

Q1 IF (now): 5.033, the journal was new at the year of submission

Meselhy GT, Sallam KR, Elshafiey MM, Refaat A, **Samir A**, Younes A a., Meselhy GT Sallam KR EMMRASAYAA (2012) Sonographic guidance for tunneled central venous catheters insertion in pediatric oncologic patients: guided punctures and guide wire localization. Chinese-German J Clin Oncol 11:484–490.

doi: 10.1007/s10330-012-1011-z

No IF yet

## Theses:

- Alfaar, A.,** Strauss, O. (2023). Thesis Topic: The role of FoxP3 in Age-related macular degeneration (Neuroscience - Ophthalmology). MD/PhD Degree.
- Alfaar, A.,** Strauss, O. (2017). *The Incidence and Survival of Pediatric Malignancies with Focus on Ocular and Orbital Tumors*. Charité Medical University. Doctor medicinae (Dr. med.) Degree.
- Alfaar, A.,** Kestler, H., & Rodriguez-Galindo, C. (2014). *Ordinal Classification of Pediatric Tumors Samples*. Ulm University. MSc Advanced Oncology
- Alfaar, A.,** Hamza, H., AbouElnaga, S., & AbdelBaki, A. (2012). *Genetic and Molecular Targeting of Retinoblastoma* (Review). Cairo University. MSc Ophthalmology

## Book Chapters:

- “Getting Started in Research: What Registries Can Do for You” in “U. Schmidt-Strassburger (ed.), Improving Oncology Worldwide, Sustainable Development Goals Series”, 2022, ISBN 978-3-030-96052-0

## Protocols and projects documentations:

- Informatics Project:** *Building a Research-oriented Follow-up System for Cancer Patients*. Supervisor: Prof. Sherif Kholief. 2010 Jan.: **PG Diploma- Medical and Biomedical Informatics**. Faculty of Information and Computer Sciences, Helwan University.
- Clinical Trial Protocol Project;** *Comparison of Bimatoprost with a fixed combination of Bimatoprost and Timolol in adult patients with primary open-angle glaucoma: an eight-week, randomized, double-blind, and parallel groups*. 2009 Nov. **Certificate- Principles and Practice of Clinical Research**. Harvard Medical School.
- eLearning Project:** *Online Training Module for Nurses on Leukemia*. 2009 Aug.: **Certificate- eLearning in Practice Course**. InWent/GIZ (Gesellschaft für Internationale Zusammenarbeit (GIZ)), DE/KE.

## Conference Presentations:

 [Blue: Oral Presentation](#)

### 2022

-  **Alfaar, AS.** The Epidemiology of Eye Malignancies in Saxon, Germany, between 1998-2015. In: *The Saxonian ophthalmological congress*. Dresden, Germany; 2022.
-  **Alfaar, A.,** P. Wiedemann, M. Rehak, and A. Wolf. 2022. “The Incidence of Retinal Detachment in Germany between 2005 and 2019.” P. S210 in *Kongress der Deutschen Ophthalmologischen Gesellschaft [The Congress of the German Ophthalmological Society]*. Berlin: Springer.
- Melekidou, W., M. Rehak, and **A. S. Alfaar**. 2022. “Die Inzidenz von Augen- Und Orbitaltraumata in Deutschland Vor Und Nach COVID 19 [The Incidence of Ocular and Orbital Trauma in Germany before and after COVID 19].” P. S333 in *Kongress der Deutschen Ophthalmologischen Gesellschaft [The Congress of the German Ophthalmological Society]*. Berlin: Springer.
-  **Alfaar, A.** 2022. “Building Registries Is Hard, How Can We Make It Even Harder?” P. S215 in *Kongress der Deutschen Ophthalmologischen Gesellschaft [The Congress of the German Ophthalmological Society]*. Berlin: Springer.
- Reyna, E. Carlos, M. Rehak, and **A. S. Alfaar**. 2022. “Epidemiologische Auswirkungen Der Covid-19- Pandemie Auf Enukeationsfälle in Deutschland [Epidemiological Effects of the Covid-19 Pandemic on Enucleation Cases in Germany].” P. S293 in *Kongress der Deutschen Ophthalmologischen Gesellschaft [The Congress of the German Ophthalmological Society]*. Berlin: Springer.
- Al-Shaibawi, H., M. Rehak, and **A. S. Alfaar**. 2022. “Die Inzidenz Der Endophthalmitis in Deutschland in Den Jahren 2019 Und 2020 Und Die Mögliche Auswirkung von COVID-19 [The Incidence of Endophthalmitis in Germany in the Years 2019 and 2020 and the Possible Impact of COVID-19].” P. S313 in *Kongress der*

Deutschen Ophthalmologischen Gesellschaft [The Congress of the German Ophthalmological Society]. Berlin: Springer.

## 2020

- 📄 **Alfaar A.** Getting started in research – What registries can do for you. Sept 2020 Online – Ulm Alumni MOAO Meeting
- 📄 **Alfaar, A., M. Rehak, A. Saad, P. Wiedemann, and K. Kraywinkel.** 2020. “The Incidence of Ocular Melanoma in Germany.” in 118. Kongress der Deutschen Ophthalmologischen Gesellschaft.
- 📄 **Alfaar, A., M. Rehak, W. Hassan, M. Mehanna, Saad A., L. Jansen, Kraywinkel K., and ‘Group GEKID Cancer Survival Working’.** 2020. “The Incidence and Survival of Adult Orbital Tumors in Germany.” in 118. Kongress der Deutschen Ophthalmologischen Gesellschaft.
- Alfaar, Ahmed S., Mahmoud M. Elzembely, Hossam Elzomor, Abdallah Shelil, and Naglaa Behiry.** 2020. “Towards Building a Map for Retinoblastoma in Egypt.” in The 52nd Annual Congress of the International Society of Paediatric Oncology.


## 2019

- Hammad, M., Hosny, M., Khalil, E., **Alfaar, A.**, Fawzy. M. (2019) Pediatric Ependymoma; An Institutional Experience from A Developing Country. SIOP (International Society of Paediatric Oncology) Lyon, France
- Zekri, W., Hammad, M., Rashed, W., Ahmed, G., Elshafie, M., Adly, M. H., Elborai, Y., Abdalla, B., Taha, H., Elkinaai, N., Refaat, A., Younis, A. **Alfaar. A. S.** (2019) Adrenocortical Carcinoma in The Pediatric Population. SIOP, Lyon, France.
- Alfaar, A., Saad, A., Elzouki, S.** (2019) Incidence and survival of Uveal Melanoma occurring as single cancer versus its occurrence as a first or second primary neoplasm. ESMO (European Society of Medical Oncology), Barcelona, Spain.
- Saad, A., **Alfaar, A.** (2019) Is radiation therapy influencing Alzheimer’s in Brain and Head and Neck Cancers? ESMO, Barcelona, Spain.
- 📄 **Alfaar, A., Saad, A., Tawfik, M., Elsherif, O.E., Osman, M.H., Strauß, O.** (2019) Second primary orbital malignancies in USA over 40 years. DOG (Deutsche Ophthalmologische Gesellschaft), Berlin, Germany
- Saad, A., **Alfaar, A.S.** (2019) Death from alzheimer’s in brain and head and Neck cancers; is it influenced by therapy?. Brain Tumor Meeting, Berlin, Germany.
- Reichhart, N., Cordes, M., Bucichowski, P., **Alfaar A.S.**, Almedawar, S., Strauß, O. (2019) Influence of mutant bestrophin-1 on L-type channel trafficking and activity in the RPE. Pro-Retina.

## 2017

- Rashed, W.M., Adly, M.H., Sobhy, M., Rezk, M.A., Ishak, M., El Shafie, A., Ali, M., **Alfaar, A.** (2017) The risk of subsequent malignancies among survivors of pediatric thyroid cancer. Conference: 49th Congress of the International Society of Paediatric Oncology (SIOP), At Washington, DC, USA.
- Rashed, W., Saad, A., Al-Husseini, M., Galal, A.M., Al-Tayep, A.M., El Shafie, A., Ali, M.A., **Alfaar, A.S.** Incidence of Adrenal gland tumor as a second primary malignancy: SEER based database, Sep 2017 European Society of Medical Oncology - ESMO

## 2016

-  **Alfaar, A. S.** Lausser, L., Rodriguez-Galindo, C., Kestler, H. (2016) Ordinal Classification of Microarray Data of Pediatric Tumors. European Molecular Biology Organization Meeting, Mannheim, Germany. (Poster and short oral)

## 2015

- Jomaa M., Gado N., Elgazawy H., .. **Alfaar, AS.** Assessment of breast cancer screening awareness among relatives of Egyptian breast cancer patients. In: Asia Congress of the European-Society-for-Medical-Oncology (ESMO). Singapore, Singapore: Oxford Univ Press, Great Clarendon St, Oxford OX2 6dp, England; 2015. P. 26.
- El-Nadi, E., Elzomor, H., Labib, R. M., **Alfaar, A. S.**, Zaghloul, M. S., Taha, H., ... & Elwakeel, M. (2015). Childhood Orbital Rhabdomyosarcoma. Report from Children's Cancer Hospital-57357-Egypt. 18<sup>th</sup> ECCO - 40<sup>th</sup> ESMO European Cancer Congress.
- Zekri, W., **Alfaar, A.**, Yehia, D., Labib, A., Zaghloul, M.S., Taha, H., ... & Younis A. (2015) Treatment and Outcomes of Anaplastic Wilms' Tumors in Egypt. The 47th Congress of the International Society of Paediatric Oncology (SIOP), Cape Town, South Africa.

## 2014



-  **Alfaar, A. S.** Ordinal Classification of Retinoblastoma (2014). Egyptian Ophthalmological Society meeting, Alexandria, Egypt
- Zekri, W., Hammad, M., ElBoraie, Y., Abdalla B., Taha H., Refaat A., Alfaar A.S., Younis A. (2014) Adrenocortical Carcinoma In The Pediatric Age Group; Experience at Children Cancer Hospital Of Egypt (CCHE). In American Society of Pediatric Hematology/Oncology.
- Alfaar, A. S.**, Labib, R., Ezzat, S., Mostafa M., Taha H., Abouelnaga S. (2014) Telepathology to Improve Collaboration and Quality of Samples Annotation in Biorepository. In the International Society for Biological and Environmental Repositories Annual Meeting.
-  Labib, R., Mostafa, M., Ezzat, S., **Samir, A.**, Abouelnaga, S. (2014) Omics-Ready Bio/Data Repository for Childhood Cancers in Egypt. In The International Society for Biological and Environmental Repositories Annual Meeting.
- Ezzat, S., Labib, R., Mostafa, M., **Alfaar, A.**, Sabry, M.S., Shaaban, K., Taha, H., Abou Naga, S. (2014) Building a State of Art Biorepository by Hybridizing Electronic Data Capture Systems in a Limited Resource Country. In "The International Society for Biological and Environmental Repositories" Annual Meeting.
-  **Alfaar, A.S.**, Labib, R. (2014) eBanking of what really matters; Children's Cancer Hospital-Egypt experience in electronic management of BioBanks. In Conference on Cancer Biobanking "Establishing the First Cancer Biobank in Jordan".
- Alfaar, A.S.**, Bakry, M.S, Ezzat, S. (2014) Childhood Orbital, Ocular and Optic nerve tumors in Egypt. In Association for Research in Vision and Ophthalmology.
- Alfaar, A. S.**, Zaki, I., Taha, I., Ismail A, Sabry M, Kamal M, Ezzat S, Abouelnaga S (2014) Accelerating innovation in outcomes and quality-of-care research through integrating clinical databases: Pediatric oncology experience in Egypt. In ASCO Conference.

## 2013

- Alei Eldin, A., Haddad, A., Elzomor, H., Medhat, Y., Taha, H., Saad, M., ... Mohamed, S. (2013). Evaluation of Retinoblastoma management in the first Multidisciplinary system in the Cancer children hospital in Egypt. In *International Society of Ocular Oncology Meeting*. Cleveland.

-  **Alfaar, A. S.,** Nour, R., Kamal, M., Bakry, M. S., & Ezzat, S. (2013). Retinoblastoma Clinical Research in Egypt, 5 years' experience. In *International Society of Genetic Eye Diseases and Retinoblastoma meeting*. Gent, Belgium.
- AlFaar, Ahmad S.,** Nour, R., Kamal, M., Ezzat, S., & Bakry, M. S. (2013). Automating clinical protocol monitoring: a model from developing countries. In *European Multidisciplinary Cancer Congress*. Amsterdam: Elsevier.
-  ElZomor, H., Nour, R., **Alfaar, A. S.,** Aleieldin, A., Zaghoul, M. S., & Taha, H. (2013). High Risk Histopathologic features of Retinoblastoma in Egypt. In *International Society of Genetic Eye Diseases and Retinoblastoma meeting*. Gent, Belgium.
- Elzomor, H., Nour, R., **Alfaar, A. S.,** Aleieldin, A., Zaghoul, M. S., Taha, H., & Elhaddad, A. (2013). Presentation of Extra-Ocular Retinoblastoma in Egypt. In *International Society of Genetic Eye Diseases and Retinoblastoma meeting*. (p. 71). Gent, Belgium.
-  Taha, H., ElZomor, H., Aleieldin, A., Elhaddad, A., Nour, R., Zaghoul, M. S., & **Alfaar, A. S.** (2013). Pathological findings of Retinoblastoma in Egypt; implementing CAP protocol in developing countries. In *International Society of Genetic Eye Diseases and Retinoblastoma meeting*. Gent, Belgium.
- Zekri, W., **Alfaar, A.,** Yehia, D., Elshafie, M., Saad Zaghoul, M., Taha, H., ... Younis, A. (2013). Clear Cell Sarcoma of the Kidney. In *European Multidisciplinary Cancer Congress*. Amsterdam: Elsevier.


## 2012

- Hanafy, N., & **Samir Al-Faar, A.** (2012). Developing A Specialized Central Venous Catheter Nursing Team In Pediatric Oncology Setting. In *International Conference on Cancer Nursing*. Prague, Czech Republic.
- Hassanain, O., Adel, N., Kamal, M., Abouelnaga, S., & **Samir AlFaar, A.** (2012). Building the First ELearning Paediatric Oncology Clinical Pharmacy Program for Developing Countries. In *European Conference of Oncology Pharmacy*. Budapest, Hungary: European Journal of Oncology Pharmacy.
- Kamal, M., Hassanain, O., AbouElNaga, S., Hosny, H., & **Samir, A.** (2012). Treatment Protocols' Monitoring Solution for Real-Time Tracking of Pediatric Cancer Patients: A Research Oriented System. In *21st Pediatric Pharmacy Conference and PPAG Annual Meeting*. Houston.
-  Kamal, M., Hassanain, O., AbouElNaga, S., Hussein, H., Hosny, H., Sabry, M., & **Samir Alfaar, A.** (2012). Integrating Treatment Protocol Monitoring System with Real-Time Statistics: A Research Oriented In-House developed Solution. In *International Society of Pediatric Neuro-oncology*. Toronto.
- Taha, G., Sallam, K., ElShafie, M., **Samir, A.,** Younes, A., & Refaat, A. (2012). Sonographic guidance for tunneled central venous catheters insertion in pediatric oncologic patients: guided punctures and guide wire localization. In *5th Scientific Annual Conference of South Egypt Cancer*. Assiut, Egypt.
-  **Alfaar, A.,** AlAsmar, M., AbdelHameed, M., Aamer, I., & Sabry, N. (2012). Integrating Virtual Reality with eLearning in Medical Education: Cost Effective Model in Developing Countries. In *Online Educa*. Berlin.
- Alfaar, A.,** Kamal, M., Hassanain, O., Sabry, M., Ezzat, S., & Abouelnaga, S. (2012). Advancing Clinical Oncology Practice in Developing Countries: Integrating Research Informatics for Continuous Process Improvement. In *European Society of Medical Oncology*. Vienna, Austria: Oxford.
- Alfaar, A.,** Kamal, M., & Sabry, M. (2012). Next Generation Cancer Registry; Opportunities of web 3.0 and physician perspective. In *European Society of Medical Oncology*. Vienna, Austria.

## 2011

- AlFaar, A. S.** (2011). Teaching Clinical Research Leadership Skills for Undergraduate Medical Students and Impact on Public Health. In *Washington DC: US Department of State Fellows Congress*.

Bakry, M. S., Kamal, M., Ezzat, S., & **AlFaar, A. S.** (2011). Integrating Web-based Real-time Analysis System with Clinical Research Database Facilitates Interim Analysis. In *European Multidisciplinary Cancer Congress* (p. p. 2.163). Stockholm: Elsevier.

 **Samir AlFaar, A.**, Ezzat, S., & AbouElNaga, S. (2011). "Bringing them together" – An essential role in retinoblastoma team; a disease coordinator. Two years' experience in a developing country. In *International Society of Genetic Eye Diseases and Retinoblastoma meeting*. (p. 62). Bangalore, India.

## 2010

**Samir, A.**, & Kamal, S. (2010). Using hybrid solutions for maximizing the return on investment from telemedicine in pharmacy education. In *5<sup>th</sup> Annual Pediatric Telehealth Colloquium* (pp. 846–854). Baltimore, Maryland, USA: Mary Ann Liebert, Inc.

## Acknowledgments

I am deeply grateful to Prof Olaf Strauß, my supervisor, for his exceptional guidance, mentorship, and support throughout this research project. He provided me with a smooth entry to the field, trained me personally on Patch-clamping and calcium imaging, and encouraged me to apply my programming skills to their data. I also want to express my heartfelt thanks to Dr. Nadine Reichhart for her unwavering support and invaluable advice.

I would like to acknowledge the lab team members between 2016-2022 who provided me with excellent support in experiments and data analysis and enriched my knowledge with their insightful discussions, especially Dr. Norbert Kociok and Dr. Stefan Mergler. I am also grateful to the doctoral and postdocs who helped me in the experiments and presentations or by providing advice, including Lucas Stürzbecher, Christophe Roubex, Magdalena Cordes, Piotr Bucichowski, Susanne Keckeis, and Sergio Crespo-García.

My sincere thanks go to Gabriele Fels, our lab technician, who made my lab life more manageable and clarified every minute detail for me. I am also grateful to the German Academic Exchange Service (DAAD) for sponsoring my scholarship between 2015 and 2019, and especially to Mrs. Margret Leopold from the DAAD team for her exceptional support and empathy.

I would like to thank Mrs. Angelika Cernitori and Pamela Glowacki from Charité International Cooperation for their support and Mr. Ralf Ansorg and Dr. Benedikt Salmen from the International neuroscience program for assistance over the seven years.

I am indebted to my wife, Salma, and my daughters, Jomana and Rofaida, for their unwavering support and encouragement throughout this journey. They stood beside me during the hard times away from the big family for such a long time, and I am deeply grateful for their love and support.

Finally, I would like to express my gratitude to my mother, Naglaa Behiry, for raising my mathematical mind, providing me with her remote support and her prayers, and being there whenever I needed her. Her efforts in Egypt enabled me to make the most of my time in Germany, and I could not have reached this point without her.